

„ Carbon nanotubes as catalysts in the catalytic oxidation of C4 hydrocarbons”

vorgelegt von
M.Sc. Physical Chemistry
Xi Liu
P.R. China

Von der Fakultät II – Mathematik und Naturwissenschaften
der Technischen Universität Berlin
zur Erlangung des akademischen Grades
Doktor der Ingenieurwissenschaften
- Dr.-Ing. -

genehmigte Dissertation

Promotionsausschuss:

Vorsitzender: Prof. Dr. M. Gradzielski

Berichter/Gutachter: Prof. Dr. R. Schlögl

Berichter/Gutachter: Prof. Dr. T. Ressler

Tag der wissenschaftlichen Aussprache: 10 September 2008

Berlin 2008
D 83

Contents

Contents	1
Abstract.....	3
Chapter 1 Introduction	8
1.1. General considerations- Economic aspect of C ₄ hydrocarbons	8
1.2. Catalytic oxidation of hydrocarbons	10
1.3. Metal catalysts for catalytic oxidation of butane to butene and butadiene	13
1.3.1. Reaction process	14
1.3.2. Factors affecting activity and selectivity	17
1.3.2.1. Surface Basicity	18
1.3.2.2. Oxygenated surface groups.....	20
1.4. Carbon catalysts for ODH of butane to butene and butadiene.....	22
1.4.1 Feature and surface nature of carbon materials	22
1.4.2. Carbon materials in catalysis	24
1.4.3. Modification of carbon materials.....	28
1.4.3.1 Oxidative treatment.....	29
1.4.3.2 Grafting modification.....	30
1.4.3.3 Phosphoric acid addition.....	31
1.5. Motivation and aim	33
References.....	34
Chapter 2 Experiment and characterization Methods	43
2.1. Set-up for the catalytic reaction tests	43
2.2. Characterization Techniques.....	47
2.2.1. Microscopic Methods (TEM, SEM)	47
2.2.2. Spectroscopic Methods (XPS, IR-spectroscopy and XRF)	48
2.2.3. Thermal characterization methods with MS (TPD, TPO and NH ₃ -TPD)	49
References.....	54
Chapter 3 Catalysts preparation and functionalization	56
3.1 Oxidation treatment	56
3.2 Chlorination and immobilization	57
3.3 Phosphoric addition	59
3.4 Carbon supported metal catalysts	60
Chapter 4 Catalytic oxidation of n-butane over carbon catalysts	61
4.1 Catalytic activity of CNTs	61

4.2 Catalytic activity of phosphoric modified CNTs	70
4.3 Catalytic activity of grafted CNTs	76
4.4 Catalytic activity of activated carbons	79
4.5 Catalytic activity of phosphoric modified activated carbons	84
4.6 Catalytic activity of other carbon materials	85
4.7 Catalytic activity of carbon supported metal catalysts	86
4.8 Conclusions	87
References	90
 Chapter 5 Characterization of carbon catalysts before and after reaction	 91
5.1 TEM	91
5.1.1 Nanocyl CNTs	91
5.1.2 PSLD CNTs	96
5.2 TPO, TPD, NH ₃ -TPD analysis of catalysts	100
5.2.1 Pristine Nanocyl CNTs	100
5.2.2 Oxidized Nanocyl CNTs	103
5.2.3 Thermally treated Nanocyl CNTs	109
5.2.4 Phosphoric modified Nanocyl CNTs	118
5.2.5 PSLD CNTs	126
5.3 XPS spectrum	131
5.4 Infrared spectrum	133
5.5 XRF	138
5.5 Conclusions	138
Reference:	139
 Chapter 6 Catalytic oxidation of butene to butadiene	 142
6.1 Catalytic performance of carbon materials	142
6.1.1 Catalytic activity of pristine carbon materials	142
6.1.2 Catalytic activity of oxidized carbon materials	146
6.1.3 Catalytic performance of phosphoric modified CNTs	147
6.2 Oxygen order measurement	150
6.2 Conclusions	152
Reference:	152
 Chapter 7 Reaction mechanism and outlook	 153
References	161
 APPENDIX	 163
Curriculum Vitae	163
Acknowledgements	164

Abstract

The catalytic performance of pristine and modified CNTs for catalytic oxidation of butane/butene to corresponding alkenes has been studied in the present work, owing to its great potential in petro-industry and considerably growing interest in metal-free catalysis. For comparison, the catalytic activity using other materials for catalytic oxidation reaction, such as activated carbons, diamond-like carbon and metal oxides, has also been investigated under the same reaction conditions. A comparative investigation on the catalysts before and after reaction has been performed by using a series of joint experimental techniques in catalysis, for example, TEM, TPO, TPD, NH₃-TPD, XPS and IR. The detailed knowledge on the chemical nature of surface functionalities has been achieved and, based on the analysis of activity-surface functionalities relationship, the reasonable reaction model has been proposed accordingly.

It has been found that the pristine CNTs display high activity but low selectivity for catalytic oxidation of butane to target products, butene and butadiene. The oxidation treatment is able to improve the catalytic performance of CNTs. A better catalytic performance can be further achieved by using phosphoric modified oxidized CNTs. In addition, molecule grafting as a new catalytic modification method has firstly been applied to modify CNTs and, significantly, the as-modified CNTs display an active and stable catalytic performance even after 40 hours reaction. The grafting modification can effectively immobilize small molecules, like 2-furoic acid and methyl cyclopentanone-2-carboxylate, to the carbon defects on the surface of CNTs. The surface investigation suggests that a variety of moieties remain on the surface of CNTs after reaction process,

thus indicating that the selective and stable catalytic performance could be attributed to the existence of the grafted functional groups.

Two kinds of reaction pathways, i.e., the total oxidation and selective oxidation, participate in catalytic oxidation of butane. The former one can be related with the non-dissociative oxygen molecules, which are chemisorbed and activated on the surface of CNTs. The latter one should be correlated with quinone groups, generated via dissociative chemisorption of gaseous oxygen. The characterization supports the non-competitive adsorption model: hydrocarbons molecules are preferably adsorbed by the quinone groups and oxygen molecules are adsorbed on the π -electron-rich surface of CNTs, forming electrophilic O_2^{2-} and O_2^- species. The following dissociation of O_2 species could occur on the carbon defects, resulting in the generation of active sites for catalytic oxidation. The oxidation treatment significantly improves the catalytic performance by generating the oxygenated surface groups acting as active sites for catalytic oxidation of butane. However, the majority of oxygen species generated via oxidation do not involve in the catalytic oxidation of butane, which has been removed during the reaction process. The improvement in catalytic performance by using the phosphoric acid modified CNTs can be attributed to the inhibition of combustion of butane. The reasonable elementary steps proposed in present work include the adsorption of hydrocarbons and dehydrogenation on the quinone groups, the recombination of hydroxyl groups and following regeneration of quinone groups via dissociative chemisorption of gaseous oxygen. The carbon oxides form as byproducts from the combustion of hydrocarbons.

Aufgrund des beträchtlichen Potentials in der Petroindustrie und des steigenden Interesses an metallfreien Katalysatoren wurde in der vorliegenden Arbeit die katalytische Leistung von unveränderten und modifizierten CNTs für die katalytische Oxidation von Butan/Buten zu den entsprechenden Alkenen untersucht. Zum Vergleich wurden auch weitere für die katalytische Oxidation genutzte Materialien, z. B. aktivierter Kohlenstoff, diamantähnlicher Kohlenstoff und Metalloxide, unter denselben Reaktionsbedingungen auf ihre katalytische Aktivität hin untersucht. Vergleichende Untersuchungen wurden an den Katalysatoren vor und nach der Reaktion mit der Katalyse verbundenen experimentellen Methoden durchgeführt, z. B. TEM, TPO, TPD, NH_3 -TPD, XPS und IR. Es wurden detaillierte Kenntnisse über die chemische Natur der funktionellen Oberflächengruppen erhalten und ein entsprechendes auf der Analyse der Beziehung zwischen diesen Oberflächengruppen und der Aktivität basierendes Reaktionsmodell vorgeschlagen.

Es stellte sich heraus, daß die unveränderten CNTs eine hohe Aktivität, aber eine geringe Selektivität für die katalytische Oxidation von Butan zu den Zielprodukten Buten und Butadien zeigen. Die oxidative Behandlung verbessert die katalytische Leistung der CNTs. Eine weitere Steigerung der katalytischen Leistung kann mit phosphorhaltigen oxidierten CNTs erreicht werden. Zusätzlich wurde die Funktionalisierung der Oberfläche durch Aufbringen von Molekülen („molecule grafting“) als neue katalytische Methode zum ersten Mal angewendet, um die CNTs zu modifizieren. Die so modifizierten CNTs zeigen eine aktive und dauerhafte katalytische Leistung auch noch nach 40 Stunden Reaktionsdauer. Kleine Moleküle, wie 2-Furoesäure und Methyl Cyclopentanon-2-Carboxylat, können durch „molecule grafting“ wirkungsvoll an

Kohlenstoffdefekten an der Oberfläche der CNTs festgelegt werden, Die Oberflächenuntersuchung deutet darauf hin, daß verschiedene Gruppen auf der CNT Oberfläche nach dem Reaktionsprozess verbleiben. Dies deutet darauf hin, daß die selektive und dauerhafte katalytische Leistung auf die Anwesenheit von funktionalen Gruppen durch “molecule grafting“ zurückgeführt werden kann.

Zwei Reaktionswege treten bei der katalytischen Oxidation von Butan auf: die Totaloxidation und die selektive Oxidation. Ersterem kann nicht dissoziierten Sauerstoffmolekülen zugeordnet werden, die chemisorbiert und aktiviert auf der CNT Oberfläche sind. Der zweite Reaktionsweg sollte mit Chinongruppen korreliert werden, die durch dissoziative Chemisorption von gasförmigem Sauerstoff entstanden sind. Das nicht-kompetitive Adsorptionsmodell wird durch die Charakterisierung unterstützt: Kohlenwasserstoffe werden bevorzugt von den Chinongruppen und Sauerstoffmoleküle auf der π -Elektronen reichen Oberfläche der CNTs adsorbiert, wobei sie elektrophile O_2^{2-} und O_2^- Spezies bilden. Die darauf folgende Dissoziation der O_2 Spezies könnte an den Kohlenstoffdefekten auftreten, woraus sich aktive Zustände für die katalytische Oxidation bilden. Die oxidative Behandlung verbessert die katalytische Leistung wesentlich, indem sie mit Sauerstoff angereicherte Oberflächengruppen als aktive Zustände für die katalytische Butanoxidation erzeugt. Der Hauptanteil der durch Oxidation erzeugten Sauerstoffspezies ist jedoch nicht die katalytische Butanoxidation einbezogen, da diese während des Reaktionsprozesses abgebaut wurden. Die Verbesserung der katalytischen Leistung von mit Phosphorsäure modifizierten CNTs kann der Hemmung der Verbrennung von Butan zugeschrieben werden. Die sinnvoll angenommenen Elementarschritte der Reaktion, die in dieser Arbeit vorgeschlagen

wurden, beinhalten die Adsorption von Kohlenwasserstoffen und die Dehydrierung an den Chinongruppen, die Rekombination von Hydroxylgruppen und die darauf folgende Regeneration der Chinongruppen durch dissoziative Chemisorption gasförmigen Sauerstoffs. Kohlenstoffoxide entstehen als Nebenprodukte bei der Verbrennung von Kohlenwasserstoffen.

Chapter 1 Introduction

Since phrase *catalysis* was coined in 1835 by Jöns Jakob Berzelius, who was the first to note that certain chemicals speed up a reaction, our civilization has been irreversibly changed and reconstructed by a variety of catalyzed chemical production. The requirement for faster-cheaper-better products pushes the development of civilization. So-called natural thing is only a fading dream for the modern homo sapiens, or just gimmick travel traps and expensive commercial products. What we do is just keeping pace with the rapidly advancing and mighty tide.

1.1. General considerations- Economic aspect of C₄ hydrocarbons

n-Butane, which was extracted from crude oil and natural gas by distillation, has a variety of industrial uses: steam cracking yields ethylene and propylene, catalytic dehydrogenation yields butenes and butadiene, acid-catalyzed isomerization provides i-butane, and maleic anhydride or acetic acid was obtained through catalytic or non-catalytic oxidations, respectively.^[1] Until 2000, the annual consumption of n-butane in US was about 1 billion cubic meter and the condensate average field gate price of butane was about 250 dollars per cubic meter.^[1]

Butene is also an important industrial raw material. The worldwide consumption of n-butene was about 18×10^6 ton in 1984 and increased to 44×10^6 ton in 2004. United states are the biggest butene producing and consuming region in the world followed by Northeast Asia, Western European and Mideast Asia.^[1] More than half of the butene was used to manufacture alkylate and polymer gasoline. Around one-third was used without

any conversion as fuel gas or blendstock for gasoline. And 10% of the n-butene was used in the manufacture of a variety of other chemical products. It plays an important role in the production of materials such as linear low density polyethylene (LLDPE): the copolymerisation of ethylene and 1-butene produces a form of polyethylene that is more flexible and more resilient. n-Butene can be used in the production of butadiene and maleic anhydride, polybutene, butylene oxide, secondary butyl alcohol (SBA), methyl ethyl ketone (MEK) and a more versatile range of polypropylene resins.^[1-4] 2-Butene is mainly used as fuel gas, but it can be converted to 2-Methylbutanol and other chemicals.^[1] In recent study, the isomerization of 2-butene was a potential valuable method to produce the important chemical monomers like propene, 1-butene and butadiene.^[1]

The importance of butadiene production can be attributed to the enormous applications of its synthetic products. One of the well-known products is butadiene–styrene rubber: the major rubber for manufacture of tires. The other synthetic products include latex and polybutadiene rubber, plastics with special mechanical properties (*i.e.* polystyrene, ABS polymers), and as raw material in a wide variety of chemical synthesis.^[1,5] Butadiene consumption in 1987 was estimated at 12 billion pounds worldwide (3.3 billion pounds in U.S) and the trend has been for this production to increase.^[6] For example, the demand for butadiene in U.S grew 2.3% annually from 1995 to 2001 and consumption of U.S. in 2001 reached 5.1 billion pounds. Butadiene is produced by one of two processes: recovery from a mixed hydrocarbon stream and oxidative dehydrogenation of n-butene.^[3] Almost all butadiene was produced by steam cracking from naphtha or liquefied petroleum gas (LPG), but catalytic dehydrogenation was also an important process. Essentially two processes were used in the United States

for butadiene synthesis: a two-phase process departing from n-butane (Phillips process), wherein butenes were converted into butadiene in the second phase, or a single-stage process using n-butane and n-butene (Houdry Catadiene process). These processes were applied to produce synthetic rubber instead of natural rubber in the United States at the beginning of the Second World War.

1.2. Catalytic oxidation of hydrocarbons

Although the unsaturated light hydrocarbons (*i.e.* ethylene, propylene, isobutene, butadiene, etc.) are mostly produced via steam cracking of LPG. The low price of light alkanes has provided enormous incentives for their use as raw materials in the chemical industry.^[1] An important example of utilization of alkanes or alkenes is their conversion to corresponding unsaturated hydrocarbons. Especially, the present-day chemical industry depends heavily on the use of crude oil as starting material, but the world crude oil supply would be exhausted in 50 years. The natural gas supply would meet the increasing demand for hydrocarbon recourse. In 2004, the estimated worldwide consumption of natural gas was 100 trillion cubic feet and butane took 1%. Indeed, the petrochemical industry's tendency seems to be the direct use of alkanes as raw materials, due to the great abundance and low price.^[2,7-9] In fact, the price of raw materials is an ultimate factor for the industrial application. A relevant example concerns styrene production via the butane–butadiene process. Till the middle of 1960s, among other large-scale catalyzed reactions, dehydrogenations of organic compound became prominent and 9.8% chemicals were produced by dehydrogenation among the 147 billion pounds of organic

products obtained via catalytic processes by the 50 top chemical industries in the United States.^[7, 11]

Compared with direct dehydrogenation, it seems that oxidative dehydrogenation (ODH) is more promising for conversion of alkanes due to its thermodynamic advantages. In reality, for light alkanes (C₂ to C₄), the DH reaction



is such that the educts are favored by the equilibrium in the low temperatures and at high pressure.^[1] Reactions are endothermic and in order to shift the equilibrium to aim to alkenes, reactions must be carried out at relatively high temperatures (from 773 to 923K).^[2,3] In addition, high operating pressure, which is usually preferred in industrial practice, is unfavorable for shifting the equilibrium towards the aiming direction. The significant deactivation of catalysts is always observed, attributed to coke formation. Specific examples are chromia–alumina catalysts (used in a commercial DH process of alkanes), requiring regeneration after a few minutes of operation.^[12] For all these reasons, dehydrogenations of alkanes with oxygen:



is an excellent alternative for the synthesis of alkenes.^[1,2] The formation of water is thermodynamically favorable for this reaction.^[1,8,12] A theoretically complete conversion can be attained even at low temperatures and high pressure, bringing advantages from the economic and process engineering points of view. The conversion of butane was significantly increased due to the existence of oxygen. Catalyst deactivation is also further reduced by the possible removal of coke and its precursors by oxygen.^[2,8] It

should be stressed, for the conversion of alkanes to the corresponding alkenes, the temperature of ODH processes is about 200 K lower than that of DH process.^[13] However, despite of those advantages mentioned above, ODH (including other catalytic-oxidation processes) has some drawbacks: due to its exothermic character it may require special care in reactor operation, explosion (explosion limits in air: butane 1.4-8.4%, butene 1.6-9.3%, butadiene 2.0-11.5%), and “hot-spot” phenomenon could be observed since there might be a distribution of feed composition of oxygen and in some range the feed composition is explosive; the desired product must be sufficiently stable in the reaction conditions in order to be removed from the product stream before it decomposes or undergoes other subsequent reactions. Indeed, oxygenated carbons, such as CO and CO₂, are the very thermodynamically favorable products. In general, the by-products in the ODH of alkanes have no economic interest when compared to the high value of hydrogen that is produced as a co-product in the conventional dehydrogenation process. The selective oxidation of alkanes to corresponding alkenes is a great challenging since the dehydrogenation products always displayed higher reactivity than educts, leading to the further oxidation and low selectivity.^[14] An alternative is to operate at low conversion levels leading to high selectivity, but removal of alkenes from the products stream needs recycling instruments.

Furthermore, it should be mentioned that gaseous oxygen is not the only choice as oxidant in the ODH reactions. It is also possible to use bromine, sulfur, or iodine compounds as dehydrogenation agents. For example, Shell and Petro-Tex developed propane ODH in the presence of iodine with high selectivity.^[2] The research on butane ODH with iodine is also known as the Idas process.^[1] In some cases, the use of nitrogen

oxide is also mentioned.^[1,2] However, the corrosive nature of the products, environmental problems and expensive cost of iodine hindered the commercialization of such processes.

1.3. Metal catalysts for catalytic oxidation of butane to butene and butadiene

The metal catalytic systems mainly applied in the ODH of n-butane are unsupported vanadium or molybdenum oxides catalysts. Numerous papers reported that the V-Mg-O system is particularly noteworthy (see Tab. 1.1).^[15] Nickel molybdate catalysts have also been investigated extensively.^[16–21] Other systems that were reported in the literature include zeolites (containing transition metals), Fe/Zn mixed oxides, Zn and Mn ferrites, supported vanadium oxide, vanadates (especially magnesium vanadate), molybdates, and nickel-based oxides.^[22–25] Supported catalytic systems were also applied in the catalytic oxidation, with either silica or alumina as supports, usually containing Ni, V, or both metals (see Tab. 1.1). Although the inactive nature of the supported materials was reported, the interaction between the active phase and support strongly influences the catalytic activity, which was attributed to the change in the size distribution, phase and acid-base character.^[26–28] More recent study is the use of membrane reactors (with an inert ceramic membrane for controlled oxygen distribution to the bed containing V-Mg-O catalysts) for catalytic oxidation of butane, displaying more efficient performance than the traditional fixed bed reactors (FBRs).^[29, 30]

Tab. 1.1 Some catalytic systems used for the catalytic oxidation of n-butane

Catalyst Composition	Temperature (K)	Con. (%)	Selec (%)	Reference
V-Mg-O	773	6.8	31.8	16
Ni-Mo-O	698	5.4	11.6	17-21
Ni-Mo-P-O	810	38.8	72.2	31
Mg-Ni-Sn-O	810	57.4	11.4	32
Mg-Ni-SO ₄	810	17.5	58.0	32
M ⁴⁺ -P-O	810	42.3	60.5	37, 42
Ni-Sn-P-K-O	839	37	71.9	34
V/SiO ₂	793	22	35	35, 36
V/Al ₂ O ₃	808	16.1	45.2	37
Metal vanadate catalysts	813	50.9	31.5	38

1.3.1. Reaction process

n-Butane is more reactive with gaseous oxygen than other alkanes with fewer carbon atoms at lower reaction temperature. Besides the corresponding alkenes (1-butene, 2-butene and butadiene) formed from the dehydrogenation reaction, other products would also be produced, like CO/CO₂ from the total oxidation, iso-butene from the isomerization and oxygen-containing organic products (acids, ketones or aldehydes). The possible reaction functions are listed below: ^[39]



All the reactions involved are exothermic or even strongly exothermic. However, the high selectivity is primarily considered from the economic point of view. How to increase the yield of desired products is a hard task, attributing to the absence of empty orbitals and low polarity of C-H bonds in alkanes. The method to increase the reactivity of reactant would decrease the selectivity to the desired products because the reactivity of desired products is increased too and it is a major pathway that the degradation products are formed from the desired products in the reaction of butane.^[39] Actually the C-H bond in the alkanes (390.8 kJ/mol butane) is stronger than that in alkenes (345.2 kJ/mol).^[40] What determines the upper limitation to selectivity has been studied recently. It was observed that, at fixed conversion, the selectivity to desired products was related with the function:

$$D^{\circ}H_{\text{C-H (reactant)}} - D^{\circ}H_{\text{C-H (products)}}$$

where $D^{\circ}H$ is the dissociation enthalpy of the weaker C-H (or C-C) bond in the reactant or in the selective oxidation product.^[41] Current experimental data revealed that that if the difference is smaller than 30 kJ/mol, high selectivities are achievable at any conversion levels, whereas for difference larger than 70 kJ/mol low selectivities are always obtained.^[15] The situation for catalytic oxidation of butane is intermediate, which is shown in Fig. 1.1. For the catalytic oxidation of butane over MgO supported V_2O_5 catalysts, the higher selectivity of 66% to 69% was obtained associated with the lower conversion of butane of 20%. When butane conversion increased to about 65% by using different loading, the significant decrease in alkenes selectivity from 68% to 32% was observed.^[37] As reported in literature, the superior catalytic performance of MgO

supported Vanadium oxide was always achieved with about 90% selectivity with respect to the 9% butane conversion.^[16, 43] It suggests that the catalytic performance with both high conversion and high selectivity for the ODH of butane could not be achieved from the thermodynamical point of view.

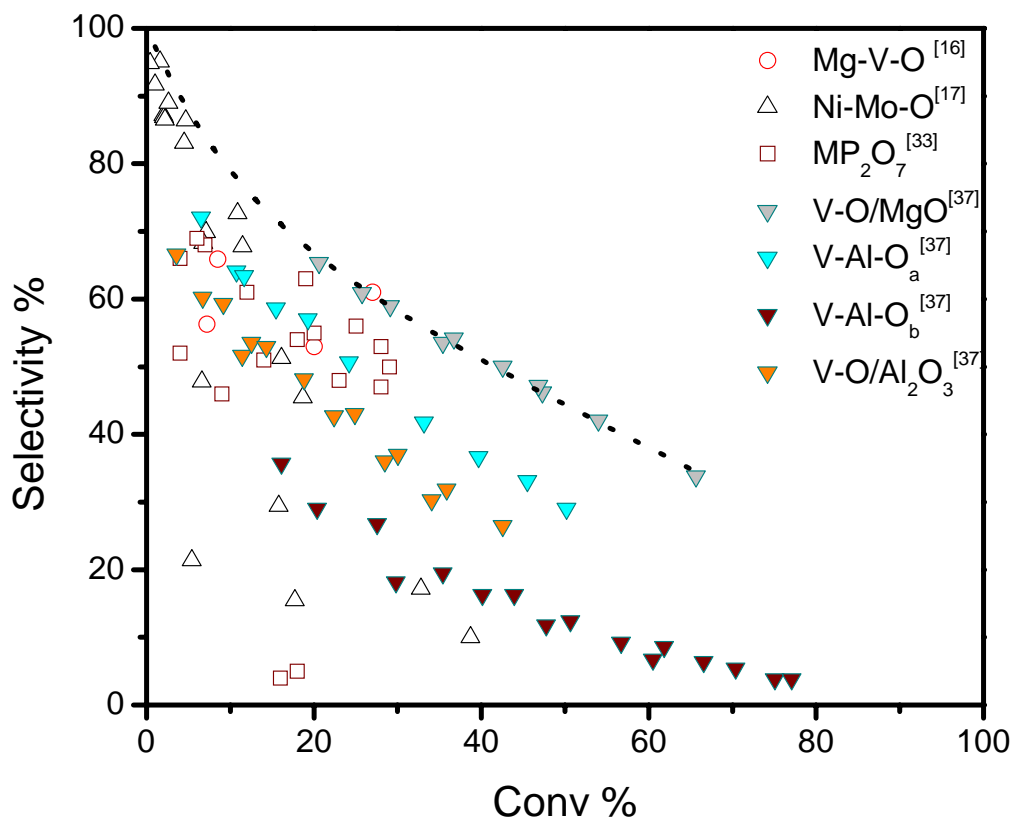


Fig. 1.1 Selectivity-conversion plot for n-butane ODH

The possible reaction pathway of catalytic oxidation was displayed in Fig. 1.2, occurring via parallel and sequential oxidation steps. Butenes are primary products and carbon oxides (CO_x) form as byproducts via butane oxidation and corresponding alkenes oxidation.^[2]

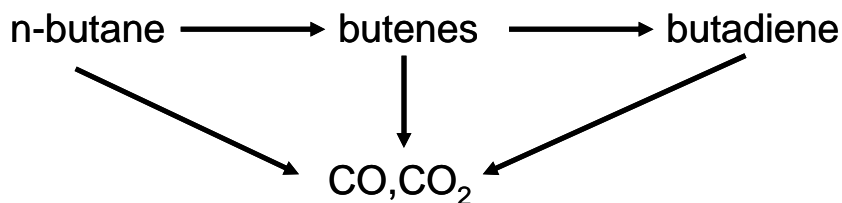


Fig. 1.2 Possible reaction network for catalytic oxidation of n-butane

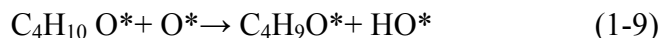
1.3.2. Factors affecting activity and selectivity

The heterogeneously catalyzed ODH of butane involves complicated kinetics, corresponding to the surface adsorption, activation and desorption process. In order to describe the kinetic dependence of alkenes formation rate on H_2O , O_2 and butane for metal catalysts, a set of elemental steps used in literature is described below.^[2]

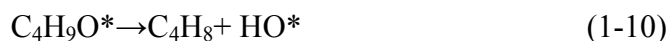
1. Non-dissociative adsorption of butane by interaction on active oxygen (O^*)



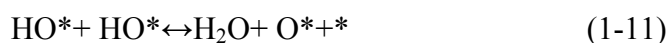
2. C-H bond activation by abstraction of H atom from adsorbed butane using neighboring active O^* atom



3. Formation of butene by cleavage of C-H bond and consecutive desorption



4. Recombination of OH groups to form water



5. Regeneration of active oxygen via dissociative chemisorption of O_2



Although the significant difference was observed between the chemical nature of metal catalysts and metal free catalysts, the research on the kinetics and chemical

properties of metal oxides still developed the systematic investigation methods for surface science and catalysis. The study on the oxygen species on the surface of metal oxides suggests the importance of chemical nature of oxygen species for C-H cleavage, which is considered as the rate-determining step for the formation of alkenes. The abundance of oxygen functionalities on surface of carbon materials will dominate the chemical nature of the surface of carbon materials and thus play an important effect on the activity and selectivity of carbon catalysts for catalytic oxidation reaction.

1.3.2.1. Surface Basicity

The alkenes molecules with C=C double bonds displayed higher electron density (nucleophilicity) than alkanes, corresponding to higher basicity. Although it is difficult to evaluate the basicity of light hydrocarbons in liquid phase due to the chemical stability of light hydrocarbons. The alternating gas phase basicity and proton affinity could be measured by using ionization threshold measurement, bracketing measurement or thermokinetic methods associated with quantum chemical calculation.^[44-45] The proton affinity of butene is 820 kJ/mol, which is higher than that of butane (648.5kJ/mol), with respect to the higher basicity.^[44-46] The difference of proton affinity between butene and butane is about 1.7eV, consistent with a by 1.5eV higher proton affinity of olefins in comparison with corresponding paraffins.^[47]

Furthermore, the consecutive reactions, the dehydrogenation of mono-olefins to diolefins (Fig. 1.2), are catalyzed on the same active sites as the dehydrogenation of paraffins to mono-olefins. It means, for catalysts used in the ODH (V_2O_5) or DH (Cr_2O_3/Al_2O_3) of butane, the preferable dehydrogenation of butenes could occur on the

surface of catalysts, resulting in the decrease in the selectivity for target products. It also suggests that the decreasing in acidity of catalysts should favor the selectivity of target products.

Therefore, the surface acidity/basicity has important influence on the catalytic activity, which has been discussed in literatures. An increase in the basicity improves the desorption of alkenes, resulting in a decrease in deeper oxidation.^[12, 48-52] When the basicity of catalyst is increased, the adsorption of hydrocarbons at active sites could be weakened, resulting in lower reactivity and high selectivity. For example, the alkali earth metal promotion in vanadium catalysts decreases the formation of oxygenate products (like maleic acid) in the reaction effluent, which is frequently found in un-promoted catalysts.^[37, 43] The high activity and low selectivity in n-butane ODH at low surface coverage can be explained by the high Bronsted acid character of octahedral V(V) species.^[48, 49] Therefore, the relationship between the desired products and catalyst basicity is shown schematically in Fig. 1.3.

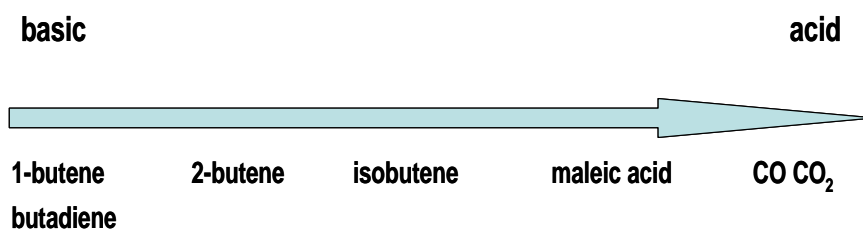


Fig. 1.3 Schematic illustration for the influence of acidity/basicity on products

Hence, the same evaluation method could be performed for metal-free catalysts by measuring their acidity/basicity. It is possible to relate the acidity/basicity with the thermal stability of oxygen functional groups on the surface of carbon by using the TPD method. The influence of basicity of oxygenated surface groups on catalytic performance

of carbon material could be tested by gradually removing the oxygen functional groups with low thermal stability from the surface of catalysts. This could point to identify that what kind of oxygen species could be the real active sites in the ODH reaction. The pioneering work suggested that quinone groups decomposed at 873 K or more could be active sites for ODH of butane.^[45]

1.3.2.2. Oxygenated surface groups

Although the pathway of oxygen adsorption and dissociation is not yet defined, the details of knowledge achieved from kinetic experiments on the metal catalysts could give some suggests about the reaction mechanism over the metal free catalysts. The kinetic investigation on Mg/Al supported vanadium catalysts was reported in literature, proposing the Langmuir-Hinshelwood adsorption model for the ODH of butane to corresponding alkenes.^[51] Under the kinetic conditions (low contact time, low conversion), it was assumed that butenes and butadiene were primary products and combustion of hydrocarbon products could be neglected (Fig. 1.4). Therefore, the reduced reaction scheme was proposed, corresponding to the dehydrogenation of butane to alkenes and combustion of butane to carbon oxides.

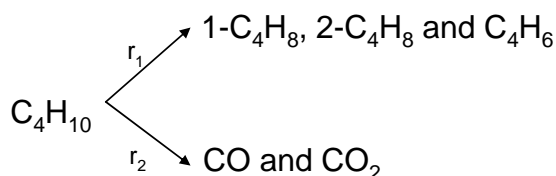


Fig. 1.4 Schematic illustration of catalytic oxidation of butane^[51]

In this work, it assumed that the controlling step was the reaction between two adsorbed reactants. Therefore, the competitive adsorption (CAM) and non-competitive

adsorption (NCAM) of butane and oxygen molecules, as well as dissociative adsorption (CAM/NCAM, $n=1/2$) and non-dissociative adsorption (CAM/NCAM, $n=1$) of oxygen were discussed. The reaction rates of CAM and NCAM were list below:

$$\text{CAM} \quad r_i = \frac{k_i K_{C_4} K_{O_2}^n P_{C_4} P_{O_2}^n}{(1 + K_{C_4} P_{C_4} + K_{O_2}^n P_{O_2}^n)^2} \quad (1-13)$$

$$\text{NCAM} \quad r_i = \frac{k_i K_{C_4} K_{O_2}^n P_{C_4} P_{O_2}^n}{(1 + K_{C_4} P_{C_4})(1 + K_{O_2}^n P_{O_2}^n)} \quad (1-14)$$

Where k_i is rate coefficient, K_i is equilibrium constant and P_i is partial pressure of educt i

Linear correlation and non-linear correlation were used to fit the experimental data to the kinetic models. Based on the calculation of linear correlation, it appeared that the non-competitive adsorption (NCAM) and non-dissociative adsorption models were more convincing than other models. However, from a non-linear correlation, it suggested that the better correlation was obtained with model NCAM-1/2 for the oxidative dehydrogenation of butane, and with model NCAM-1 for the combustion of butane to carbon oxides.

The further investigation was performed and the final reaction mechanism was proposed: 1) the non-competitive adsorption model was a convincing reaction mechanism, meaning there were two kinds of active site for adsorption of butane and oxygen, respectively; 2) the dissociated and non-dissociated oxygen were both involved in the selective oxidation and deep oxidation, while the non-dissociated oxygen might have more contribution to the formation of CO_x.

This study is significantly helpful to consider the reaction mechanism in the ODH using carbon materials as catalysts. The adsorption of oxygen on the surface of carbon

materials has been studied till 1980s due to its significant importance from the industrial point of view.^[52-56] The study on the role of molecular oxygen on the surface of graphitic carbon pointed out that, oxygen molecule was adsorbed on the surface of π -electron-rich active site (generally it is big aromatic ring) and activated, forming the O_2^{2-} specie. The short-life O_2^{2-} species could dissociate into the O^- and react with the neighbour π -electron-poor active site (defect with more sp^3 composition), resulting in a carbon-oxygen bond. For activated carbon and CNTs with abundant carbon defects on the surface, the adsorption and activation of oxygen molecules could happen extensively, thereby greatly influencing the surface chemical properties of carbon materials.

Therefore, we can distinguish two kinds of oxygenated species on the surface of carbon material: one is oxygen functional groups and another is weakly adsorbed oxygen species, concerning the strength between oxygen and carbon defects. It suggested that the chemical nature of oxygen species had influence to catalytic activity, attributed to the nucleophilicity or electrophilicity of active sites.

1.4. Carbon catalysts for ODH of butane to butene and butadiene

1.4.1 Feature and surface nature of carbon materials

The extent of application of carbon materials in 1900s was not bigger than that in 1500s, although more detailed knowledge was achieved by modern investigation methods. More efforts were focused on the fabrication and application of activated carbons from an industrial point of view. The discovery of fullerene in 1985 and carbon nanotube in 1991 was the cornerstone of great revolution of carbon chemistry, revealing an availability of rolling and curving of 2D graphene sheet. These materials display a great potential in

many fields of industry because of their unique chemical and physical properties. The microstructures of various carbon forms are displayed in Fig. 1.5.

In the present work, the attention would be focused on the surface chemical properties and functionalization methods of multi-walled CNTs since the nature of oxygenated surface groups is the key factor for the oxidative dehydrogenation reaction. Fullerene and single-walled carbon nanotubes were not used in this work, owing to the thermal stability and commercial feasibility, respectively. In literature, the carbon nanofilaments with cavity microstructure could also be called “nanotube”, even with so-called “herringbone” or “stacked cup” structure. We would not make distinguishment between herring-boned microstructure and parallel microstructure and all the nano carbons with hollow-tubular microstructure would be labelled as CNTs.^[57]

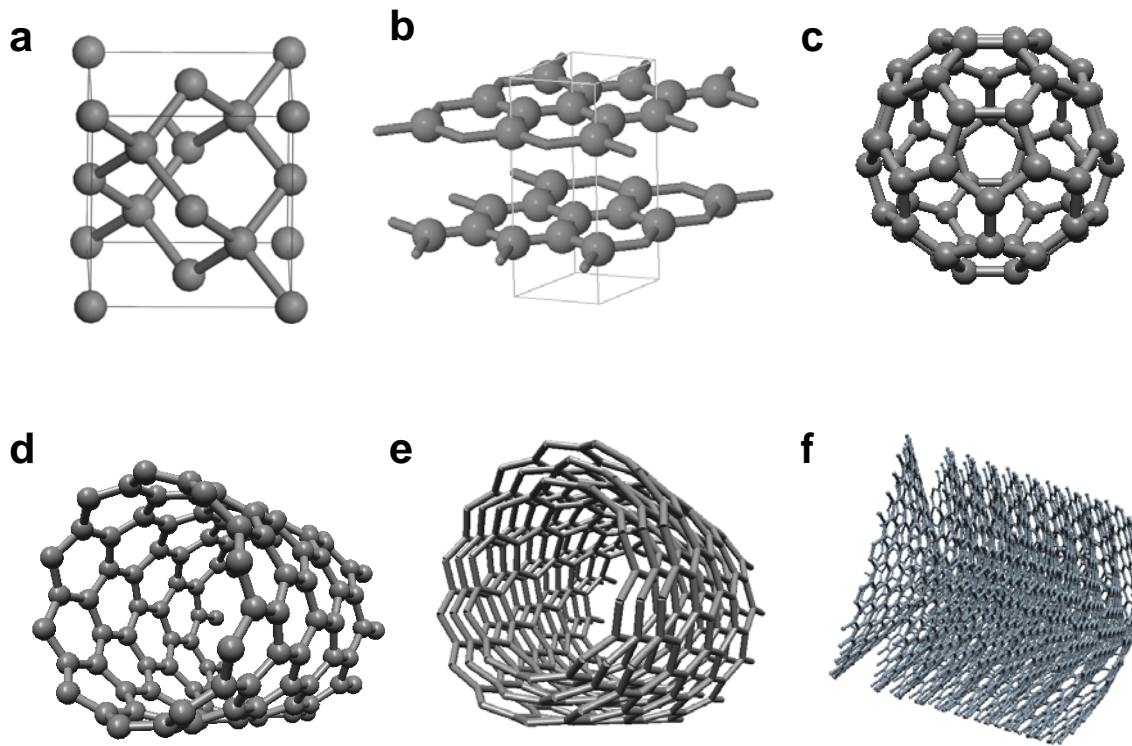


Fig. 1.5 Morphologies of different carbon materials a) diamond, b) graphite, c) fullerene, d) single-walled carbon nanotube, e) multi-walled carbon nanotube, f) herring-boned carbon nanofilament

1.4.2. Carbon materials in catalysis

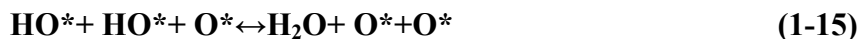
Carbon materials, including CNTs, are mainly used as supports for the active phase in heterogeneous catalysis.^[48] The catalytic application of carbon materials could be backdated to the use of activated carbons in the treatment of waste water and gas. It has been proved those activated carbons display good catalytic performance in the dechlorination and desulfation of the waste gases. Other reactions using activated carbons as catalysts include elimination of hydrogen halogens, oxidation of SO_2 to H_2SO_4 , synthesis of COCl_2 , NO reduction, dehydration and dehydrogenation of 2-propanol and ethanol, oxidative dehydrogenation and dehydrogenation of methanol, propanol and propanal, H_2SO_3 oxidation, oxidative dehydrogenation of cyclohexanol, and isoborneol oxidation, oxidation of phenol, among others.^[58-67] It was assumed that, for carbon supported catalysts, there should be a good correlation between the activity of catalysts and surface area of carbon supports (mostly activated carbons). However, in most cases, the correlation was not found when using activated carbons with different feature for a given catalytic reaction.^[67] It means that a variety of catalytic performance of carbon materials should be related with the chemical nature of surface of carbon catalysts. The investigation on the relationship between the chemical properties of carbon materials and the catalytic activity has been performed in several decades. Generally, two approaches have been widely performed in the surface chemistry of carbon, one is “solid state chemistry” approach and another is “organic surface groups” approach. The former one

focuses on the crystalline microstructure of carbon materials and the latter one focuses on the organic character of the surface groups. In the “solid state chemistry” approach, the defects on the surface of carbon materials are considered as active sites since the edge-side carbon atoms are more chemically reactive. As well the “organic surface groups” approach deals with the nature and the functionality of surface complexes of oxygen and other compounds chemisorbed at the surface defects. Obviously, the combination of both approaches could lead to a deeper insight to the real reaction process taking place on the surface of carbon materials. For instance, the dependence of chemical nature of activated carbon on the raw material and preparation history was always observed, suggesting that the microstructure should be the key factor for the reaction activity. On the other hand, activated carbon annealed in H_2 exhibited no activity for the dehydration and dehydrogenation of alcohols while the oxidation treatment by nitric acid considerably increased the activity of same carbon by two orders of magnitude, suggesting that the catalytic activity should be attributed to the surface functionalities.^[64]

The use of carbon materials as catalysts in the ODH could be traced to 1970s, as it was noted that carbon deposition over the metal catalysts was favorable for the catalytic performance in the ODH of ethylbenzene to styrene.^[68-71] The observation suggested that the active sites were not located on the initial catalyst surface, but on a carbon deposit. Later, activated carbons were used as catalysts in the ODH of ethylbenzene, displaying the remarkable catalytic performance.^[72-78] It was found that the operating temperature (623-673K) in the ODH of ethylbenzene to styrene over carbon materials could be 100 K lower than those with mixed oxide catalysts (723-823K). Figueredo’s work on the thermal treated activated carbons suggested that the catalytic performance could be

related to the amount of oxygenated surface groups, especially the thermal stable functionalities.^[73] The superior catalytic performance of activated carbons than that of graphite could be attributed to its mesoporous microstructure and highly functionalized surface properties. However, it is difficult to develop activated carbons as industrial catalysts since they are not stable during the reaction process. The rapid deactivation observed is attributed to the blockage of micropores by coke.^[76] We have to mention here, activated carbons display a great variety in the chemical nature due to their fabrication processing, hindering the investigation and industrial application. The discovery of fullerene and its family derivatives, carbon nanotubes (CNTs), stimulated an enormous interest in chemical society. The superior stability and ultimate physicochemical properties suggest their promising future in material science. In addition, the sp^3 -like bonds were introduced by curvature of graphene layers and acted as electronic promoter, resulting in the increase in the reactivity. The homogeneous microstructure, highly functionalized surface properties and non-porosity are attractive in the catalysis community since they might be good catalysts instead of activated carbons. The use of carbon nanotubes/nanofilaments in the ODH of ethylbenzene was reported in the literature, displaying a promising catalytic activity and stability.^[79-83] The investigation confirmed that the quinone groups should be active sites for the oxidative dehydrogenation of ethylbenzene to styrene. The possible reaction pathway has been proposed that the cleavage of C-H bonds occurred on the quinone groups and regeneration of quinone groups followed via removal of water. The elementary steps were similar to equation 1-10 to 1-12, wherein quinone groups worked as active sites instead of activated oxygen. But it was proposed that formation of water resulted from

the oxidation of hydroxyl groups by dissociative chemisorption oxygen species (eq 1-15).^[82] However, this step has never been tested in previous work.



It is notable that effort was mostly put on the conversion of ethylbenzene, only few works have been done on the conversion of alkanes.^[84-86] One possible reason is that the intermediate product produced in the ODH of ethylbenzene is much more stable than those in the ODH of alkanes, while the radical is stabilized by the delocalized π bonds. The catalytic performance of various carbon catalysts were shown in Tab. 1.2. The catalytic activities of coals were predominantly related with the reaction temperature and the best catalytic performance of about 7% C₄ yield was achieved at 973K. The combustion of catalyst was also observed in the work, suggesting that the stability of carbon catalysts should be carefully considered.^[84] The catalytic activity of CNTs was also tested for the ODH of propane to propene.^[85] It was found that a significant catalytic performance could be also achieved at high temperature, associated with the gasification of catalysts. However, the phosphoric oxide addition could remarkably decrease the reaction temperature with respect to the considerable catalytic performance. Various activated carbons were used for ODH and DH of iso-butane to iso-butene, revealing the correlation between the catalytic activity and amount of oxygenated surface groups.^[86] However, the formation of coke was also found in the used catalysts.

Tab. 1.2 Catalytic performance of carbon catalysts in the ODH of light hydrocarbons

Catalysts	Reactants	Products	Temperature K	Conv. %	Selec. %	Yield %
Coal ^[84]	butane	butene, butadiene	973	~40	~17	7
CNTs ^[85]	propane	propene	773	42	40	17
Activated carbons ^[86]	iso-butane	iso-butene	648	25	60	15

1.4.3. Modification of carbon materials

It was proposed that the catalytic performance of carbon materials was attributed to the nature of the surface of carbon materials, especially the amount of quinone groups.^[67] However, less knowledge was obtained about the surface chemical kinetic process. Chemistry of graphite and graphene derivatives, like CNTs, have been widely developed and various functionalization/modification methods have been reported, providing us with a valuable platform to functionalize the surface of carbon materials in a controlled manner. It was reported in the literature that the increased amount of stable oxygenated surface groups could remarkably favour the catalytic performance. The grafted small organic molecules with different oxygen functional groups could also be used as molecules probes for mechanism investigation. Phosphoric addition was also used since it is a commercial modification method, not only for modification of carbon materials, but for preparation of inorganic catalysts.^[85, 87] The change in catalytic behaviour of carbon materials by using different modification methods could be related

with the change in the chemical nature of surface of catalysts, which would be potentially helpful on investigating the reaction mechanism.

1.4.3.1 Oxidative treatment

The oxidative treatment covers the gaseous oxidative treatment and wet oxidative treatment. The gaseous oxidants include oxygen, ozone and N_2O . Gaseous oxidation is used to remove impurity, open end and create functional groups. It is an efficient but rough functional method applied in the laboratory work. It has been used to modify activated carbon catalysts in the oxidative dehydrogenation of ethylbenzene to styrene. The improvement in the catalytic performance was observed but the catalytic performance decreased as a function of reaction time, meaning the oxygen functional groups generated by gaseous oxygen were instable.^[88] The similar trend was observed when N_2O was used as oxidant in the pre-treatment.^[88] Ozone is a weak but particularly efficient oxidant in ozonolysis reaction, which reacts with $C=C$ double bonds and fabricates two hydroxyl functional groups on the neighbor carbon atoms. The ozonized CNTs were mainly used to fabricate the poly-composite. There is no report about the application of ozone in the catalytic modification of CNTs.^[92]

In wet chemical approach, the primary oxidant is nitric acid due to its strong oxidative ability and convenient post-treatment (no residue after treatment). But it has similar situation like gaseous oxygen since the deactivation of catalytic activity was also observed in literature.^[88] The oxygenated surface groups might be carboxylic acid, anhydride, lactone, phenol, quinone and other aromatic carbonyl. H_2O_2 is also used as a weaker oxidant in the functionalization of CNTs. Compared with the oxidation by nitric

acid, more alkyl hydroxyl/carboxyl functional group could be achieved under the proper conditions due to its weak oxidative ability. The other oxidant, like sulfuric acid, has been reported in literature, but the existence of residue could hinder its further application.^[89-93]

1.4.3.2 Grafting modification

The ordinary method for molecules immobilization was applied by using chlorination or fluorination and subsequent substitution of organic molecules (Fig. 1.6).^[94] This method has been widely used in the fabrication of carbon nanotube composite since it was very convenient to graft the moieties on the surface of CNTs with respect to the low efficiency of directive immobilization. The reaction followed such steps: the ends and defects of CNTs were oxidized by HNO₃ or other oxidants, forming hydroxyl functional groups on the surface of CNTs; the consecutively nucleophilic substitution occurred with replacement of hydroxyl by chloride group; the further nucleophilic substitution was performed by using identical moieties, resulting in the immobilization of grafting materials via covalent linkage with CNTs. The immobilized molecular moieties include inorganic molecules such as ammonia, organic molecules, polymers, protein and even DNA/RNA. The prevailing advantages of immobilization have been proposed that it is a useful method to anchor the expected functional groups on the surface of carbon materials. The immobilized carbon materials can be used directly as gas sensor and bio-sensor and also be used as precursor for further modifications to synthesize polymer and composite mechanical materials.^[95-101] Under the proper condition, the direct immobilization is also possible, but the requirement for the activity of immobilized molecules would limit its fabrication.^[102]

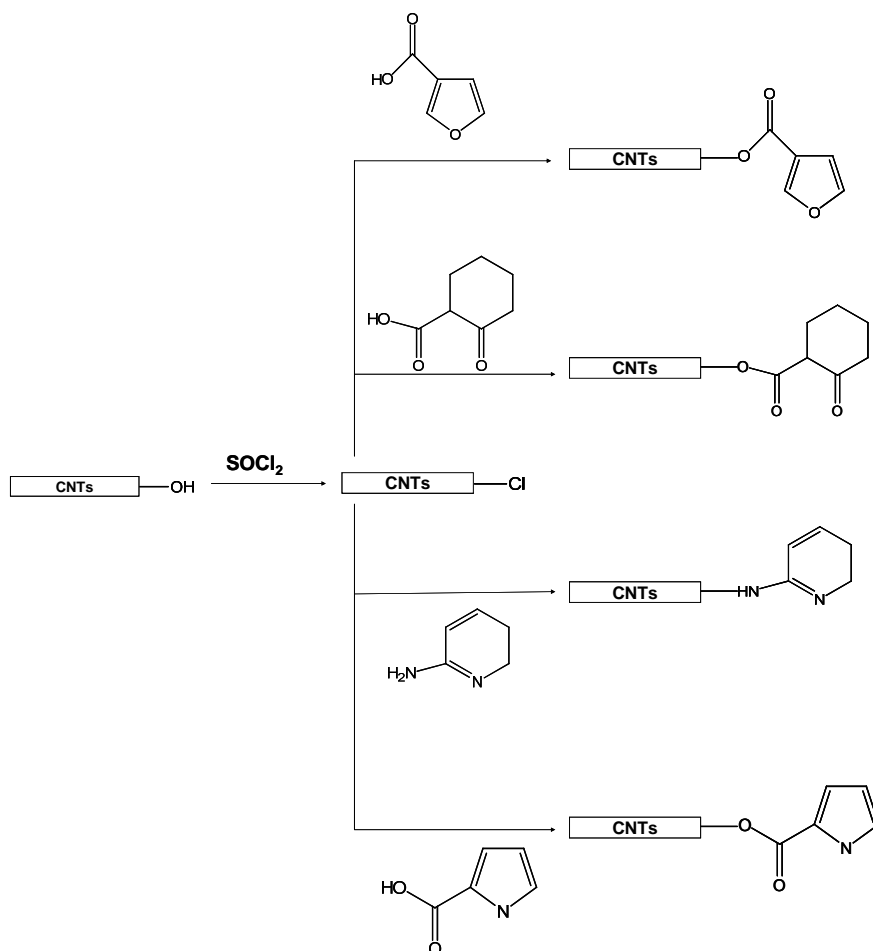


Fig. 1.6 Chlorination and subsequent substitution in the CNTs

In this work, we have applied the chlorination method to immobilize the different small acid or amine molecules on the surface of carbon materials (shown in Fig. 1.5). The as-modified carbon materials with different surface functionalities have been used as catalysts for the catalytic oxidation of butane.

1.4.3.3 Phosphoric acid addition

The phosphoric modified activated carbons were used as catalysts in the ODH of alcohols since the addition of phosphoric compounds could prolong the catalysts life.^[103] Some works suggested that phosphoric modification of activated carbon could improve

the amount of acid sites, resulting in the better absorbance ability for metal ions.^[104-107] The microstructure of phosphorus oxide is quite complicated. It was believed that polyphosphoric acid was formed during the calcination process and polyphosphoric acid was connected with carboxylate group by C-O-P bond, confirmed by IR and XPS measurements.^[108-110] The chemical bonding was thermally stable even at 800°C.

The acidity of polyphosphoric acid was related with the amount of protons on the surface of support using phosphoric acid as precursor, its H_0 value (Hammett acidity) ranging from -5.0 to 5, as well as the H_0 of benzoic acid is only 4.2.^[111-113] The acidity of phosphoric modified materials was always higher than that of non-modified carbon materials. The acidity of modified materials was related with the amount of the relic cations, like proton or ammonium, which was determined by the calcination temperature. The higher calcination temperature favored higher polymerization degree and decreased the amount of cations, resulting in the decrease in the acidity. Thus, it was interesting that, in some cases, the promotion of phosphoric acid was unfavorable to improve the surface acidity, resulting in a decrease in absorbance of metal ions.^[105] The phosphoric modified materials also covered so-called “solid phosphoric acid (SPA)” catalysts by using SiO_2 , TiO_2 or other oxides as supports. They were widely used as strong acid catalysts in organic chemistry, even in the ODH of ethane.^[111-118] Detailed knowledge about relationship between reaction mechanism and catalytic behavior was still insufficient. The catalytic potential of phosphoric oxide in the ODH reaction has never been confirmed by other work.^[116]

In addition, the inhibition effect of phosphoric addition to combustion of carbon-carbon composite has been widely reported.^[119] It proposed that there should be two

approaches for the inhibition of catalytic oxidation of carbon-carbon composites: (a) surface coating (acting as a diffusion barrier), and (b) active sites poisoning. However, the reaction mechanism is still in debate.

1.5. Motivation and aim

The unique physical and chemical nature of CNTs, such as the homogenous microstructure, the enormous availability of functionalization, the superior thermal conductivity and electronic conductivity, the strong mechanical properties, make it a promising future as advanced materials and supports. These significant properties also favor the catalytic behavior of catalysts. However, less effort was focused in the catalytic performance of CNTs. It would be an interesting and valuable attempt to develop the industrial application of CNTs.

In the present work, the catalytic behavior of CNTs for the ODH of C_4 hydrocarbons was studied. Various modification methods would be applied to improve the catalytic performance of carbon materials. The improvement in catalytic activity by using functionalization methods would be related with the alteration of the chemical properties of surface functional groups. A series of joint experimental techniques in catalysis, including thermal programmed desorption coupled with mass spectroscopy, TEM, SEM, XPS and IR, would be used to investigate the change of chemical nature of surface of carbon materials during the modification process and catalysis process. In particular, the role of oxygen and carbon defects in the catalysis reaction would be studied to identify the real active sites for the ODH. Ultimately, the reasonable reaction

model on carbon materials catalysts would be proposed based on the microstructure-activity analysis.

References

1. Bohnet M, et al. Eds. Ullmann's Encyclopedia of Industrial Chemistry, 6th Ed.; Wiley-VCH: Weinheim, Germany, 1999; Electronic Release.
2. Mamedov EA, Corberan VC, Oxidative Dehydrogenation of Lower Alkanes on Vanadium Oxide-Based Catalysts. The Present State of the Art and Outlooks. Appl. Catal. A: Gen. 1995, 127 (1–2), 1–40.
3. Satterfield CN, Heterogeneous Catalysis in Practice; McGraw-Hill: New York, 1980.
4. Hucknall DJ, Selective Oxidation of Hydrocarbons; Academic Press: London, 1974.
5. Matar S, Mirbach MJ, Tayim HA, Catalysis in Petrochemical Processes; Kluwer Academic Publishers: Dordrecht, 1989.
6. Morrow NL, The Industrial Production and Use of 1,3-Butadiene, Environmental Health Perspectives 1990, 86, 7-8
7. Oyama ST, Desikan AN, Hightower JW, Research Challenges in Selective Oxidation. In Catalytic Selective Oxidation; ACS Symposium Series No. 523, Oyama ST, Hightower JW, Eds.; American Chemical Society: Washington, DC, 1993, 1–15.
8. Moro-oka Y, Ueda W, Partial Oxidation and Ammoxidation of Propane: Catalysts and Processes. Catalysis; Specialist Periodical Report; Royal Society of Chemistry: Cambridge, 1994; 11, 223–245.
9. Wittcoff HA, New Technology and Chemical Feedstocks. Chemtech 1990, 20, 48–53.
10. Tianjin Lingang Industrial Area Administration Commission, Investment Instruction for Propylene Oxide /Styrene Monomer Joint Production Project, http://www.Tanggu.gov.cn/zsy/016_4.html 2006.
11. Thomas JM, Thomas WJ, Principles and Practice of Heterogeneous Catalysis; VCH: Weinheim, Germany, 1997.
12. Carra S, Fomi L, Catalytic Dehydrogenation of C4 hydrocarbons Over Chromia-Alumina, Catalysis Reviews 1972, 5, 159-198.
13. Figueiredo JL, Desidrogenac AO, Oxidativa de Hidrocarbonetos. Proceedings of the XVth Ibero-American Symposium on Catalysis, Facultad Regional Cordoba, Universidad Tecnologica Nacional, Cordoba, Argentina, Sept 16–20, 1996, 1996, 1, 29–38.
14. Harding WD, Kung HH, Kozhevnikov VL, Poeppelmeier, K.R. Phase Equilibria and Butane Oxidation Studies of the MgO–V₂O₅–MoO₃ System. J. Catal. 1993, 144 (2), 597–610.

15. Madeira LM, Portela MF, Catalytic Oxidative Dehydrogenation of n-Butane, *Catalysis Reviews* 2002, 44(2), 247-286
16. Kung HH, Oxidative Dehydrogenation of Light (C2 to C4) Alkanes. *Advances in Catalysis* 1994, 40, 1-38.
17. Martin-Aranda RM, Portela MF, Madeira LM, Freire F, Oliveira M, Effect of Alkali Metal Promoters on Nickel Molybdate Catalysts and Its Relevance to the Selective Oxidation of Butane. *Appl. Catal. A: Gen.* 1995, 127 (1-2), 201-217.
18. Maldonado-Hodar FJ, Madeira LM, Portela MF, Martin-Aranda RM, Freire F, Oxidative Dehydrogenation of Butane: Changes in Chemical, Structural and Catalytic Behavior of Cs-Doped Nickel Molybdate. *J. Mol. Catal. A: Chem.* 1996, 111 (3), 313-323.
19. Maldonado-Hodar FJ, Madeira LMP, Portela MF, The Effects of Coke Deposition on NiMoO₄ Used in the Oxidative Dehydrogenation of Butane. *J. Catal.* 1996, 164 (2), 399-410.
20. Madeira LM, Herrmann JM, Freire FG, Portela MF, Maldonado FJ, Electrical Conductivity, Basicity and Catalytic Activity of Cs-Promoted α -NiMoO₄ Catalysts for the Oxidative Dehydrogenation of n-Butane. *Appl. Catal. A: Gen.* 1997, 58 (1-2), 243-256.
21. Madeira LM, Martin-Aranda RM, Maldonado-Hodar FJ, Fierro JLG, Portela MF, Oxidative Dehydrogenation of n-Butane over Alkali and Alkaline Earth-Promoted α -NiMoO₄ Catalysts. *J. Catal.* 1997, 169 (2), 469-479.
22. Armendariz H, Toledo JA, Aguilar-Rios G, Valenzuela MA, Salas P, Cabral A, Jimenez H, Schifter I, Oxidative Dehydrogenation of n-Butane on Zinc-Chromium Ferrite Catalysts. *J. Mol. Catal.* 1994, 92 (3), 325-332.
23. Armendariz H, Aguilar-Rios G, Salas P, Valenzuela MA, Schifter I, Arriola H, Nava N, Oxidative Dehydrogenation of n-Butane on Iron-Zinc Oxide Catalysts. *Appl. Catal. A: Gen.* 1992, 92 (1), 29-38.
24. Toledo JA, Armendariz H, Lopez-Salinas E, Oxidative Dehydrogenation of n-Butane: A Comparative Study of Thermal and Catalytic Reaction using Fe-Zn Mixed Oxides. *Catal. Lett.* 2000, 66 (1-2), 19-24.
25. Cavani F, Trifiro F, Selective Oxidation of C4 Paraffins. *Catalysis; Specialist Periodical Report; Royal Society of Chemistry: Cambridge*, 1994, 11, 246-317.
26. Huff M, Schmidt LD, Production of Olefins by Oxidative Dehydrogenation of Propane and Butane over Monoliths at Short Contact Times. *J. Catal.* 1994, 149 (1), 127-141.
27. Yokoyama C, Bharadwaj SS, Sameer S, Schmidt LD, Catalytic Oxidative Dehydrogenation Process and Catalyst. US Patent 6,072,097, June 6, 2000.
28. Hoang M, Pratt KC, Mathews J, Catalysts for Oxidative Dehydrogenation of Hydrocarbons. US Patent

5,759,946, June 2, 1998.

29. Tellez C, Menendez M, Santamaria J, Oxidative Dehydrogenation of Butane Using Membrane Reactors. *AIChE J.* 1997, 43 (3), 777–784.

30. Tellez C, Menendez M, Santamaria J, Simulation of an Inert Membrane Reactor for the Oxidative Dehydrogenation of Butane. *Chem. Eng. Sci.* 1999, 54 (13), 2917–2925.

31. Bertus BJ, Catalyst and Process for Oxidative Dehydrogenation. US Patent 4,094,819, June 13, 1978.

32. Bertus BJ, US Patents 3,886,090; 3,886,091, 1975.

33. Marcua IC, Sandulescu I, Millet MJM, Oxidehydrogenation of *n*-Butane over Tetravalent Metal Phosphates Based Catalysts, *Applied Catalysis A: General* 2002, 227, 309–320

34. Kimble JB, Oxidative Dehydrogenation of Paraffins. US Patent 4,751,342, June 14, 1988.

356. Owens L, Kung HH, Effect of Cesium Modification of Silica-Supported Vanadium-Oxide Catalysts in Butane Oxidation. *J. Catal.* 1994, 148 (2), 587–594.

36. Owens L, Kung HH, The Effect of Loading of Vanadia on Silica in the Oxidation of Butane. *J. Catal.* 1993, 144 (1), 202–213.

37. Nieto JML, Concepcion P, Dejoz A, Knozinger H, Melo F, Vasquez MI, Selective Oxidation of *n*-Butane and Butenes over Vanadium-Containing Catalysts, *Journal of Catalysis* 2000, 189, 147–157

38. Kung HH, Chaar MA, Oxidative Dehydrogenation of Alkanes to Unsaturated Hydrocarbons, US Patent 4,777,319, October 11, 1988.

39. Perry RH, Green DW, (Eds.) *Perry's Chemical Engineers' Handbook*; McGraw-Hill: New York, 1984.

40. Kung MC, Kung HH, Oxidative Dehydrogenation of Cyclohexane over Vanadate Catalysts. *J. Catal.* 1991, 128 (1), 287–291.

41. Batiot C, Hodnett BK, The Role of Reactant and Product Bond Energies in Determining Limitations to Selective Catalytic oxidations. *Appl. Catal. A: Gen.* 1996, 137 (1), 179–191.

42. Marcua IC, Sandulescu I, Millet JMM, Oxidehydrogenation of *n*-Butane over Tetravalent metal Phosphates Based Catalysts, *Applied Catalysis A: General* 2002, 227, 309–320

43. Chaar MA, Patel D, Kung MC, Kung HH, Selective Oxidative Dehydrogenation of Butane over VMgO Catalysts. *J. Catal.* 1987, 105 (2), 483–498; Selective Oxidative Dehydrogenation of Propane over VMgO Catalysts. *J. Catal.* 1988, 109 (2), 463–467.

44. Lias S, Liebman JL, Levin RD, Evaluated Gas Phase Basicities and Proton Affinities of Molecules: Heat of Formation of Protonated Molecules, *J. Phys. Chem Refe. Data* 1984, 13, 3, 695-808

45. Hunter EPL, Lias S, Evaluated Gas Phase Basicity and Proton Affinities of Molecules: An Update, *J. Phys. Chem Refe. Data* 1998, 27, 3, 413-655

46. Esteves PM, Alberto GGP, Ramirez-Solis A, Mota CJA, The n-Butonium Cation ($n\text{-C}_4\text{H}_{11}^+$): the Potential Energy Surface of Protonated n-Butane, *J. Phys. Chem. A* 2000, 104, 6233-6240
47. Kazansky VB, Senchenya IN, Frash M, A Quantum-chemical Study of Adsorbed Nonclassical Carbonium Ions as Active Intermediates in Catalytic Transformations of Paraffins. I. Protolytic Cracking of Ethane on High Silica Zeolites, *Catalysis Letters* 1994, 27, 345-354
48. Albonetti S, Cavani F, Trifiro, F. Key Aspects of Catalyst Design for the Selective Oxidation of Paraffins. *Catal. Rev.—Sci. Eng.* 1996, 38 (4), 413–438.
49. Blasco T, Galli A, Nieto J.ML, Trifiro F, Oxidative Dehydrogenation of Ethane and n-Butane on $\text{VOx}/\text{Al}_2\text{O}_3$ Catalysts. *J. Catal.* 1997, 169 (1), 203–211.
50. Pereira MFR, Orfao JJM, Figueiredo JL, Oxidative Dehydrogenation of Ethylbenzene on Activated Carbon Catalysts 1. Influence of Surface Chemical Groups. *Applied Catalysis A: General* 1999, 184, 153-160.
51. Dejoz A, Nieto JML, Melo F, Vazquez I, Kinetic Study of the Oxidation of n- Butane on Vanadium Oxide Supported on Al/Mg Mixed Oxide. *Ind. Eng. Chem. Res.* 1997, 36, 2588-2596.
52. Atamny F, Blöcker J, Dübotzky A, Kurt H, Timpe O, Loose G, Mahdi W, Schlögl R, Surface Chemistry of Carbon: Activation of Molecular Oxygen, *Molecular Physics* 1992, 76, 4, 851-886
53. Chen S, Yang'A R, New Surface Oxygen Complex on Carbon: Toward a Unified Mechanism for Carbon Gasification Reactions, *Ind. Eng. Chem. Res.* 1993,32, 2835-2840
54. Zhu X, Lee S, Lee Y, Frauenheim T, Adsorption and Desorption of an O_2 Molecule on Carbon Nanotubes, *Physical Reviews Lett.* 2000, 85, 13, 2757-2760
55. Li C, Brown T, Carbon Oxidation Kinetics from Evolved Carbon Oxide Analysis during Temperature-programmed Oxidation, *Carbon* 2001, 39, 725-732
56. Xu Y, Li J, The Interaction of Molecular Oxygen with Active Sites of Graphite: A Theoretical Study, *Chemical Physics Letters* 2004, 400, 406–412
57. Martin-Gullon I, Vera J Conesa JA, González JL, MerinoC, Differences between Carbon Nanofibers Produced Using Fe and Ni Catalysts in a Floating Catalyst Reactor, *Carbon* 2006, 44(8), 1575-1580
58. Serp P, Corrias M, Kalck P, Carbon Nanotubes and Nanofibers in Catalysis, *Applied Catalysis A: General* 2003, 253, 337–358
59. Yang J, Mestl G., Herein D, Schlögl R, Find J, Reaction of NO with Carbonaceous Materials - 1. Reaction and Adsorption of NO on Ashless Carbon Black, *Carbon* 2000, 38, 715-727.
60. Szymanski G, Rychlicki G, Catalytic Conversion of Propan-2-ol on Carbon Catalysts, *Carbon* 1993, 31, 247-257.

61. Szymanski G, Rychlicki G, Terzyk AP, Catalytic Conversion of Ethanol on Carbon Catalysts, *Carbon* 1994, 32, 265-271.
62. Grunewald GC, Drago RS, Carbon Molecular Sieves as Catalysts and Catalysts Supports, *J. Am. Chem. Soc.* 1991, 113, 1636-1639.
63. Stöhr B, Boehm HP, Schlögl R. Enhancement of the Catalytic Activity of Activated Carbons in Oxidation Reactions by Thermal Treatment with Ammonia or Hydrogen Cyanide and Observation of a Superoxide Species as a Possible Intermediate, *Carbon* 1991, 36, 707-720.
64. Szymanski GS, Rychlicki G, Importance of Oxygen Surface Groups in Catalytic Dehydration and Dehydrogenation of Butan-2-ol Promoted by Carbon Catalysts, *Carbon* 1991, 29, 4-5, 489-498
65. Silva IF, Vital J, Ramos AM, Valente H, Botelho do Rego AM, Reis MJ, Oxydehydrogenation of Cyclohexanol over Carbon Catalysts, *Carbon* 1998, 36, 1159-1165.
66. Yang SX, Zhu WP, Li X, Wang JB, Zhou YR, Multi-walled Carbon Nanotubes (MWNTs) as an Efficient Catalyst for Catalytic Wet Air Oxidation of Phenol, *Catalysis Comm.* 2007, 8, 2059-2063
67. Rodriguez-Reinoso F, The Role of Carbon Materials in Heterogeneous Catalysis, *Carbon* 1998, 36, 3, 159-175
68. Zhyznepvskiy V, Tsybukh R, Gumenetskiy V, Physico-chemical and Catalytic Properties of Fe-Bi-Mo-O-x Catalysts in the Oxidative Dehydrogenation of Ethylbenzene. *React. Kinet. Catal. Lett.* 2000, 71(2), 209-215.
69. Cracium R, Dulamita N, Ethylbenzene Oxidative Dehydrogenation on MnOx/SiO₂ Catalysts. *Ind. Eng. Chem. Res.* 1999, 38, 1357-1363.
70. Ogranowski W, Hanuza J, Kepinski L, Catalytic Properties of Mg-3(VO₄)(2)-MgO System in Oxidative Dehydrogenation of Ethylbenzene. *Appl. Catal. A: General* 1998, 171(1), 145-154.
71. Ogranowski W, Hanuza J, Drulis H, Mista W, Macalik L, Promotional Effect of Molybdenum, Chromium and Cobalt on a V-Mg-O Catalyst in Oxidative Dehydrogenation of Ethylbenzene to Styrene. *Appl. Catal. A: General* 1996, 136(1), 143.
72. Alkhozov TG, Lisovskii AE, Ismailov YA, Kozharov AI, Oxidative Dehydrogenation of Ethylbenzene on Activated Carbons. I. General Characteristics of the Process, *Kinet, Catal.* 1978, 19(3), 611-614.
73. Pereira MFR, Orfao JJM, Figueiredo JL, Oxidative Dehydrogenation of Ethylbenzene on Activated Carbon Catalysts. I. Influence of Surface Chemical Groups. *Appl. Catal. A: General* 1999, 184, 153-160.
74. Pereira M.F.R., Orfao J.J.M., Figueiredo J.L. Oxidative Dehydrogenation of Ethylbenzene on Activated Carbon Catalysts 2. Kinetic Modelling. *Appl. Catal. A: General* 2000, 196, 43-54.

75. Macia-Agullo JA, Cazorla-Amoros D, Linares-Solano A, Wild U, Su DS, Schlögl R. Oxygen Functional Groups Involved in the Styrene Production Reaction Detected by Quasi In-situ XPS. *Catal. Today* 2005, 102, 248-253.
76. Pereira MFR, Orfao JJM, Figueiredo JL. Oxidative Dehydrogenation of Ethylbenzene on Activated Carbon Catalysts 3. Catalyst Deactivation, *Applied Catalysis A: General* 2001, 218, 307-318.
77. Guerrero-Ruiz A, Rodriguez-Ramos I, Oxydehydrogenation of Ethylbenzene to Styrene Catalyzed by Graphites and Activated Carbons, *Carbon* 1994, 32, 23-29.
78. Boehm HP, Mair G., Stoehr T. Rincón A.R., Tereczki B. Carbon as a Catalysts in Oxidation Reactions and Hydrogen Halide Elimination Reactions, *Fuel* 1984, 63, 1061-1063.
79. De Jong KP, Geus JW, Carbon nanofibers: Catalytic Synthesis and Applications, *Catal. Reviews-Sci. and Eng.* 2000, 42 (4): 481-510.
80. Mestl G, Maksimova NI, Keller N, Roddatis VV, Schlögl R, Carbon Nanofilaments in Heterogeneous Catalysis: An Industrial Application for New Carbon Materials? *Angew. Chem. Inter. Edit.* 40 2001, (11), 2066-2068
81. Pereira MFR, Figueiredo JL, Orfao JJM, Serp P, Kalck P, Kihn Y, Catalytic Activity of Carbon Nanotubes in the Oxidative Dehydrogenation of Ethylbenzene, *Carbon* 2004, 42 (14), 2807-2813.
82. Su DS, Maksimova N, Delgado JJ, Keller N, Mestl G, Ledoux MJ, Schlögl R, Nanocarbons in Selective Oxidative Dehydrogenation Reaction, *Catalysis Today* 2005, 102, 110-114.
83. Delgado JJ, Vieira R, Rebmann G, Su DS, Keller N, Ledoux MJ, Schlögl R, Supported Carbon Nanofibers for the Fixed-bed Synthesis of Styrene, *Carbon* 2006, 44 (4), 809-812.
84. Maldonado-Hodar FJ, Madeira LM, Portela MF, The Use of Coals as Catalysts for the Oxidative Dehydrogenation of n-Butane. *Applied Catalysis A: General* 1999; 178: 49-60.
85. ZJ. Sui, JH. Zhou, Dai YC, Yuan WK, Oxidative Dehydrogenation of Propane over Catalysts Based on Carbon Nanofibers. *Catal. Today* 2005; 106: 90-94.
86. Velasquez JDD, Suarez LAC, Figueiredo JL, Oxidative Dehydrogenation of Isobutane over Activated Carbon Catalysts, *Applied Catal. A general* 2006, 311, 51-57
87. Krawietz TR, Lin P, Lotterhos KE, Torres PD, Barich DH, Clearfield A, Haw JF, Solid Phosphoric Acid Catalyst: A Multinuclear NMR and Theoretical Study, *J. Am. Chem. Soc.* 1998, 120, 8502-8511
88. Pereira MFR, Orfao JJM, Figueiredo JL. Oxidative Dehydrogenation of Ethylbenzene on Activated Carbon Catalysts 1. Influence of Surface Chemical Groups. *Applied Catalysis A: General* 1999, 184, 153-160.

89. Sham ML, Kim JK, Surface Functionalities of Multi-wall Carbon Nanotubes after UV/Ozone and TETA Treatments, *Carbon* 2006, 44(4), 768-777.
90. Olstowski F, Watson JD, Acid Catalysts of Reaction, US patent, 1971, 3584061
91. Suslick KS, The Chemical Effects of Ultrasound. *Sci. Am.* 1989, 260, 80-86.
92. Niyogi S, Hamon MA, Hu H., ZHAO B, Bhowmik P, Sen R, Itkis ME, Haddon RC, Chemistry of Single-Walled Carbon Nanotubes. *Acc. Chem. Res.* 2002, 35, 1105-1113
93. Sui ZJ, Zhao TJ, Zhou JH, Li P, Dai YC, Microstructure of Carbon Nanofibers and Their Catalytic Performance for Oxidative Dehydrogenation of Propane. *Chinese Journal of Catalysis* 2005, 26(6), 521-526
94. Ellison MD, Crotty MJ Koh, D, Spray RL, Tate KE, Adsorption of NH₃ and NO₂ on Single-Walled Carbon Nanotubes. *J. Phys. Chem. B* 2004, 108, 7938-7943.
95. Niyogi S, Hamon MA, Hu H, Zhao B, Bhowmik P, Sen R, Chemistry of Singlewalled Carbon Nanotubes, *Acc. Chem. Res.* 2002, 35, 1105–1113.
96. Valentini L, Bavastrello V, Stura E, Armentano I, Nicolini C, Kenny JM, Sensors for Inorganic Vapor Detection Based on Carbon Nanotubes and Poly(o-anisidine) Nanocomposite Material, *Chemical Physics Letters* 2004, 383, 617–622
97. Cai H, Cao X, Jiang Y, He P, Fang Y, Carbon Nanotube-enhanced Electrochemical DNA Biosensor for DNA Hybridization Detection, *Anal Bioanal Chem* 2003, 375, 287–293
98. Valentina L, Armentano I, Kenny JM, Bidalib S, Marianib A, Interaction of Oxygen with Nanocomposites Made of n-Type Conducting Polymers and Carbon Nanotubes: Role of Charge Transfer Complex Formation between Nanotubes and Poly(3-octylthiophene), *Thin Solid Films* 476 2005, 162– 167
99. Velasco-Santosi C, Martinez-Hernandez AL, Castanoi VM, Carbon Nanotube-polymer Nnocomposites: the Role of Interfaces, *Composite Interfaces* 2005, 11, 8-9, 567–586
100. Staii1 C, Johnson AT, DNA-decorated Carbon Nanotubes for Chemical Sensing, *Nano Lett.* 2005, 5 (9), 1774-1778.
101. Ma X, Zhang X, Yu L, Li G, Wang M, Chen H, Mi Y, Preparation of Nano-Structured Polyaniline Composite Film via “Carbon Nanotubes Seeding” Approach and its Gas-Response Studies, *Macromol. Mater. Eng.* 2006, 291, 75–82
102. Bianco A, Kostarelos K, Partidos CD, Prato M, Biomedical Applications of Functionalised Carbon Nanotubes. *Chem. Comm* 2005, 5, 571-577
103. Zhu ZP, Su DS, Weinberg G, Jentoft RE, Schloel R, Wet-Chemical Assembly of Carbon Tube-in-Tube Nanostructures. *Small* 2005, 1(1), 117-120.
104. Stanley MH, Catalytic dehydrogenation of alcohols, US patent, 2220430, 1940

105. Toles CA, Marshall WE, Johns MM, Phosphoric Acid Activation of Nutshells for Metals and Organic Remediation: Process Optimization. *J. Chem Technol Biotechnol* 1998, 72, 255-263.
106. Toles CA, Marshall WE, Johns MM, Surface Functional Groups on Acid-activated Nutshell Carbons. *Carbon* 1999, 37, 1207-1214.
107. Dastgheib SA, Rockstraw DA, Pecan Shell Activated Carbon: Synthesis, Characterization, and Application for the Removal of Copper from Aqueous Solution, *Carbon* 2001, 39 (12), 1849-1855.
108. Figueiredo JL, Pereira MFR, Freitas MMA,, Orfao JJM, Modification of the surface chemistry of activated carbons, *Carbon* 1999, 37, 1379-1389.
109. Puziy AM, Poddubnaya OI, Martinez-Alonzo A, Suarez-Garcia F, Tascon JMD, Synthetic Carbon Activated with Phosphoric Acid I. Surface Chemistry and Ion Bonding Properties, *Carbon* 2002, 40, 1493-1505.
110. Puziy AM, Poddubnaya OI, Martinez-Alonzo A, Suarez-Garcia F, Tascon JMD, Synthetic Carbon Activated with Phosphoric Acid II. Porous Structure, *Carbon* 2002, 40, 1507-1519.
111. Puziy AM, Poddubnaya OI, Martinez-Alonzo A, Suarez-Garcia F, Tascon JMD, Synthetic Carbon Activated with Phosphoric Acid III. Carbon Prepared in Air, *Carbon* 2003, 41, 1181-1191.
112. Popp FD, McEwven WE, Polyphosphoric Acid as Reagent in Organic Chemistry II, *Transactions Kansas Academy of Science*, 1960 63, 3, 169-193
113. Fougret CM, Atkins MP, Holderich WF, Influence of the Carrier on the Catalytic Performance of Impregnated Phosphoric Acid in the Hydration of Ethylene, *Applied Catalysis A: General* 1999, 181, 145-156
114. Stine LO, Abrevaya H, Frame RR, Process for Oligomer Production and Saturation, US Patent 6689927, 2004
115. Zhu ZR, Xie ZK, Chen YF, Wang RF, Yao YP, Free Phosphoric Acid of Diatomite-Phosphoric Acid and Its Catalytic Performance for Propylene Oligomerization, *Reat. Kinet. Catal. Lett.* 2000, 70, 2, 379-388
116. Fougreta CM, Atkinsb MP, Hoeldericha WF, Influence of the Carrier on the Catalytic Performance of Impregnated Phosphoric Acid in the Hydration of Ethylene, *Applied Catalysis A: General* 1999, 181, 145-156
117. Maiti A, Govind N, Kung P, King-Smith D, Effect of Surface Phosphorus on the Oxidative Dehydrogenation of Ethane: A First-Principles Investigation, *Journal of Chemical Physics* 2002, 117, 17, 8080-8088
118. Klerk AD, Nel JJR, Schwarzer R, Oxygenate Conversion over Solid Phosphoric Acid, *Ind. Eng. Chem. Res.* 2007, 46, 2377-2382

119. Wu X, Radovic LR, Inhibition of Catalytic Oxidation of Carbon/carbon Composites by Phosphorus, Carbon 44 (2006) 141–151

Chapter 2 Experiment and characterization Methods

2.1. Set-up for the catalytic reaction tests

The catalytic tests were carried out in the set-up, shown schematically in Figure 2.1. The fix-bed reactor allowed one to perform catalytic tests with full control of all reaction parameters, and to conduct the process in the presence of He, O₂, hydrocarbons or mixtures of these gases. He was always used as purging gas. The gaseous reactants were led to the reactor by mass flow controllers (Bronkhorst). The catalytic tests were performed in quartz tubular reactors (30 cm length, 8.0 mm i.d.) placed inside of an vertical electrical heating oven, which was controlled by an Eurotherm PID temperature controller. The diluted or undiluted catalysts were held in the isothermal oven zone between two quartz fiber supports, supported by another thinner quartz tube. The products stream was sampled in the micro gas chromatography (Micro-GC, Varian 4900) with TCD detectors. The molecular sieve column 5A (length of 10 m) with Ar as carrier gas was used to separate the oxygen and carbon monoxide. The 19CB column (length of 10 m) with He as carrier gas was used to separate the hydrocarbons. The PPQ column (length of 6 m) with He as carrier gas was used to separate the carbon dioxide.

The reactor was also used as heating apparatus as a part of TPA system. The outlet of reactor was connected with vacuum chamber of Mass spectrometer by capillary. The details of investigation were described in chapter 2.2.3.

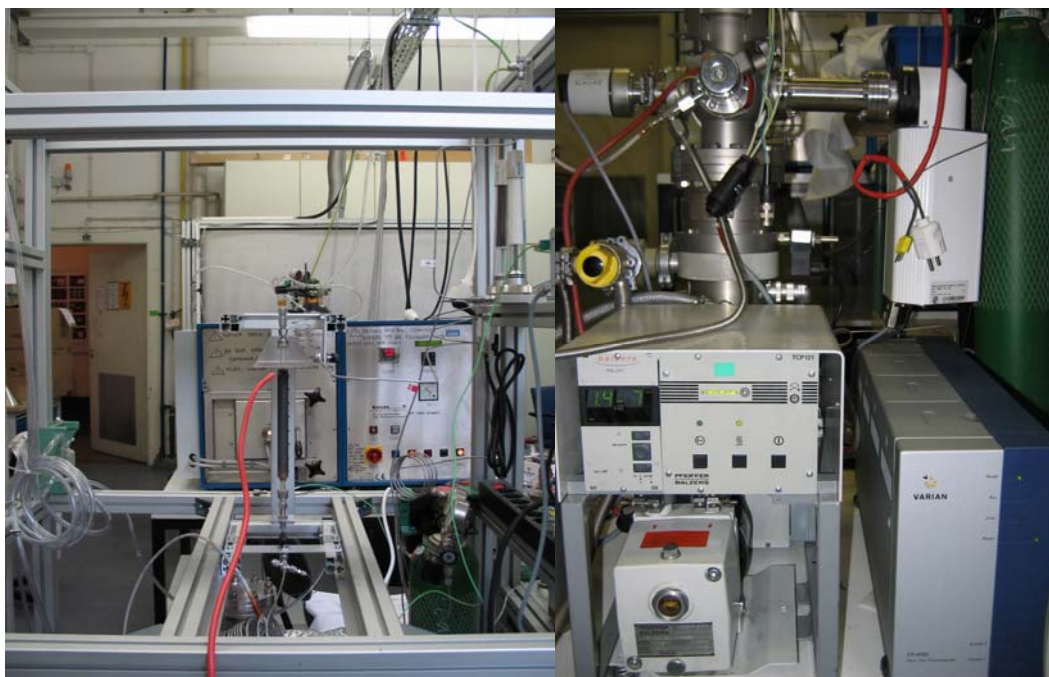
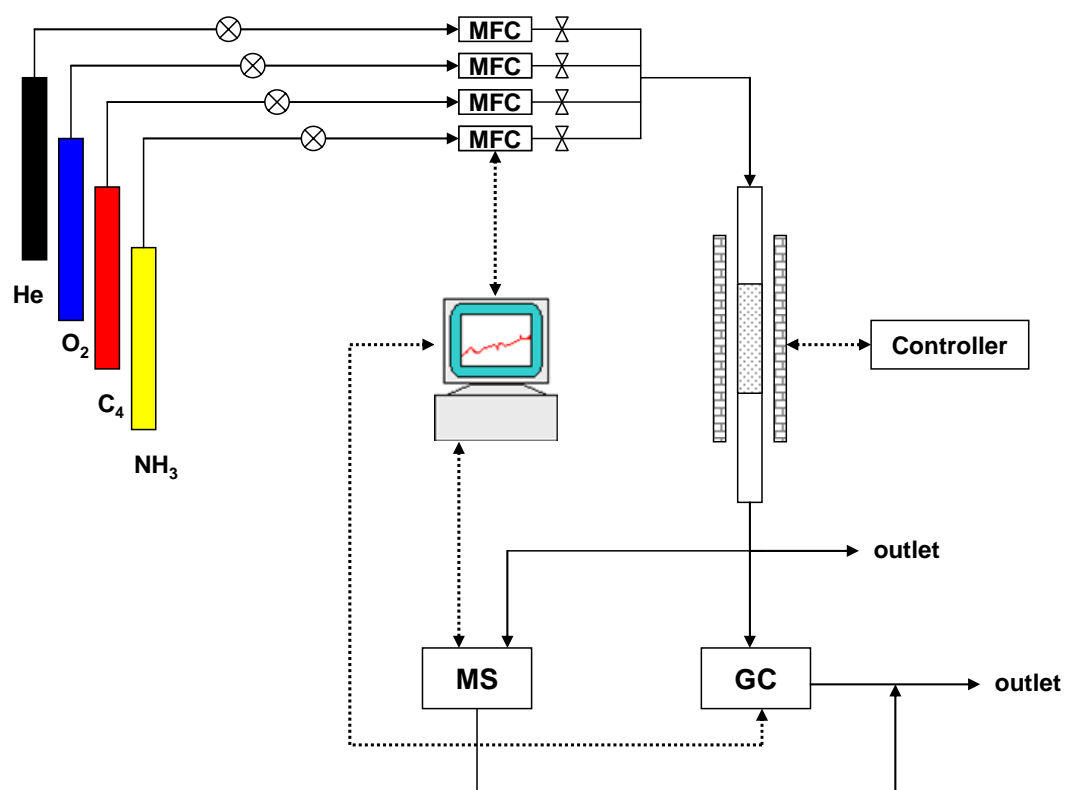


Fig. 2.1 Schematic illustration and photo of the reactor set-up used for the catalytic experiments and TPD apparatus

The parameters of the catalytic performance were defined by the following equations, where F is the molar flow rate and subscript i and o mean measured at the inlet and outlet:

$$\text{Conversion: } Con_{butane} = (F_{butane(i)} - F_{butane(o)}) / F_{butane(i)} \quad (2.1)$$

$$\text{Selectivity to product: } S_{1-butene} = F_{1-butene} / (F_{butane(i)} - F_{butane(o)}) \quad (2.2)$$

$$S_{2-butene} = F_{2-butene} / (F_{butane(i)} - F_{butane(o)}) \quad (2.3)$$

$$S_{butadiene} = F_{butadiene} / (F_{butane(i)} - F_{butane(o)}) \quad (2.4)$$

$$\text{Product yield: } Y_{1-butene} = F_{1-butene} / F_{butane(i)} \quad (2.5)$$

$$Y_{2-butene} = F_{2-butene} / F_{butane(i)} \quad (2.6)$$

$$Y_{butadiene} = F_{butadiene} / F_{butane(i)} \quad (2.7)$$

The normalized catalytic yield by amount and surface area was calculated by the following equation:

$$Rs = F_{product} / (m \times s)$$

with m being the weight of the catalyst in grams, and s the BET surface area in m^2/g of the catalyst measured after reaction.

The carbon balance was calculated from the ratio of sum of the reaction products to educt to obtain information about possible carbon deposition or combustion taking place during catalytic reaction process. The experimental error in the carbon balance did not exceed 5%.

The blank experiments and comparative experiments were hold at 673 K and 723K to test if there was contribution from homogeneous reaction. 180mg SiC with 100 mesh

particle size used as catalysts showed a very low catalytic activity, with only 1% conversion and 0% selectivity.

Generally, 180mg catalyst was filled in the quartz reactor for one catalytic test. The length of isothermal zone was about 5 cm and the length of catalysts ranged from 0.5cm to 3cm. The reactants were induced into the reactor and consecutively reactor temperature was rapidly increased to the set-point. Spontaneously the outlet gas was injected into the Micro-GC for analysis. All values were taken at steady state. Higher reaction temperature should favor the catalytic performance of carbon catalysts, although the combustion of catalysts should feasibly occur. Therefore, the reaction temperature was set at 673 to 723 K, lower than the gasification temperature of corresponding CNTs. For catalytic oxidation of butene, the same contact time (0.72g·h/ml) was used as that used in carbon catalyzing ODH of ethylbenzene in previous work, facilitating the comparison. Ratio of concentration of oxygen to that of hydrocarbon, reaction temperature and total flow rate were tuned to achieve higher conversion and selectivity, combined with low concentration of butane/butene. The details of reaction conditions were list in Tab. 2.1. Although it was proposed that the reaction was running during the isothermal condition. The mass transfer and heating transfer were still an important problem. The outer diffusion and inner diffusion would happen simultaneously in the quartz reactor due to the microporous structure of CNTs. Generally, the diffusion could not be avoided by using so-called “integral reactor” with a large amount of catalysts, resulting in a distribution of concentration of educts and products along the quartz tube. Consequently, a significant drawback was: although carbon catalysts displayed different catalytic performance, but their conversion or selectivity was similar due to the serious

diffusion. Therefore, for kinetic analysis, the less catalysts amount, smaller particle size and high flow rate were required to eliminate the influence of diffusion on catalytic performance.

Tab. 2.1 Optimal reaction conditions of catalytic oxidation of C₄ hydrocarbons

C ₄ Hydrocarbons	Conc. C ₄ vol%	Conc. O ₂ vol%	Flow rate ml/min	Temperature K	Catalysts amount mg
n-Butene	0.67	1.32	15	673	180
n-Butane	2.64	1.32	10	723	180

2.2. Characterization Techniques

2.2.1. Microscopic Methods (TEM, SEM)

Transmission electron microscopy (TEM) is a very important characterization method for the local investigation at atom-scale, uniquely providing detailed information about the size, shape and microstructure of carbon materials. Therefore, the change in the structure and chemical properties of catalyst during the reaction could be identified by TEM. Two TEMs were used in the present work. The normal one is Philips CM 200 LaB₆ operated at an accelerating voltage of 200 kV with an energy dispersive X-ray analysis (EDX) detector and another is Phillips CM200 FEG field-emission gun electron microscope operated at an accelerating voltage of 200 kV equipped with an energy dispersive X-ray analysis (EDX) (DX-4) and electron energy loss spectroscopy (EELS) detectors (Gatan 100) for elemental analysis. The samples were prepared by suspending the solid powder in ethanol or chloroform under ultrasonic vibration. One drop of the thus prepared suspension was brought onto holey carbon films on copper grids.

TEM is a powerful characterization method for nano materials. The localized information about morphology, microstructure and defects could be obtained using imaging technique. However, the disadvantage of TEM is also remarkable since it is not suitable method for characterization of oxygenated surface groups. EELS is theoretically available for identification of oxygen functional groups, depending on the abundance of oxygenated surface groups. However, for multi-walled carbon nanotubes, the signal from oxygen element was always covered by the signal from carbon.

2.2.2. Spectroscopic Methods (XPS, IR-spectroscopy and XRF)

X-ray photoelectron spectroscopy (XPS, also called electron spectroscopy for chemical analysis, ESCA) is an electron spectroscopic method that uses X-rays to eject electrons from inner-shell orbitals. The kinetic energy of these photoelectrons is determined by the energy of the x-ray radiation and the electron binding energy. The electron binding energies are dependent on the chemical environment of the atoms, making XPS useful to identify the oxidation state and ligands of an atom. XPS is an invaluable analytical tool for the identification of the chemical composition of the oxygenated surface groups in present work. The C1s and O1s spectra of the carbon samples before and after catalysis were recorded and investigated, correlated with the change of chemical properties of carbon surfaces. XP spectra were recorded on a modified Leybold Heraeus spectrometer (LHS12 MCD) with Mg K α radiation (1253.6 eV) and a power of 240 W. The bandpass energy was set to 50 eV. X-ray satellites and Shirley backgrounds were subtracted. The peak areas were normalized with the theoretical cross-sections to obtain the relative surface compositions. The C1s and O1s

peaks were fitted by combined convoluted Gauss Lorentz functions. The quantification of concentration of oxygen on the surface of catalysts was calculated following the given function:

$$n_o = \frac{I_o/\delta_o}{\sum_i (I_i/\delta_i)} \quad (2.4)$$

where I is intensity of XPS peak (peak area) and σ is atomic sensitivity factor.

Infra-red (IR) spectroscopy uses electromagnetic radiation of a wavelength longer than that of visible light, but shorter than that of radio waves. It is one of the primary tools in the organic chemical investigation since it could differentiate the nature of different functional groups on the surface of carbon materials. The detailed information about the change in the category and amount of oxygenated surface groups could be obtained. IR-spectra were obtained using a Fourier transform spectrometer (Perkin-Elmer System 2000). The samples were prepared as suspensions by pressing in alkali metals halides (KBr).

Elemental analysis of carbon sample was conducted by X-ray fluorescence spectrometry (XRF, Bruker S4 Pioneer, Rh-anode 60kv, 4kW) since the influence of metal impurities should be taken into account. It should be clarified if the difference in catalytic performance should be attributed to the concentration of metal impurities,

2.2.3. Thermal characterization methods with MS (TPD, TPO and NH₃-TPD)

Thermogravimetry-differential thermal (TGA, TG/DTA) analysis determines the temperature- and time-dependent changes in the mass of a sample that occur during a specific temperature program and in a defined atmosphere. If analysis is combined with

mass spectrometer (MS), it could be used to analyze the outlet gas composition during the temperature program. Temperature-programmed Oxidation (TPO) and Temperature-programmed Desorption (TPD) were used to analyze thermal stability and oxygen functional groups of carbon material. The correlation between the size distribution and gasification temperature of graphene sheets was reported, investigated by using TPO method.^[1]

TPD investigation could offer valuable detailed information about the chemical nature of catalyst surface, since the desorption temperature of CO and CO₂ could be associated with the thermal stability of different oxygen functional group. Almost all the possible functionalities in the individual graphene sheet were schematically summarized in Fig. 2.2. However, inconsistent data were achieved about the chemical desorption temperature of oxygen functional groups since the desorption significantly depended on the chemical environment and feature. Therefore, the difference of desorption temperatures of some functional group in literature could be almost 373K or more (Tab. 2.2). Generally, only desorption temperature of carboxylic acid and quinone groups was undoubtedly identified (the lowest and highest desorption temperature). Therefore, the deconvolution of TPD profiles and consequent investigation must be confirmed by other characterization methods.

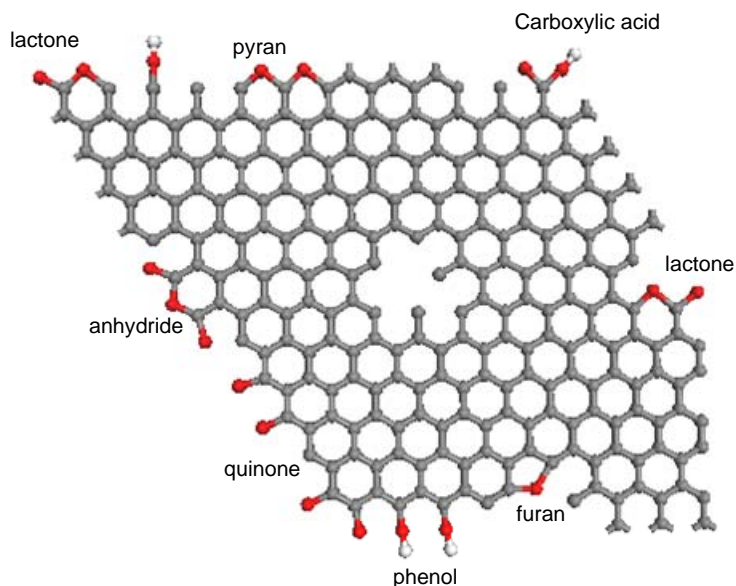


Fig. 2.2 Schematic representation of the main chemical features in a graphene sheet, with its typical surface functionalities

Tab. 2.2 Desorption temperature of oxygen functional groups in carbon materials

Oxygen functional groups	Desorption products	Desorption temperature K
carboxylic acid	CO ₂	623 ^[2] , 373-573 ^[3,4] , 473-523 ^[5] ,
anhydride	CO ₂ +CO	900 ^[6] , 823 ^[4] , 523-773 ^[5] ,
lactone	CO ₂	900 ^[6] , 933 ^[4] , 463-923 ^[7] , 623-6730 ^[5] ,
phenol	CO	903 ^[4] , 873-973 ^[5]
ether	CO	873 ^[6]
quinone and half quinone	CO	1073 ^[4] , 1073-1173 ^[5] , 873-1223 ^[7]

The TPD and TPO characterization also could be conducted individually using vertical heating oven coupled with a QMS200 mass spectrometer (Thermostar, Pfeiffer Vacuum) for the investigation of the evolved gaseous oxidation/desorption products as a function of temperature (Fig. 2.1). Although the information about thermogravimetry was missed during the characterization, the intensity of H₂O, CO and CO₂ as a function of

temperature can also be recorded and analyzed. For TPO, 20mg catalysts were used with a linear heating rate of 2K/min and 13.3vol% O₂ in He (15ml/min total flow rate). 20mg sample was used in TPD investigation, preheated at 473 K for half hour and consequently heated with 10 K/min linear heating rate and 15 ml/min He flow rate.

NH₃-TPD is a valuable analytical tool to identify the surface acidity/basicity of solid acids. By using the mass spectrometer, the ammonia desorption signal was recorded during the temperature-programmed process. 20mg sample was used in NH₃-TPD investigation, preheated at 473 K and helium atmosphere for half hour and consequently cooled down to room temperature. Then the sample was flushed by 33% ammonia with 30 ml/min total flow rate for 1 hour. Afterward, the saturated sample was purged by He with 20ml/min flow rate for 1 hour. 10 K/min linear heating rate was used with 15 ml/min He flow rate.

The well-known technical problem, diffusion, was also taken into account. The characterization conditions, like catalysts amount, heating ramp and diluters, were changed to obtain the optimum result. The Figure 2.3 showed the NH₃ profiles obtained from NH₃-TPD with different heating ramp and blank experiment.

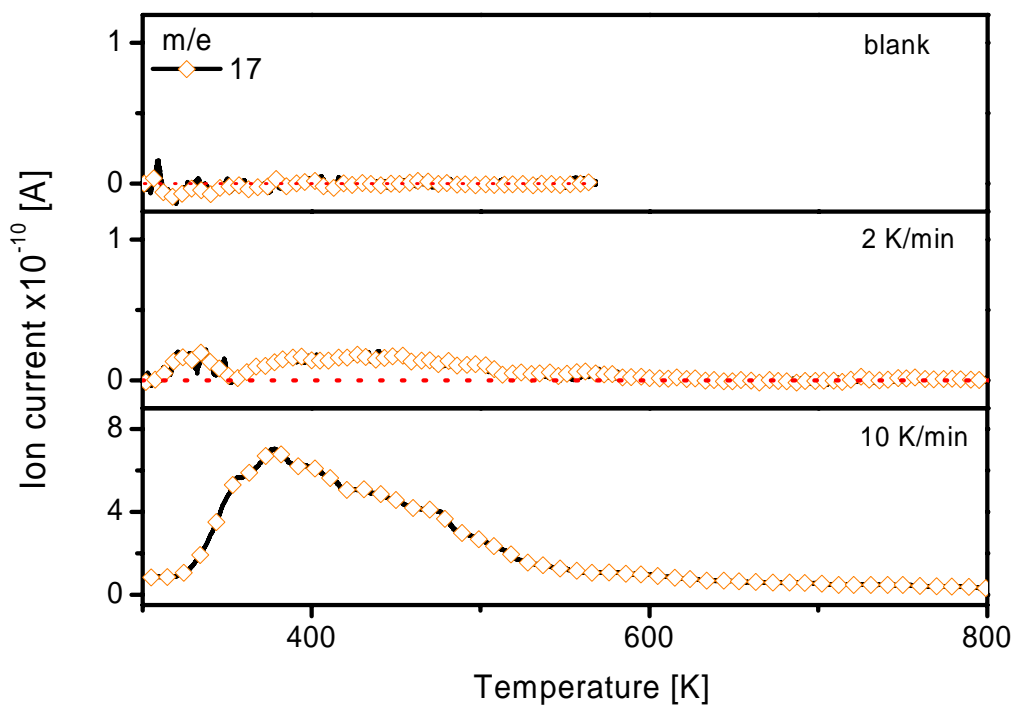


Fig. 2.3 NH₃-TPD profiles of oxidized Nanocyl CNTs with different heating ramp

To achieving the remarkable profiles during TPD performance, the heating ramp of 10K /min was also chosen in the characterization. For TPO profiles, a low heating ramp was possible for characterization due to the strong intensity of CO₂ signal (m/e=44). The TPO-CO₂ profiles (Fig. 2.4) showed that gasification temperature of CNTs decreased from 1099 to 913K when the heating ramp decreased from 10K /min to 2K /min. Although the intensity decreased by almost one order of magnitude, the peak shape could be identified for further analysis.

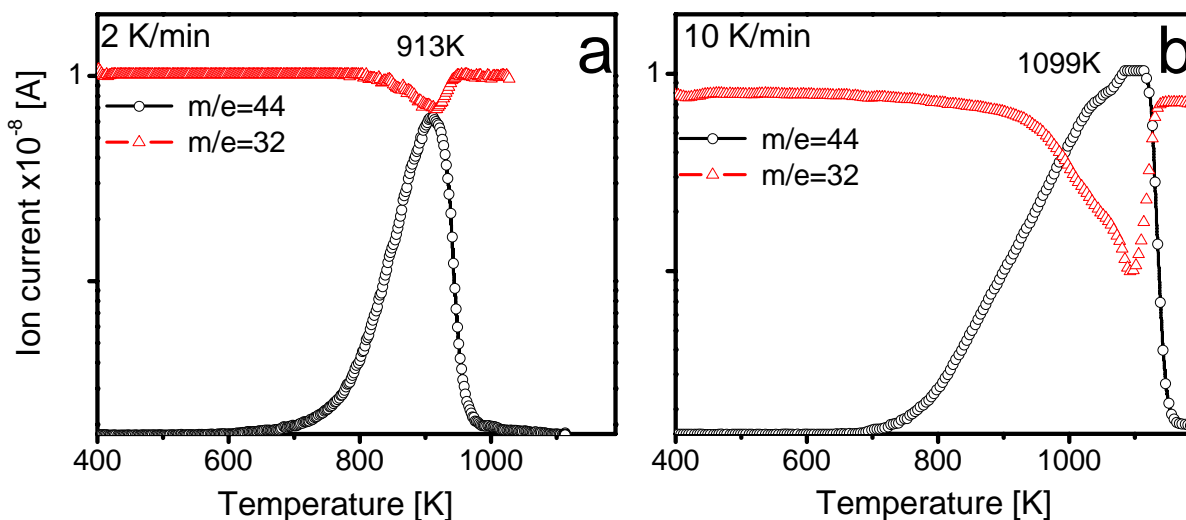


Fig. 2.4 CO₂-TPO profiles of oxidized Nanocyl CNTs with different heating ramp a) 2K/min and b) 10K/min

References

1. Aso H, Matsuoka K, Sharma A, Tomita A, Evaluation of Size of Graphene Sheet in Anthracite by a Temperature-Programmed Oxidation Method, *Energy Fuels*, 2004, 18, 1309 -1314.
2. Otake Y and Jenkins RG, Characterization of oxygen-containing surface complexes created on a microporous carbon by air and nitric acid treatment, *Carbon* 1993, 31, 109-121.
3. Zhuang QL, Kyotany T and Tomita A, The change of TPD pattern of O₂-gasified carbon upon air exposure, *Carbon* 1994, 32, 539-540.
4. Figueiredo, JL; Pereira, MFR; Freitas, MMA, Modification of the surface chemistry of activated carbons, *Carbon* 1999, 37, 1379-1389
5. U. Zielke, K.J. Huttinger and W.P. Hoffman. Surface-oxidized carbon fibers: I. Surface structure and chemistry, *Carbon* 1996, 34, 983-998

6. Zhuang QL, Kyotany T and Tomita A, DRIFT and TK/TPD Analyses of Surface Oxygen Complexes Formed during Carbon Gasification, *Energy and Fuels* 1994, 8, 714-718
7. Marchon B, Carrazza J, Heinemann H and Somorjai GA, TPD and XPS studies of O₂, CO₂, and H₂O adsorption on clean polycrystalline graphite, *Carbon* 1988, 26, 507-514

Chapter 3 Catalysts preparation and functionalization

Several kinds of commercial CNTs and other carbon materials were used in this work, listed in the Tab. 3.1. Detailed information about the modification of carbon catalysts was denoted in this chapter. Effort was mainly focused on two kinds of CNTs (PSLD and Nanocyl) with different microstructure (herring-boned nanofilament and carbon nanotube).

Tab. 3.1 Carbon catalysts used for the ODH of C₄ hydrocarbon

	Serial Nr	BET area [m ² /g]	Diameter [nm]	Database Nr	label
CNTs	PSLD-24	41	50-200	2467	PSLD
	Baytube	286	5-20	3832	Bay
	Nanocyl	313	15	3833	Nanocyl
AC	Alfar Aesar	836.7		4000	AA
	Palmshell	1011		3721	PS
	Noritrox	790		4272	Norit

3.1 Oxidation treatment

The oxidation treatment was applied following such steps: firstly, carbon materials were dispersed into concentrated nitric acid with concentration of 1g solid per 100 ml acid solution. The mixture was refluxed for hours and subsequently cooled down to room temperature. Afterwards, the solution was filtered and washed by deionized water several times. Then the obtained black solid was dry at 353K over night. The refluxing time ranged from 2 hour to 40 hour. The calcination treatment was hold at helium atomosphere,

removing oxygen functional groups with low thermal stability. The detailed information about oxidation and calcination conditions was displayed in Tab. 3.2. The influence of metal impurities on catalytic activity has been taken into account since metal residues in carbon materials might be active species for the ODH of butane. The elements analysis and HCl purification were performed, proving that catalytic activity of metal impurities was negligible.

Tab. 3.2 Preparation conditions of oxidized carbon material

	time of Refluxing (hour)	Calcination		SN	Label
		Temperature (K)	Time (min)		
PSLD-24	4	No		3235	PSLD-4
	10	No		3236	PSLD-10
	40	No		3237	PSLD-40
Nanocyl	2	No		4779	Nanocyl-1
	2	723	120	4480	Nanocyl-2
	2	873	30	5346	Nanocyl-3
	2	973	30	4633	Nanocyl-4
Alfa Aesar	2	No		4628	AA-1
	2	973	30	4631	AA-2

3.2 Chlorination and immobilization

2g oxidized CNTs were dispersed in 40 ml anhydrous tetrahydrofuran (THF) by sonication to give a suspension that was then added 20 ml of thionyl chloride (SOCl_2) and 2 drops of dimethyl formamide (DMF). The suspension was stirred at 338K for 24 h at the nitrogen atmosphere. The excess thionyl chloride was removed by filtering under

vacuum. Afterwards the resulting black solid (MWNT-Cl) was washed with anhydrous THF and consecutively vacuum-dried at 313K for 12 h. A mixture of 500 mg of MWNT-Cl, 1g moieties and 40 ml anhydrous THF were refluxed for 72 h. After cooled to room temperature, the black suspension was filtered and washed, which was subsequently dried at 353K in air. The used moieties included 3-furoic acid, methyl cyclopentanone-2-carboxylate, 2-amino pyridine, ethylenediamine and pyrrole-2-carboxylic acid. The schematic reaction process was display in Fig. 3.1 and detailed information about preparation conditions was shown in the Tab. 3.3.

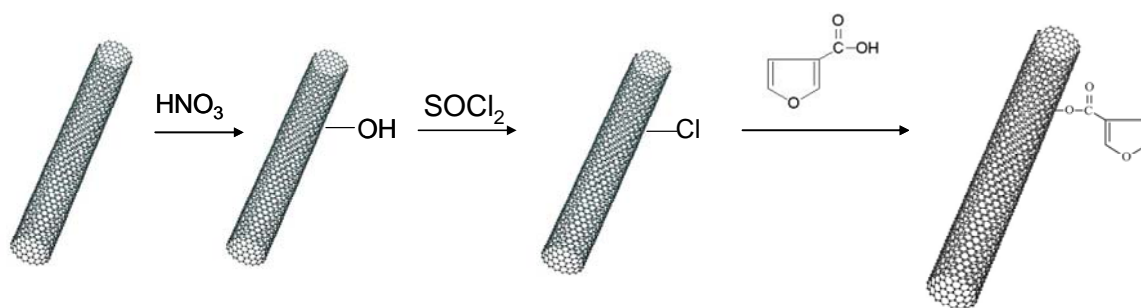


Fig 3.1 Schematic illustration for chlorification and substitution

Tab. 3.3 Preparation of immobilized carbon material

Matrix	Moieties	SN	Label
PSLD-10	3-furoic acid	4880	M-PSLD-1
	methyl cyclopentanone-2-carboxylate	4879	M-PSLD-2
	2-amino pyridine	4877	M-PSLD-3
	ethylenediamine	4876	M-PSLD-4
	pyrrole-2-carboxylic acid	4878	M-PSLD-5
Nanocyl-1	3-furoic acid	4720	M-Nanocyl-1
	pyrrole-2-carboxylic acid	4721	M-Nanocyl-2

3.3 Phosphoric addition

Two kinds of phosphoric precursors (ammonium hydrophosphate and phosphoric acid) were used in the preparation. The loading amount of phosphoric acid was calculated by weight of P_2O_5 . The loading amount ranged from 2wt% to 20wt%, by using PS LD CNTs, Nanocyl CNTs and two kinds of activated carbons as matrix. The modified CNTs were prepared by incipient-wetness impregnation method. The impregnated samples were hold at room temperature overnight and consecutively calcined at Helium atmosphere and 873K for 15 min. The phosphoric modified CNTs were labelled in Tab. 3.4.

Tab. 3.4 Phosphoric acid modified carbon materials

support	precursor	P_2O_5 wt%	SN	label
Nanocyl-2	$(NH_4)_2HPO_4$	2	4504	2% P_2O_5 (N)-Nanocyl
Nanocyl-2	H_3PO_4	2	5344	2% P_2O_5 (P)-Nanocyl
Nanocyl-2	$(NH_4)_2HPO_4$	5	4505	5% P_2O_5 (N)-Nanocyl
Nanocyl-2	H_3PO_4	5	5100	5% P_2O_5 (P)-Nanocyl
Nanocyl-2	$(NH_4)_2HPO_4$	10	4506	10% P_2O_5 (N)-Nanocyl
Nanocyl-2	H_3PO_4	10	5101	10% P_2O_5 (P)-Nanocyl
Nanocyl-2	$(NH_4)_2HPO_4$	20	4507	20% P_2O_5 (N)-Nanocyl
PSLD-10	$(NH_4)_2HPO_4$	2	5105	2% P_2O_5 (N)PSLD
PSLD-10	H_3PO_4	2	5106	2% P_2O_5 (N)PSLD
PSLD-10	$(NH_4)_2HPO_4$	5	5102	5% P_2O_5 (N)PSLD
PSLD-10	H_3PO_4	5	5107	5% P_2O_5 (P)PSLD
PSLD-10	$(NH_4)_2HPO_4$	10	5103	10% P_2O_5 (N)PSLD
PSLD-10	H_3PO_4	10	5108	10% P_2O_5 (P)PSLD
AA	$(NH_4)_2HPO_4$	5	4513	5% P_2O_5 AA
AA-1	$(NH_4)_2HPO_4$	5	4629	5% P_2O_5 AA-1
PS	$(NH_4)_2HPO_4$	5	4715	5% P_2O_5 PS

3.4 Carbon supported metal catalysts

For comparison, carbon supported iron(III) phosphate catalysts were also prepared by incipient-wetness impregnation method. The impregnated samples were held at room temperature overnight and consecutively calcined at Helium atmosphere and 873K for 15 min. The catalysts were labelled in Tab. 3.5. $\text{Mg}_3\text{V}_2\text{O}_8$ (orthovanadate) and $\text{Mg}_2\text{V}_2\text{O}_7$ (pyrovanadate) catalysts were also used in present work, prepared by wet calcination method. 3g $\text{Mg}(\text{NO}_3)_2$ and 0.91g NH_4VO_3 salts were dissolved in a diluted HNO_3 solution (5 drops concentrated HNO_3 in 250 ml H_2O) and then dried at 353K. By following calcination at 823K for 6 hours, $\text{Mg}_3\text{V}_2\text{O}_8$ white powder was obtained. To prepare $\text{Mg}_2\text{V}_2\text{O}_7$ sample, the weight of $\text{Mg}(\text{NO}_3)_2$ and NH_4VO_3 was 3g and 1.37g, respectively. The same preparation method was performed as describe above.

Tab. 3.5 Carbon supported phosphoric iron catalysts

support	precursor	P_2O_5 wt%	SN	label
Nanocyl-2	FePO_4	5	4517	$\text{FePO}_4\text{Nanocyl}$
AA	FePO_4	5	4514	FePO_4AA
AA-1	FePO_4	5	4630	$\text{FePO}_4\text{AA-1}$

Chapter 4 Catalytic oxidation of n-butane over carbon catalysts

In this chapter, the catalytic performance of various carbon catalysts, for instance, CNTs and activated carbons, for catalytic oxidation of butane was tested. The comparison was also hold between the catalytic activity of non-modified and modified carbon catalysts. The significant difference in the catalytic performance of carbon materials before and after modification was observed. Carbon catalysts displayed superior catalytic activity to metal oxides catalysts. The catalytic test combined with TPD investigation was performed in present work to identify the role of oxygenated surface groups during the reaction process.

4.1 Catalytic activity of CNTs

Two kinds of commercial CNTs were conducted as catalysts in the catalytic oxidation of n-butane to corresponding alkenes. The pristine PSLD CNTs displayed a high activity for the oxidation of butane at 673K and molar ratio of $O_2:C_4$ equal to 2, but the selectivities to C_4 alkenes were no more than 4%. The similar catalytic performance was observed using the pristine Nanocyl CNTs, whose selectivities was lower than 5% (Fig. 4.1). CO and CO_2 took a prevailing percentage in the products. For both catalysts, carbon balance kept at 1 during reaction process. It means that the pristine CNTs are active, but not selective for the catalytic oxidation of butane.

Two tested CNTs displayed different initial catalytic performance. PSLD CNTs initially displayed the highest conversion of butane, which decreased gradually and reached the stable state 15 hours later. The same trend was observed on the selectivities to corresponding alkenes. Nanocyl CNTs displayed initial catalytic performance with the

highest selectivities but lowest conversion. However, a rapid decrease in selectivities was observed with respect to increase in conversion as a function of reaction time. Then the catalysts reached the stable state after 2 hours reaction. For both samples, the decrease in selectivity to corresponding alkenes during the reaction process was observed, suggesting that no active sites for ODH of butane were generated during the reaction.

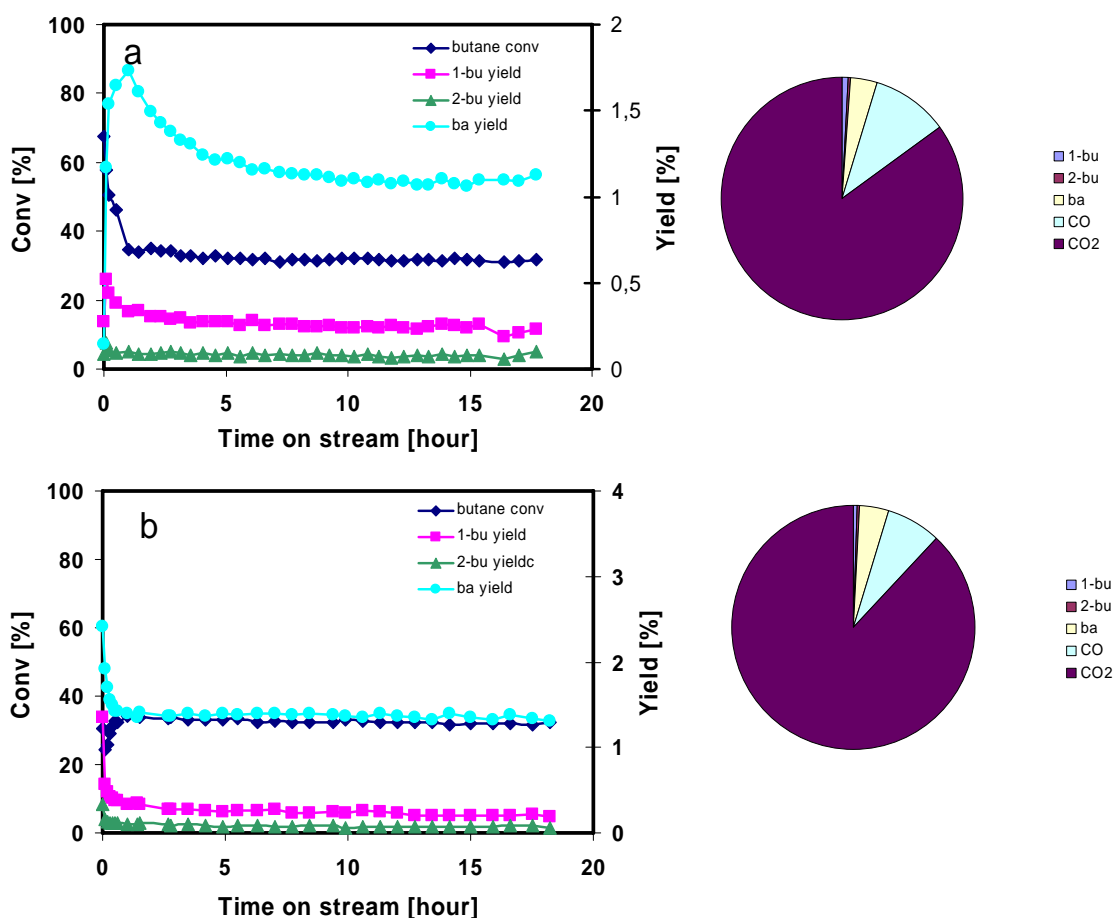


Fig. 4.1 a) Catalytic performance of PSLD: left side, butane conversion and alkenes yield; right side, selectivities to all main products; b) catalytic performance of Nanocyl: left side, butane conversion and alkenes yield, right side, selectivities to all main products; reaction

conditions: 673K, O₂ vol%=1.32% and ratio of O₂:butane=2, 15ml/min, 180mg catalysts. 1-bu, 2-bu and ba are the abbreviation of 1-butene, 2-butene and butadiene, respectively.

The catalytic performance of oxidized Nanocyl CNTs (Nanocyl-2) was shown in Fig. 4.2. At initial period, catalytic performance with higher conversion but less selectivity was observed, probably due to the unequilibrated state. Then selectivity to alkenes increased rapidly and following decrease in selectivity to butenes as function of reaction time was observed, with respect to the decrease in butane conversion. After 4 hours reaction, the catalyst reached the steady-state, corresponding to the catalytic performance with 17% alkenes selectivity. It means that the oxidation treatment is favorable for the catalytic performance.

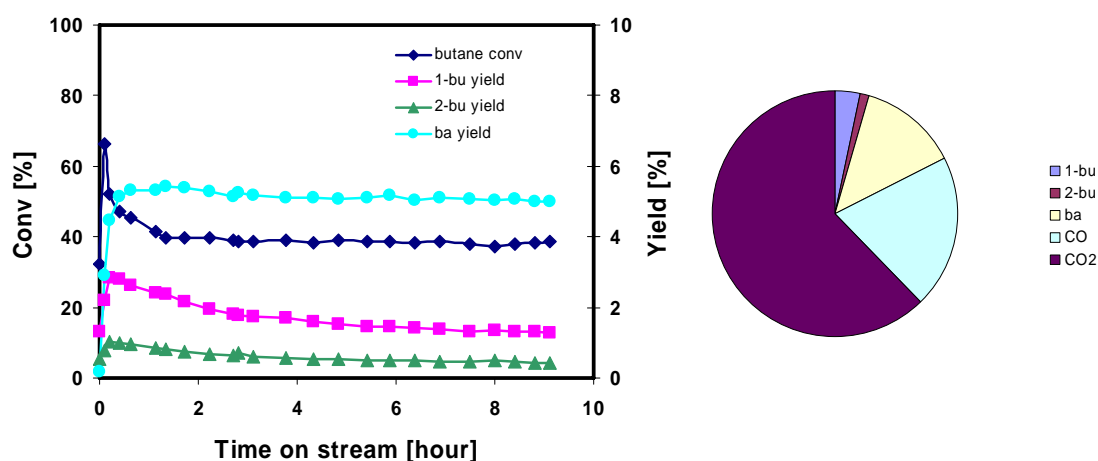


Fig. 4.2 Catalytic performance of Nanocyl-2: left side, butane conversion and alkenes yield, right side, selectivities to all main products; reaction conditions: 673 K, O₂ vol%=1.32% and ratio of O₂:butane=2, 15ml/min, 180mg catalysts.

The reaction conditions were optimized to achieve better catalytic performance and eliminate the total oxidation. The optimization process would be described in the latter part (chapter 4.7). From above experiments, it was notable that the high butane

concentration, low flow rate and high reaction temperature were favourable for the selective oxidation. Then the reaction conditions were chosen as 723K, O₂ vol%=1.32% and ratio of O₂:butane=0.5. The amount of catalysts used was 180mg and total flow rate was 10ml/min. The catalytic performance of oxidized Nanocyl CNTs (Nanocyl-2) was displayed below (Tab. 4.1).

Tab. 4.1 Catalytic performance of the Nanocyl-2 under the optimized conditions

Sample	Conv. %	Selec. %		$\Sigma C_{4=}$ yield %
		COx	$\Sigma C_{4=}$	
Nanocyl-2	11	79	21	2.4

Butane activation is a complex reaction since butadiene can be produced from further dehydrogenation of butane, but also from the following ODH reaction of 1-butene/2-butene since the catalyst also catalyzes the selective oxidation of unsaturated hydrocarbons. In addition, the secondary total oxidation of butenes and butadiene could also take place. Re-adsorption and diffusion effect must be considered since a large amount of catalysts with remarkable high BET surface area were used in the reaction and reaction was conducted in an integral reactor.

To obtain the necessary information about this reaction, the contact time of catalyst was changed to decrease the influence of diffusion and consecutive reaction (Tab. 4.2 and Fig. 4.3). It was observed that the catalytic selectivities to butenes increased from 24% to 48%, following the decrease in catalysts amount from 180 mg to 10 mg. However, the alkenes selectivity was much less than 100%, indicating that the direct butane combustion reactions occurred in parallel with ODH.^[1] The alkenes selectivity decreased

with increasing the contact time, which was contributed to the conversion of products to carbon oxides via secondary combustion pathways. Obviously, butenes were the primary olefin products and butadiene formed from the further dehydrogenation of butenes since the selectivity to butenes increased with respect to the decreasing residence time. Therefore, the catalytic oxidation of butane occurred via parallel and sequential oxidation steps, which is proposed in Fig. 4.4.

Tab. 4.2 Catalytic activity of Nanocyl-2 with different residence time

Catalyst amount (mg)	W/F s g/ml	Conv %	Selec. %			Formation rate mmol/g h ⁻¹	
			$\Sigma C_{4=}$ *	ba*	CO _x	$\Sigma C_{4=}$ *	Ba
90	0.36	15	24	7	75	0.11	0.031
40	0.16	8	30	7	70	0.16	0.038
20	0.08	5	34	7	66	0.24	0.050
10	0.04	3	48	7	52	0.34	0.052

***ba is the abbreviation of butadiene, $\Sigma C_{4=}$ represent all alkenes products**

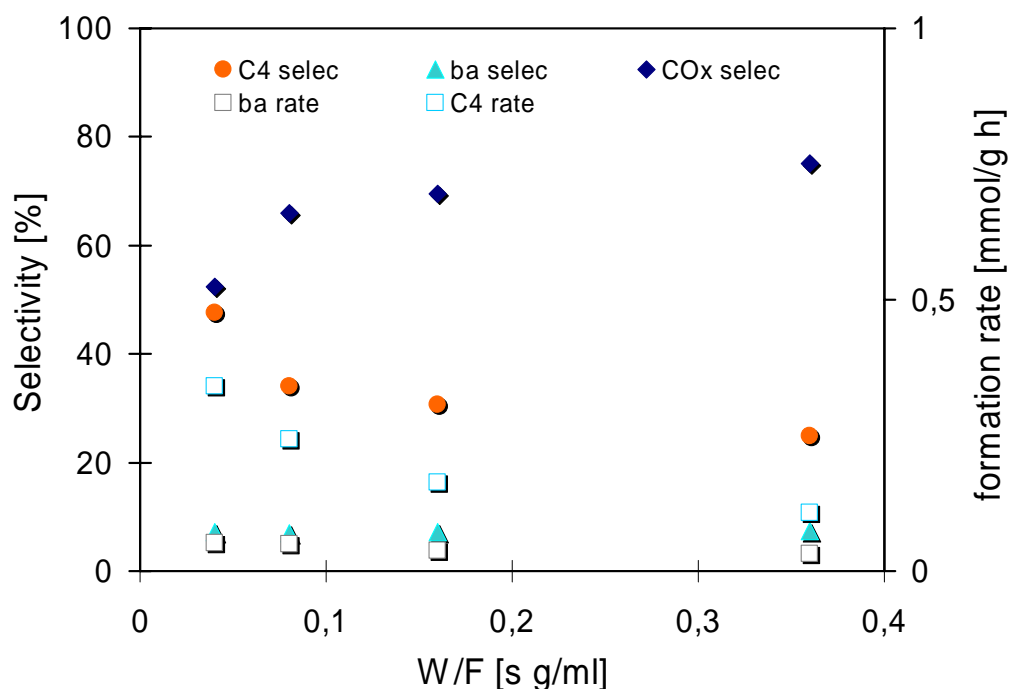


Fig. 4.3 Dependence of alkenes selectivities and formation rates on residence time

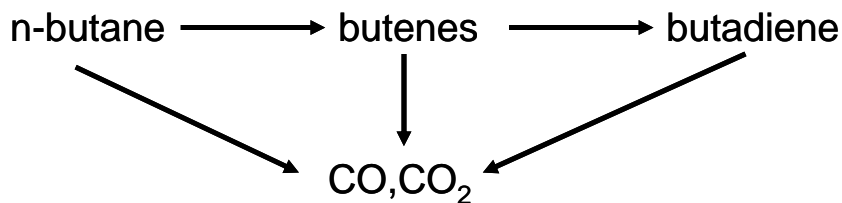


Fig. 4.4 Possible reaction network for catalytic oxidation of n-butane

For evaluation of the possible sequential oxidation reaction, the catalytic activities of Nanocyl-2 in the catalytic oxidation of 1-butane, 1-butene and butadiene were tested under the same reaction conditions (Tab. 4.3). A remarkably catalytic activities of Nanocyl-2 catalyst were observed. This confirms the contribution of the catalytic oxidation of re-adsorbed species to the catalytic oxidation of butane. Compared to the catalytic oxidation of butane, higher catalytic performance with 55% conversion and 54% selectivity was achieved by using same catalysts in the catalytic oxidation of butene. It

proved that production of butadiene in the catalytic oxidation of butane mainly resulted from the consecutive dehydrogenation of butene, in agreement with the kinetic measurement (Tab. 4.1), confirming the possible reaction network illustrated in Fig. 4.4.

Tab. 4.3 Catalytic activities of Nanocyl-2 in different reactions

Reaction	W/F	Conv.	alkenes Selec.
	s g/ml	%	%
Catalytic oxidation of butane	0.72	38	18
Catalytic oxidation of butene	0.72	55	54
Catalytic oxidation of butadiene	0.72	27	

In literature, it was proposed that the carbonyl functional groups were active sites for the ODH of ethylbenzene.^[2] By using the thermal treatment to remove the oxygenated surface groups, the correlation between the oxygenated surface species and catalytic behaviour of carbon catalysts was investigated. The catalytic activity of thermal-treated CNTs was tested in present work, displayed in Fig. 4.5 and Tab. 4.4. Firstly, Nanocyl-2 sample was used in the catalytic oxidation of butane. After six hours, the reaction was quenched by rapid decreasing reaction temperature and replacing reactants input with He. The catalyst was flushed at room temperature by He for two hours and following TPD was performed. After TPD, the reactant gases were injected inside the reactor and the catalytic oxidation of butane was performed again under same reaction condition. When the reaction reached steady state, it was stopped, following the same process described above. Then TPD was performed in sequence. The catalytic test and TPD recycling turn were held three times. It is noted that the catalyst has never been taken out of reactor and

exposed to atmospheric environment. During the third catalytic test, isotopic oxygen ($^{18}\text{O}_2$) was used instead of ordinary oxygen ($^{16}\text{O}_2$) for 1.5 hours.

After the TPD at maximum temperature of 1123K, the conversion of butane decreased slightly from 11% to 10% as well as $\text{C}_{4=}$ products selectivity decreased from 21% to 19%. It means that the thermal treatment did not lead to the deactivation of the catalyst. The active sites were not removed from the surface of CNTs or they regenerated during the further reaction cycling. In addition, the activation process of TPD-treated CNTs was very short, illustrating the quick regeneration process of active sites for catalytic oxidation. The less change in the butane conversion and alkenes selectivity observed in the second, third and forth catalytic tests suggested that the chemical nature of carbon surface should not be changed by further TPD performance. Notably, the proportion of butadiene in all alkene products increased almost 2 times after TPD treatment. It means that the sequential dehydrogenation is preferable on the surface of TPD-treated sample.

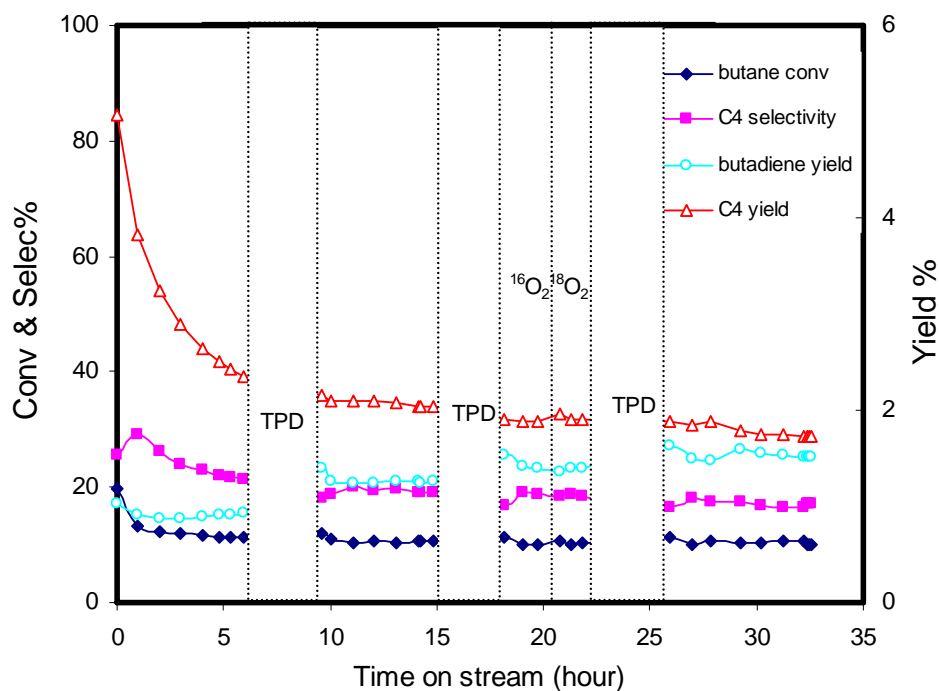


Fig. 4.5 ODH-TPD cycle of catalytic oxidation of butane catalyzed by Nanocyl-2

Tab. 4.4 Catalytic activities of Nanocyl-2 in different reaction runs

	Conv. %	Selec. %				C ₄₌ yield %
		butenes	ba*	ΣC ₄₌	S _{ba} /ΣS _{C₄₌}	
1st	11	13	8	21	0.40	2.3*
2nd	11	7.4	12	19	0.61	2.0
3rd	10	5	14	18	0.73	1.9
4th	10	2	15	17	0.88	1.7

* **ba is the abbreviation of butadiene, value taken at steady-state

The kinetic measurements of TPD-treated CNTs (after fourth catalytic tests, Fig. 4.6 and Tab. 4.5) illustrated the increase in C₄₌ products selectivity and decrease in CO_x selectivity with respect to the decrease in residence time. It means that the reaction network should be similar to the oxidized CNTs before TPD performance (Fig. 4.4).

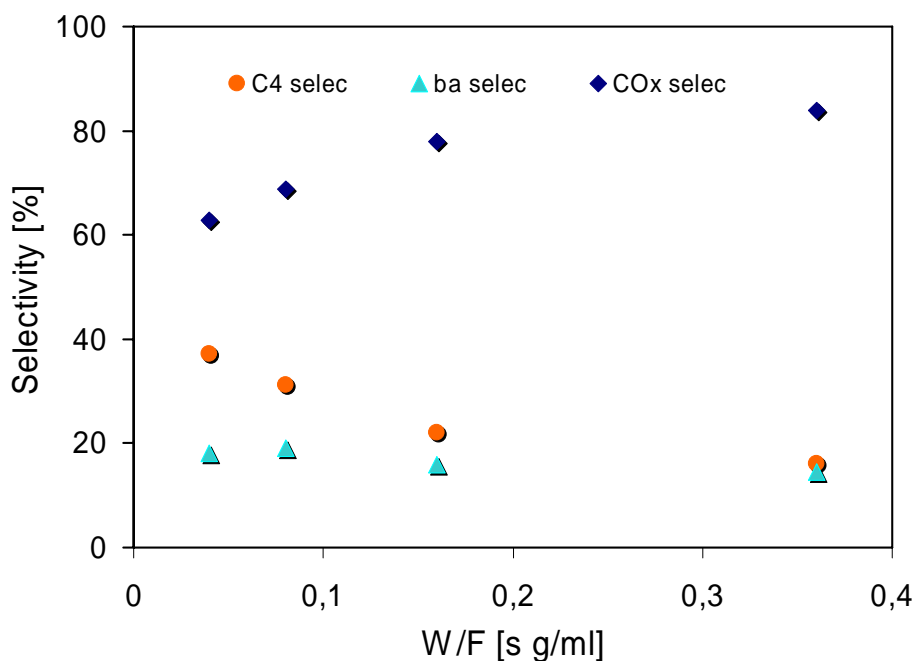


Fig. 4.6 Dependence of alkenes selectivities on residence time

Tab. 4.5 Catalytic activities of Nanocyl-2 with different residence time

Catalyst amount (mg)	W/F s g/ml	Conv %	Selec. %		
			$\Sigma C_{4=}$	ba*	COx
90	0.36	10	16	14	84
40	0.16	8	22	16	78
20	0.08	6	31	19	69
10	0.04	4	37	18	62

*ba is the abbreviation of butadiene

4.2 Catalytic activity of phosphoric modified CNTs

The catalytic performance of 2%P₂O₅(N)-Nanocyl as function of reaction time was shown in Fig. 4.7a. The catalysts reached steady state after 2 hours reaction and no significant deactivation was observed even after 20 hours reaction. The catalytic

performance with 40% butane conversion and 33% alkenes selectivity was achieved at steady state, with respect to the 30% CO₂ selectivity and 37% CO selectivity.

In addition, the reaction conditions were optimized to achieve better catalytic activity (Fig. 4.7 b-d). It was observed that change in the flow rate had less influence on the catalytic performance, but increase in temperature and ratio of butane to O₂ could remarkably improve the catalytic performance. Higher reaction temperature was mainly favourable for butane conversion and lower O₂:butane ratio could prominently improve catalytic selectivity to alkenes from 30% to almost 80%. The highest selectivity was achieved at 723K with O:butane ratio equal to 0.5. Therefore, the stoichiometric condition has been used as the optimum reaction conditions: 723K, O₂ vol%=1.32% and ratio of O₂:butane=0.5, 10ml/min, 180mg catalysts.

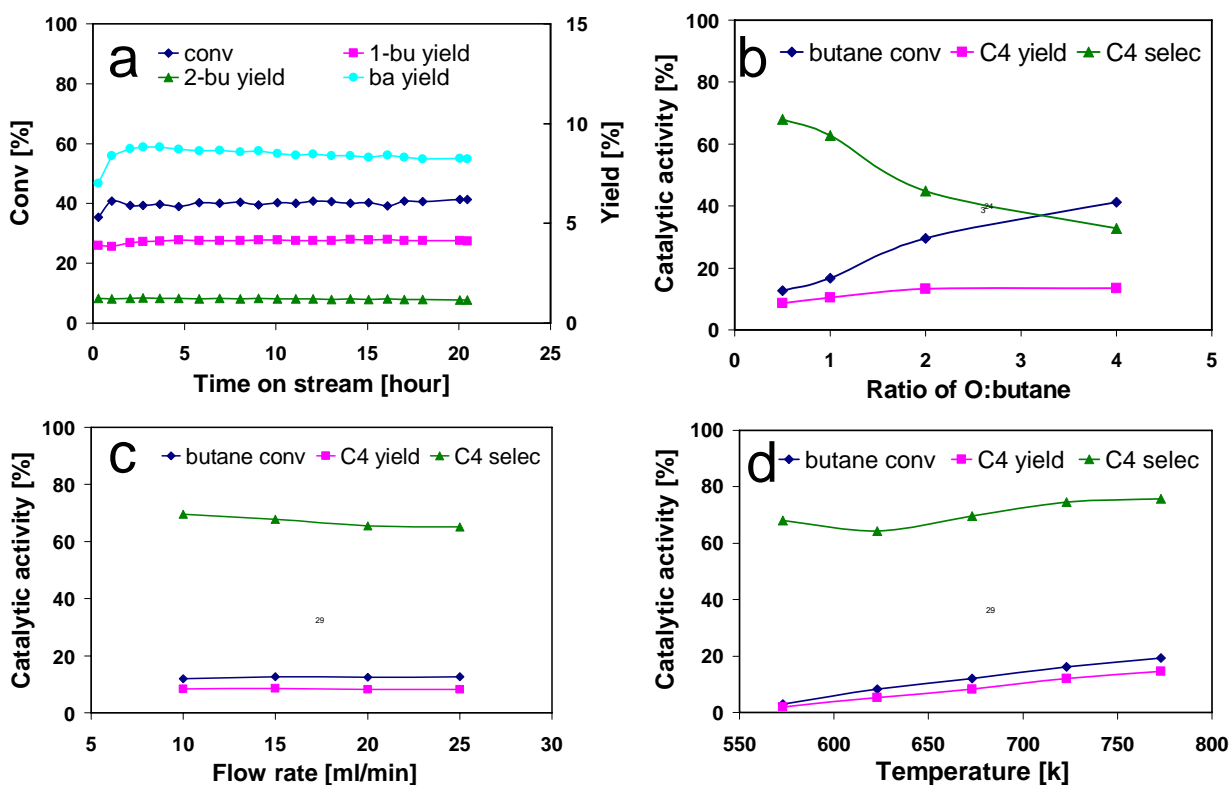


Fig. 4.7 a) Catalytic performance of 2%P₂O₅(N)-Nanocyl as function of time on stream, reaction conditions: 673 K, O₂ vol%=1.32% and ratio of O₂:butane=2, 15ml/min flow rate, 180mg catalysts; b) Dependence of catalytic activity on the ratio of oxygen concentration to butane concentration; c) Dependence of catalytic activity on the flow rate; d) Dependence of catalytic activity on the temperature

The effect of additive amount was also tested by change phosphoric oxide loading amount from 2wt% to 20% (Fig. 4.8). Low loading addition (no more than 5wt%) was favourable for catalytic performance. When the loading amount was higher than 5wt%, both butane conversion and alkenes selectivities decreased, attributed to the over-loading effect.

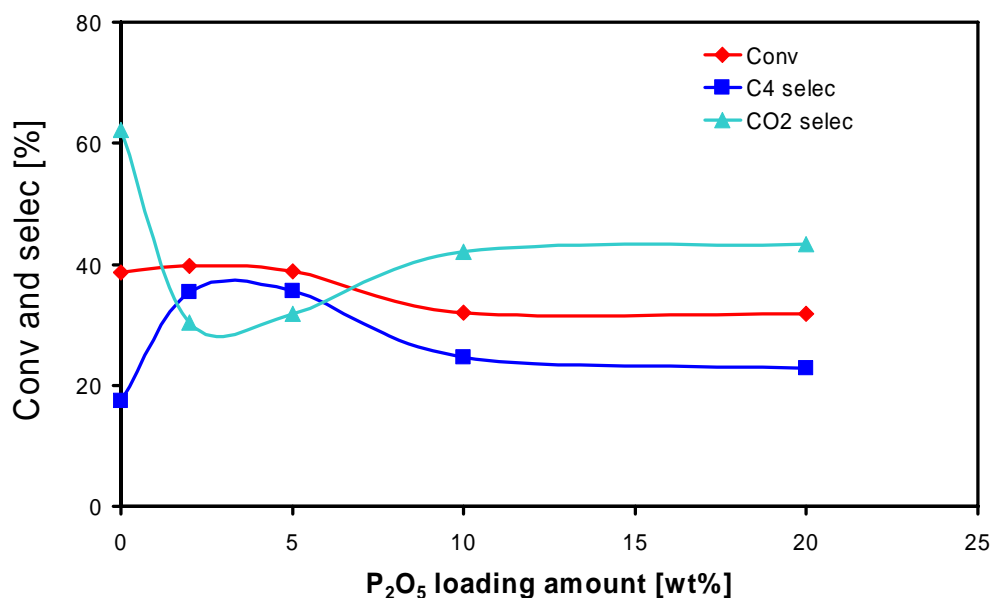


Fig. 4.8 Catalytic performance of phosphoric modified CNTs as a function of P₂O₅ loading amount (reaction conditions: 673 K, O₂ vol%=1.32% and ratio of O₂:butane=2, 15ml/min, 180mg catalysts)

The influence of precursor was also investigated (Fig. 4.9). It was shown that, with low loading amount, modified CNTs prepared by using phosphoric acid as precursor had much higher selectivity than that obtained by using $(\text{NH}_4)_2\text{HPO}_4$ as precursor, but its selectivity decreased rapidly when the loading amount increased to 5wt% or more. Obviously, as precursor, H_3PO_4 was more acidic than $(\text{NH}_4)_2\text{HPO}_4$. However, it is difficult to draw any concludes since the phosphoric carbon complexes could formed during the calcination. A remarkable difference in acidity of phosphoric modified materials has been discussed in chapter 1.4.3.3.

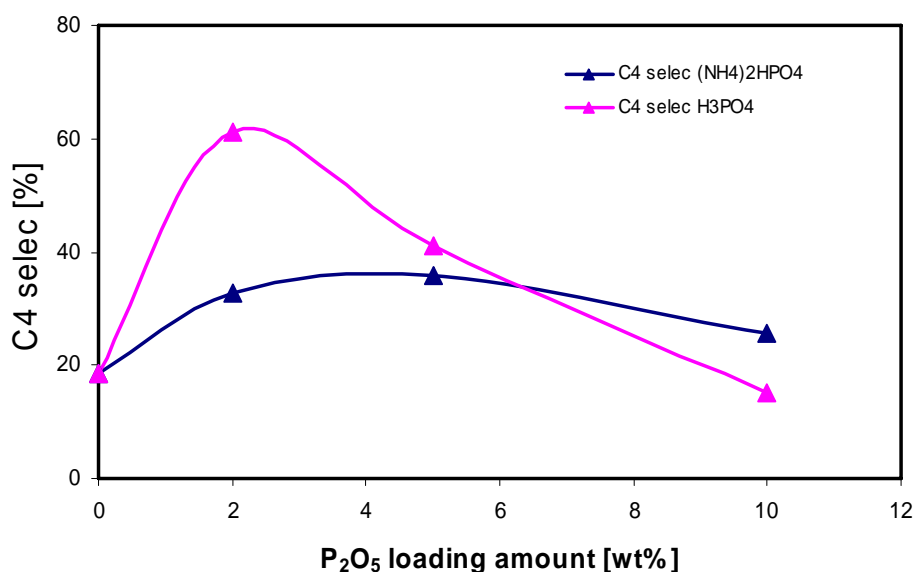


Fig. 4.9 Comparison between selectivity of phosphoric modified CNTs by using different precursors: H_3PO_4 and $(\text{NH}_4)_2\text{HPO}_4$, (reaction conditions: 673 K, O_2 vol%=1.32% and ratio of O_2 :butane=2, 15ml/min, 180mg catalysts)

The test for catalytic stability of 5% $\text{P}_2\text{O}_5(\text{N})$ -Nanocyl was displayed in Fig. 4.10. At the beginning of reaction, the combustion of butane was observed, corresponding to the high conversion and low selectivity. Consecutively, the increase in $\text{C}_4=$ products

selectivity as well as decrease in CO_x selectivity was observed. After 6 hours reaction, slightly deactivation was observed. No significant deactivation was observed after 30 hours reaction with respect to the catalytic performance of 52% C₄₌ products selectivity and 9.2% C₄₌ products yield, which was about almost four times higher than that obtained over non-modified samples. The catalytic performance was also very stable, yet after 100 hours reaction. During the whole reaction process, carbon balance kept at 100%.

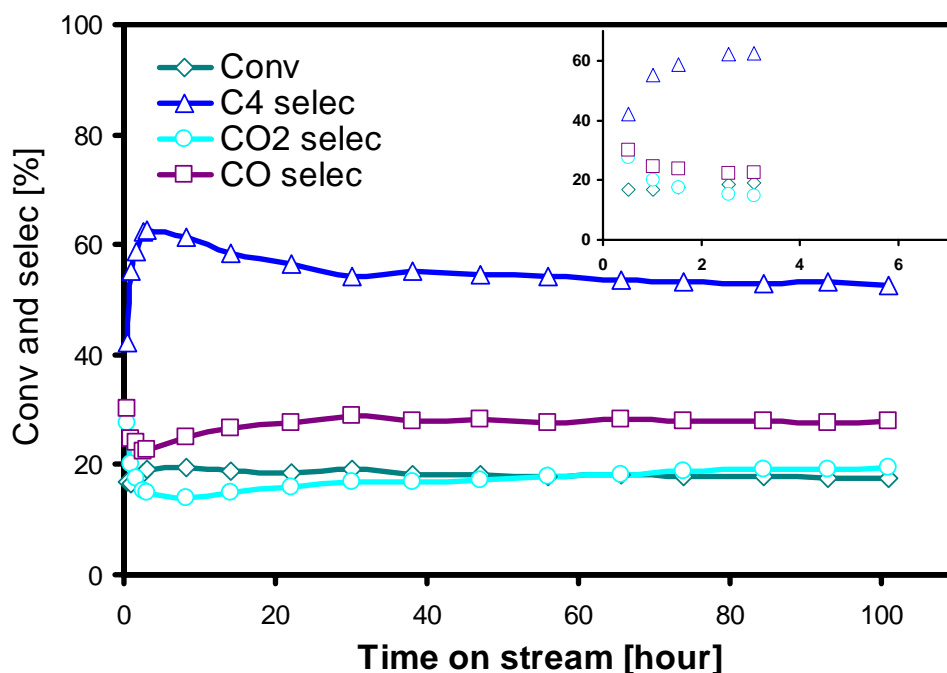


Fig. 4.10 Catalytic performance of sample 5%P₂O₅(N)-Nanocyl as a function of reaction time (upper right corner: initial period of catalytic reaction), reaction conditions: 723 K, O₂ vol%=1.32% and ratio of O₂:butane=0.5, 10ml/min, 180mg catalysts

The dependence of catalytic performance of phosphoric modified CNTs (5wt% loading) on the residence time was displayed in Fig. 4.11. Compared with Nanocyl-2 catalyst, the combustion of butane over phosphoric modified CNTs was significantly reduced. By using 10mg CNTs and phosphoric modified CNTs, no significant difference in alkenes formation rate was observed and ratio of butenes selectivity to butadiene

selectivity constantly kept 6. It means the phosphoric addition improves the catalytic performance by inhibiting butane combustion, not generating new active sites.

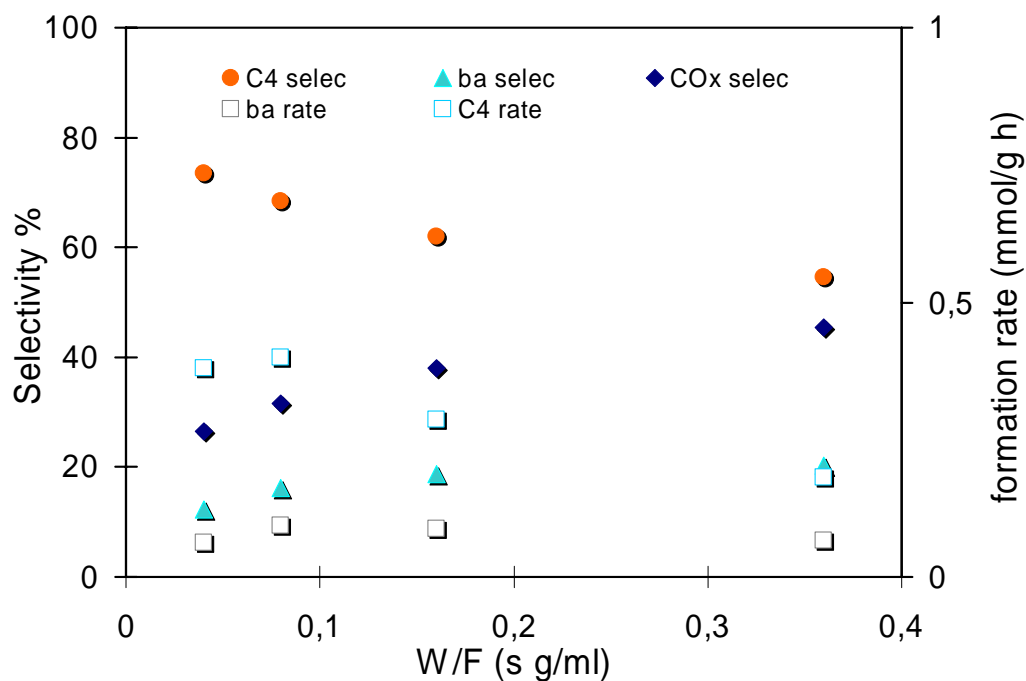


Fig. 4.11 Dependence of alkenes and butadiene formation rate on residence time

Tab. 4.6 Catalytic activity of 5%P₂O₅(N)-Nanocyl with different residence time

Catalyst amount (mg)	W/F s g/ml	Conv %	Selec. %			Formation rate mmol/g h ⁻¹	
			ΣC ₄₌	ba*	COx	ΣC ₄₌	ba
90	0.36	11	55	20	45	0.18	0.067
40	0.16	7	62	19	38	0.29	0.087
20	0.08	4	68	16	32	0.40	0.094
10	0.04	2	73	12	27	0.38	0.063

*ba is the abbreviation of butadiene

4.3 Catalytic activity of grafted CNTs

The catalytic activity of grafted carbon nanotubes at different temperature is displayed in Fig. 4.12. The activation process of catalyst was observed at low temperature (573K and 673K), corresponding to the increase of C₄₌ products selectivity as a function of reaction time. In addition, the increase in reaction temperature favored both butane conversion and alkenes selectivity at low temperature (≤ 673 K). At 673 K, a catalytic performance of 5% butane conversion and 52% C₄₌ products selectivity was achieved at steady state after 9 hours reaction. However, a decrease in C₄₌ products selectivity with respect to an increase in butane conversion was observed as the reaction temperature increased from 673 K to 723 K, indicating the loss of active sites for catalytic oxidation of butane. The comparison of catalytic performance of grafted CNTs (M-Nanocyl-1 and M-Nanocyl-2) and matrix (Nanocyl-1) as a function of reaction time was shown in Fig. 4.12b and Tab. 4.7. Notably, the carbon balance of three carbon catalysts always kept at 100% during reaction process. It was observed that grafting modification significantly improved the catalytic performance even at high temperature, with respect to the increase in catalytic selectivity to alkenes products from 22% to 39% associated with the similar butane conversion. No obvious deactivation was observed after 15 hours reaction, indicating the remarkable stability of modified catalysts.

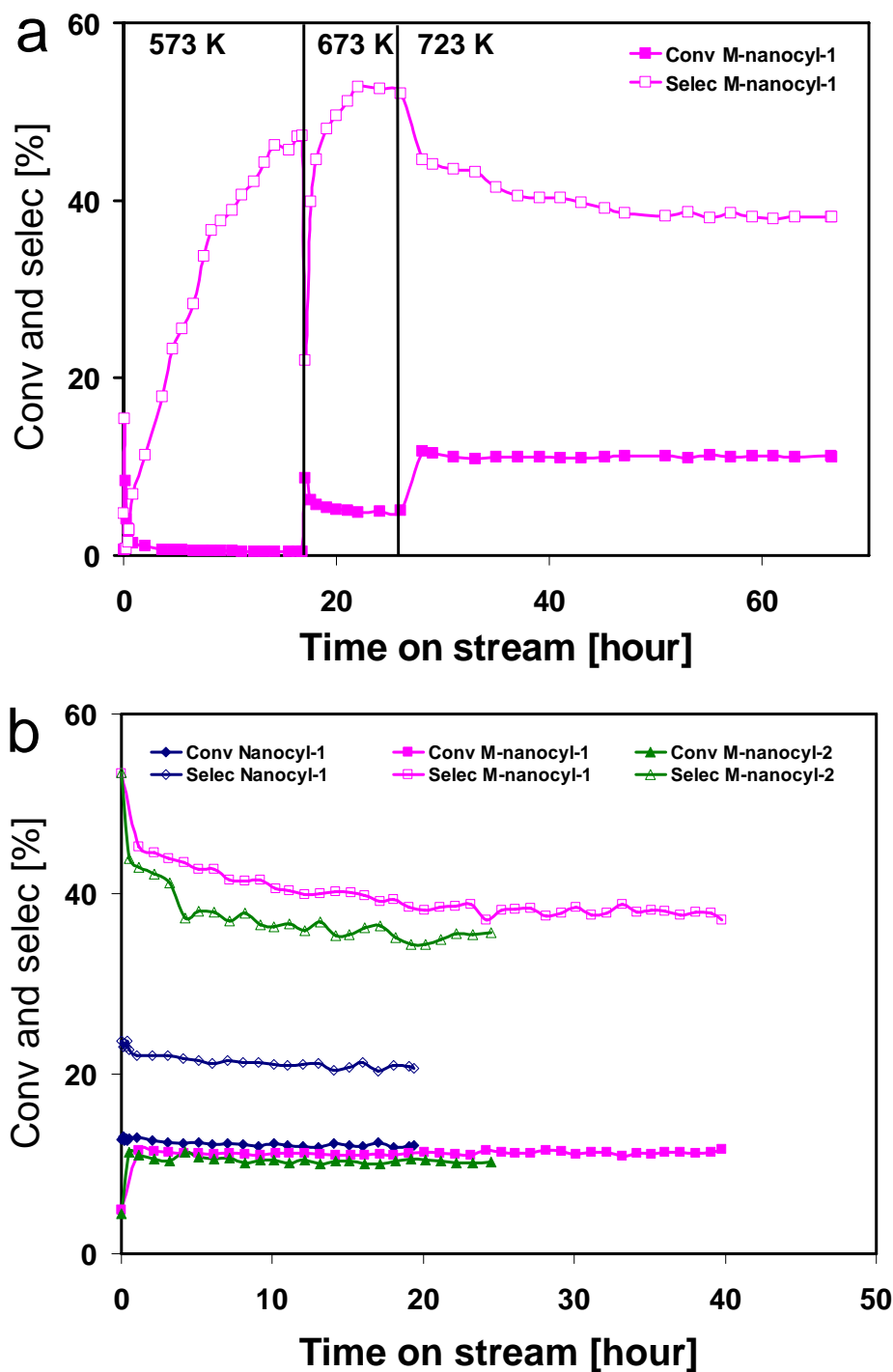


Fig. 4.12 Upper: catalytic performance of grafted Nanocyl CNTs M-Nanocyl-1 at different temperature; lower, comparison of Catalytic performance of non-grafted and grafted Nanocyl CNTs at 723 K (SN4720: M-Nanocyl-1, SN 4721: M-Nanocyl-2 and SN4779:

Nanocyl-1). For all reactions, O₂ vol%=1.32% and ratio of O₂:butane=0.5, 10ml/min, 180mg catalysts

Tab. 4.7 Catalytic performance of grafted Nanocyl CNTs

Moieties		Conv. %	Selec. %				$\Sigma C_4=$ yield %
			1-bu	2-bu	ba	$\Sigma C_4=$	
Nanocyl-1		13	12	3.9	7.4	23	3.0
M-Nanocyl-1	3-Furoic acid	11	14	4.0	20	39	4.2
M-Nanocyl-2	methyl cyclopentanone-2-carboxylate	10	12	3.5	20	36	3.6

***1-bu, 2-bu and ba are the abbreviation of 1-butene, 2-butene and butadiene, respectively, all values were taken at steady state.**

PSLD CNTs were also used as matrix for grafting modification. The catalytic performance as a function of reaction time was displayed in Fig. 4.13. A similar activation process was observed even at higher temperature, indicating the thermal stability of grafted sample. The difference in initial catalytic performance of immobilized Nanocyl CNTs and PSD CNTs should be attributed to the difference in the microstructure (Fig. 5.2 and Fig. 5.5). After modification by grafting methyl cyclopentanone-2-carboxylate moiety, the catalytic selectivity in steady state increased from 33% to 48%. The catalytic activity kept stable even after 10 hours reaction and no apparent deactivation was observed. In addition, the carbon balance of three carbon catalysts always kept at 100% during reaction process. The remarkable catalytic activity and stability suggested that this grafting modification could be a good modification method for catalysts preparation. Actually, the grafting modification has been used widely for mechanical material, like CNTs composite, but it has never been used for catalysts modification. The results here strongly suggest that this method could improve

the catalytic selectivity by introducing functional groups. For pyridine grafted CNTs, less change in catalytic performance was observed.

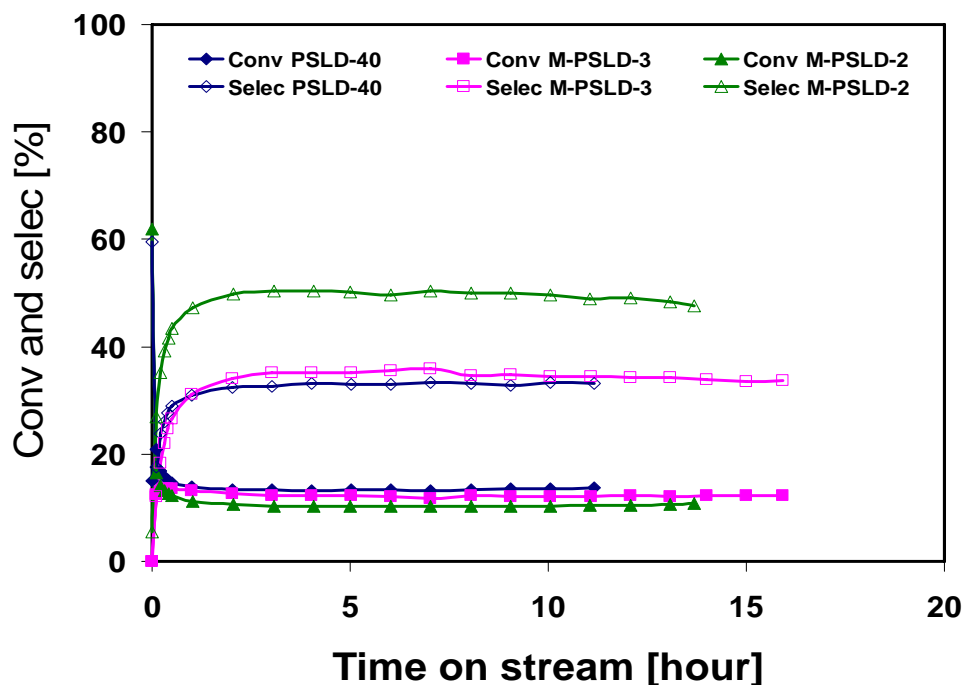


Fig. 4.13 Catalytic performance of grafted PSLD CNTs (SN4877: M-PSLD-2, SN4879: M-PSLD-3) and oxidized PSLD CNTs (SN3237: PSLD-10), reaction conditions: 723K, O₂ vol%=1.32% and ratio of O₂:butane=0.5, 10ml/min, 180mg catalysts

Tab. 4.8 Catalytic performance of grafted PSLD CNTs

Moieties		Conv. %	Selec. %			$\Sigma C_4=$ yield %	
			1-bu	2-bu	ba		
PSLD-10		13	18	5.9	9.2	33	4.5
M-PSLD-2	methyl cyclopentanone-2-carboxylate	11	25	8.0	14	48	5.1
M-PSLD-3	2-amino-pyridine	12	18	5.6	9.5	34	4.1

*1-bu, 2-bu and ba are the abbreviation of 1-butene, 2-butene and butadiene, respectively; all values were taken at steady state.

4.4 Catalytic activities of activated carbons

Three kinds of activated carbons were used as catalysts in the ODH of butane. AA and Norit were commercial acid-washed activated carbons and PS was supplied by

University of Malaysia also washed by acid. The catalytic performance of activated carbons was displayed in Fig. 4.14. During the initial period, catalytic activities with high conversion and low selectivity were observed in both AA and Norit samples due to the unequilibrated state. Then selectivity rose to maximum, subsequently decreased as a function of reaction time. The corresponding decrease in butane conversion was always observed, due to the deactivation of activated carbon. For PS sample, more stable initial catalytic performance was observed. The carbon balance of three carbon catalysts always kept at 100% during reaction process. Although the steady-state conversion of butane obtained from AA and Norit was similar to that from PS, they displayed the opposite catalytic performance: the butenes selectivity from either AA or Norit (47% and 45%, respectively) was almost one time higher than that from PS (29%); on the contrary, the butadiene selectivity from PS (17%) was much higher than that from AA or Norit (5.7% and 3.4%, respectively). The total selectivities to alkenes were similar, meaning AA and Norit preferred catalyzing formation of butene and PS preferred catalyzing formation of butadiene. For three catalysts, the conversion of butane kept stable after 5 hours reaction, but the selectivities to alkenes progressively decreased during the reaction process. The deactivation of activated carbon was reported in the literature, which was attributed to blockage of its porous microstructure.^[3] Activated carbon with lower BET surface area (Alfar Aesar, 836 m²/g) displayed better catalytic performance than that with higher BET surface area (Palm shell, 1011 m²/g), confirming that it is difficult to relate the catalytic performance of activated carbon with its microstructure due to its complicated chemical properties. The elemental analysis (XRF) displayed that there was low metal content ($\leq 0.08\text{wt}\%$) in activated carbon samples (Tab. 5.2). The difference in catalytic activity of

activated carbons should not be attributed to the impurities in activate carbons since PS sample with highest impurities had better catalytic performance than Norit sample, but AA sample with lowest impurities had best catalytic performance than PS or Norit samples . However, the deactivation suggests it is not a good stable catalyst in the ODH, even its catalytic performance is better than that of CNTs.

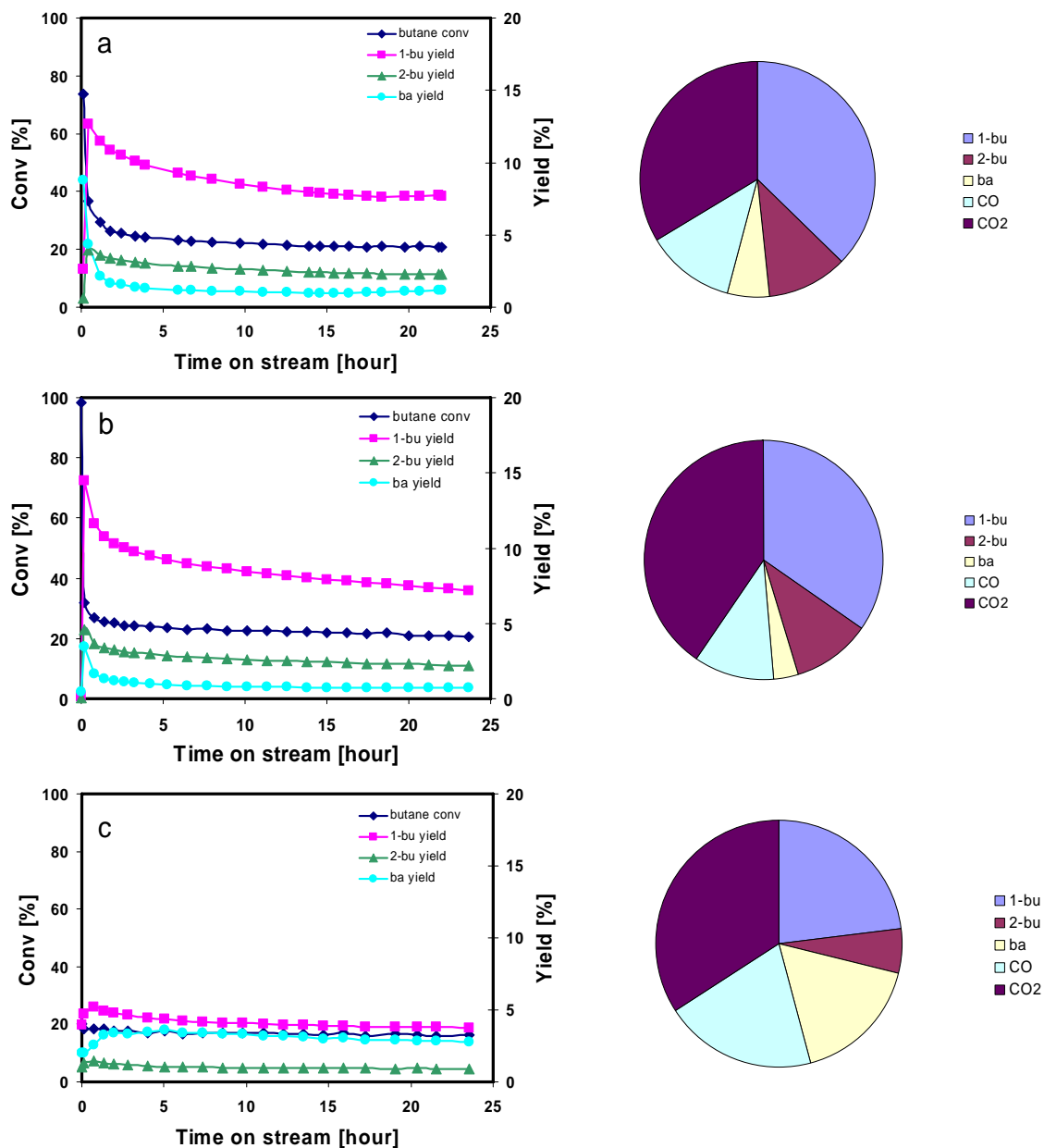


Fig. 4.14 Catalytic performance of activated carbons a) catalytic performance of AA: left side, butane conversion and alkenes yield; right side, selectivities to all main products; b)

catalytic performance of Norit: left side, butane conversion and alkenes yield, right side, selectivities to all main products; c) catalytic performance of PS: left side, butane conversion and alkenes yield; right side, selectivities to all main products; reaction conditions: 723K, O₂ vol%=1.32% and ratio of O₂:butane=0.5, 10ml/min, 180mg catalysts.

Tab. 4.9 Catalytic performance of activated carbons

	Conv.	Selec. %						ΣC ₄₌ yield
	%	1-bu	2-bu	ba	ΣC ₄₌	CO	CO ₂	%
AA	20	37	11	5.7	54	12	34	11
Norit	21	35	10	3.4	49	11	40	10
PS	16	23	5.7	17	46	20	34	7.5

***1-bu, 2-bu and ba are the abbreviation of 1-butene, 2-butene and butadiene, respectively, all values were taken at steady state (after 20 hours reaction)**

The catalytic performance of oxidized activated carbon (AA-1) was displayed in Fig. 4.15a. For comparison, the catalytic activity of oxidized activated carbon after thermal treatment (AA-2) was also displayed in Fig. 4.15b, which was calcined at 973 K in He to remove thermally unstable oxygen functionalities. For sample AA-1, initial catalytic performance with high conversion but low selectivity was observed, following a long activation process. On the contrary, the catalytic performance of thermal treated sample (AA-2) kept stably even at initial point. The carbon balance of two carbon catalysts always kept at 100% during reaction process. For both samples, the same catalytic performance with about 16% butane conversion and 39% C₄₌ products selectivity was obtained in the steady state, lower than that of pristine activated carbon. It suggests that oxidation treatment destroyed the active sites for dehydrogenation on the activated carbon, resulting in the decrease in the catalytic performance. Although the

sample AA-1 has higher amount of oxygenated surface groups than the thermal treated sample, a longer activation process was observed in the catalytic performance of AA-1. It means that those oxygenated surface groups generated via oxidation do not favor the catalytic oxidation reaction.

However, the oxidation treatment had opposite influence on the catalytic behavior of CNTs and activated carbons, the different influence of oxidation on the catalytic performance of CNTs and activated carbons could be attributed to their feature and chemical nature. Although CNTs could be damaged during the oxidation, they kept the graphitic framework and the functionalization only occurred on the end and surface of CNTs. For activated carbon, the oxidation could change its porous microstructure.

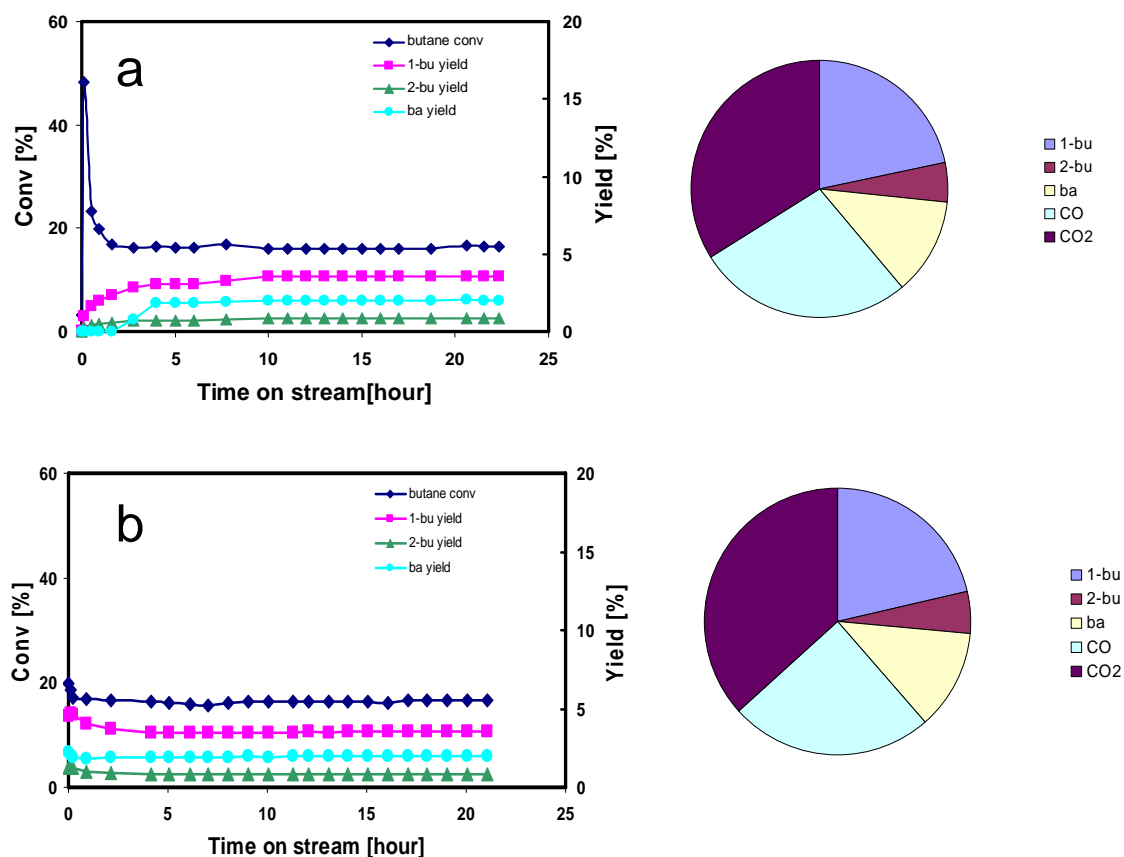


Fig. 4.15 Catalytic performance of oxidized activate carbons before and after thermal treatment (a: AA-1 and b: AA-2): left side, butane conversion and alkenes yield, right side, selectivities to all main products; reaction conditions: 723K, O₂ vol%=1.32% and ratio of O₂:butane=0.5, 10ml/min, 180mg catalysts.

Tab. 4.10 Catalytic performance of oxidized activated carbons

	Conv.	Selec. %				ΣC ₄₌ yield
	%	1-bu	2-bu	ba	ΣC ₄₌	%
AA-1	16	22	5	12	39	6.4
AA-2	17	21	5	12	38	6.4

*1-bu, 2-bu and ba are the abbreviation of 1-butene, 2-butene and butadiene, respectively, all values were taken at steady state (after 20 hours reaction)

4.5 Catalytic activity of phosphoric modified activated carbons.

Phosphoric addition was conducted to modify activated carbon materials. Activated carbons (AA and PS) were used as matrix. For comparison, the oxidized activated carbon (AA-1) was also used. Both loading amount of phosphoric acid were 5wt% by using (NH₄)₂HPO₄ as precursor and all the preparation conditions and reaction conditions were same. The catalytic activity of phosphoric modified activated carbons in steady state was displayed in Tab. 4.11. The carbon balance of three carbon catalysts always kept at 100% during reaction process. It showed that, for both pristine and oxidized activated carbons, the phosphoric addition slightly improved the C₄₌ products selectivity, but significantly eliminated the total oxidation since the selectivity to CO₂ decreased.

Tab. 4.11 Catalytic performance of phosphoric modified activated carbons

	Conv. %	Selec. %					$\Sigma C_4 =$ yield %	
		1-bu	2-bu	ba	$\Sigma C_4 =$	CO	CO ₂	
5wt%P ₂ O ₅ /AA	21	40	12	10	62	24	14	13
5wt%P ₂ O ₅ /PS	14	21	7.0	23	52	19	29	7.1
5wt%P ₂ O ₅ /AA-1	13	16	4.3	13	30	41	29	4

reaction conditions: 723K, O₂ vol%=1.32% and ratio of O₂:butane=0.5, 10ml/min, 180mg catalysts. *1-bu, 2-bu and ba are the abbreviation of 1-butene, 2-butene and butadiene, respectively, all values were taken at steady state (after 15 hours reaction)

4.6 Catalytic activity of other carbon materials

Nano diamond was used as catalyst in this reaction, and its catalytic performance as a function of reaction time was shown in Fig. 4.16. It showed that, after 4 hours reaction, the catalyst reached stable stage and 10% butane conversion and 56% C₄= products selectivity were achieved. The carbon balance always kept at 100% during reaction process. 1-Butene took main percentage in all C₄= products. During the reaction, CO₂ yield was much higher than CO yield, which was also observed by using activated carbons and CNTs as catalysts in this reaction.

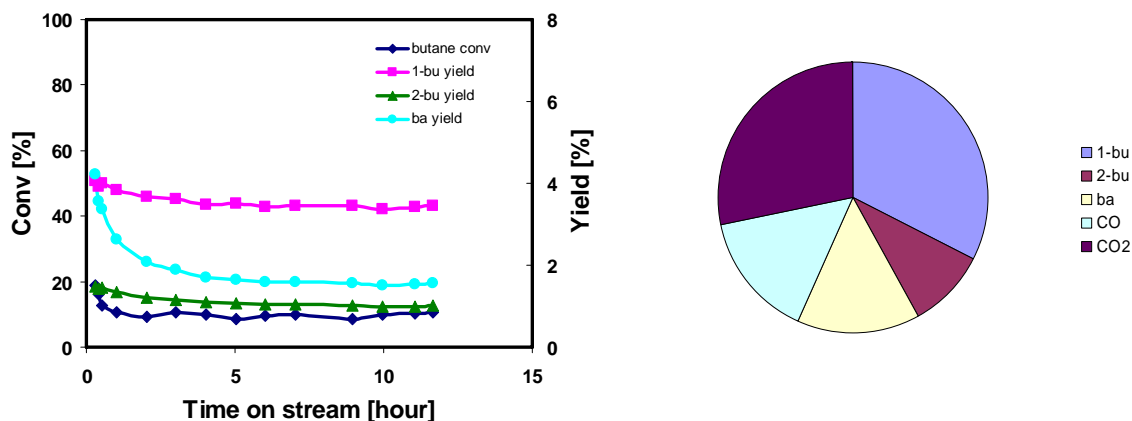


Fig. 4.16 Catalytic performance of nano-diamond, left side, butane conversion and alkenes yield, right side, selectivities to all main products; reaction conditions: 723K, O₂ vol%=1.32% and ratio of O₂:butane=0.5, 10ml/min, 180mg catalysts.

Tab. 4.12 Catalytic performance of nano-diamond

	Conv.	Selec. %				ΣC ₄ = yield %
	%	1-bu	2-bu	ba	ΣC ₄ =	
Nano-diamond	11	32	9.4	15	57	6.0

*1-bu, 2-bu and ba are the abbreviation of 1-butene, 2-butene and butadiene, respectively, all values were taken at steady state (after 10 hours reaction)

4.7 Catalytic activity of carbon supported metal catalysts

The widely use of metal or metal oxide catalysts in the catalytic oxidation of butane has been discussed in Chapter 1. As comparison, two kinds of typical metal catalysts, FePO₄ and V-Mg-O, were used as catalysts under the same reaction conditions. The catalytic performance of metal catalysts in the ODH of butane was displayed in Tab. 4.13. Obviously, the metal catalysts display worse catalytic performance than that of modified carbon materials. The best catalytic performance over metal catalysts was achieved using activated carbon supported iron catalysts, which was even worth than that of support.

Tab. 4.13 Catalytic performance of activated carbons

	Conv.	Selec. %				ΣC ₄ = yield
	%	1-bu	2-bu	ba	ΣC ₄ =	%
FePO ₄ Nanocyl	15	21	6	14	41	3.4
FePO ₄ AA	19	30	8.4	10	48	5.8
FePO ₄ AA-1	16	19	4.7	11	35	3.0
Mg ₃ V ₂ O ₈	10	26	9.1	6.1	41	4.1

Mg ₂ V ₂ O ₇	19	5.5	1.9	1.3	9.1	1.7
---	----	-----	-----	-----	-----	-----

reaction conditions: 723K, O₂ vol%=1.32% and ratio of O₂:butane=0.5, 10ml/min, 180mg catalysts. *1-bu, 2-bu and ba are the abbreviation of 1-butene, 2-butene and butadiene, respectively, all values were taken at steady state (after 8 hours reaction)

4.8 Conclusions

The catalytic performance of different carbon catalysts was summarized in Tab. 4.14. Obviously, nano-diamond displayed a superior catalytic performance to others materials. But the highest yield was achieved by using phosphoric modified activated carbon (Alfar Aesar Co.). The phosphoric addition was a useful method to prepare catalysts with better catalytic performance since the inhibition of total oxidation was observed by using phosphoric modified carbon materials. Furthermore, the grafting modification could improve the catalytic activity remarkably. Generally, carbon materials can unselectively activate butane, and then additional modification is needed to improve the selectivity. In addition, the modified carbon materials displayed a superior catalytic stability even after 100 hours (in case of phosphoric modified CNTs).

For activated carbons, the decrease in the catalytic performance was observed after oxidation treatment with respect to the increase in the functionalization degree. On the contrary, the functionalization significantly favored the catalytic performance of CNTs. In addition, the removal of oxygenated surface groups of oxidized activated carbon had less influence to the catalytic performance in steady state. It means that the catalytic activity of activated carbons could not be directly related with the functionalities. The microstructure and feature should be the most important factor for catalytic performance of activated carbons, which could be easily changed due to the low graphitic feature. However, the influence of functionalities on the catalytic performance should be

considered since the difference in the initial catalytic performance of oxidized activated carbons before and after thermal treatment was observed.

A great diversity in catalytic performance of various carbon catalysts was also observed, which has been normalized by surface area. The highest products formation rate was achieved by using modified CNTs, which was almost ten times higher than that of activated carbons. It suggests that the catalytic performance should not be directly related with the microstructure of various carbon catalysts. It means the “solid state chemistry” might not be appropriate method in present work.

The reaction network was built up based on the kinetic measurement by using CNTs as catalysts, displaying the parallel and sequential oxidation steps. Butenes were primary products from the dehydrogenation of butane and butadiene formed from the further dehydrogenation of butenes. Carbon oxides formed as byproducts from the total oxidation of butanes. However, the combustion of hydrocarbon products had also contribution to the formation of carbon oxides. It suggests that there were two reaction pathways during the catalytic oxidation of butane over CNTs catalysts, one is selective oxidation and the other is total oxidation. The phosphoric addition didn't change the former reaction process, but significantly decreased the total oxidation since the phosphoric addition decreased the ratio of CO₂ yield to CO yield with respect to the same butane conversion and alkenes selectivity in the case of activated carbon. The decrease in total oxidation is attributed to the blockage of active sites for total oxidation by phosphoric addition, confirmed by kinetic measurement by using phosphoric modified CNTs as catalysts. The thermal treatment had less influence on the butane conversion and

alkenes selectivity, suggesting that no more active sites generated during the thermal treatment. However, the increase in butadiene yield was observed, implying that the higher butadiene yield should be attributed to the stronger adsorption and consequent dehydrogenation of alkenes molecules at the active sites.

Obviously, activated carbons are not good target catalysts due to their complicated microstructure, obvious deactivation and low alkenes formation rate. The long range ordering of carbon atoms in CNTs is much higher than that in activated carbon, giving the thermal and chemical stability of CNTs. Therefore, the change in the microstructure of CNTs during the reaction process could be neglected, which has been confirmed in the chapter 5 since no significant difference was observed in TEM images of pristine CNTs, oxidized CNTs and CNTs after reaction. The change in catalytic performance should be mainly related with the functional nature of CNTs.

The influence of chemical functionalization on the catalytic performance of CNTs has been described in this chapter. Both oxidation treatment and phosphoric addition remarkably improved the catalytic performance of CNTs. The kinetic measurement displays the similar alkenes formation rates of oxidized CNTs under different treatment. It assumes that the amount of active sites should be similar. However, the increase in butadiene yield should be related with the stronger interaction between the hydrocarbons and active sites.

Tab. 4.14 Catalytic performance of carbon materials

	Conv. %	Sele. %				$\Sigma C_{4=}$ yield %	$C_{4=}$ formation rate $\mu\text{mol}/\text{m}^2 \text{h}^{-1}$
		1-bu	2-bu	ba	$\Sigma C_{4=}$		
<i>Nano-diamond</i>	11	32	9.4	15	57	6.0	0.56
<i>Nanocyl-2</i>	12	10	3	9	22	2.6	0.33
<i>PSLD-10</i>	13	18	5.9	9.2	33	4.5	4.3
<i>AA</i>	20	37	11	5.7	54	11	0.52
<i>Norit</i>	21	35	10	3.4	49	10	0.5
<i>PS</i>	16	23	5.7	17	46	7.5	0.99
<i>M-Nanocyl-1</i>	11	14	4.0	20	39	4.2	0.53
<i>M-Nanocyl-2</i>	10	12	3.5	20	36	3.6	0.45
<i>M-PSLD-2</i>	11	25	8.0	14	48	5.1	4.9
<i>M-PSLD-3</i>	12	18	5.6	9.5	34	4.1	3.9
<i>5wt%P₂O₅/AA</i>	21	10	12	10	62	13	0.61
<i>5wt%P₂O₅/PS</i>	14	21	7.0	23	52	7.1	0.33
<i>5%P₂O₅(N)-Nanocyl</i>	17	26	6	20	52	8.8	1.1

References

1. Chen KD, Khodakov A, Yang J, Bell AT, Iglesia E, Isotopic Tracer and Kinetic Studies of Oxidative Dehydrogenation Pathways on Vanadium Oxide Catalysts, *Journal of Catalysis* 1999, 186, 325–333
2. Pereira MFR, Orfao JJM, Figueiredo JL. Oxidative dehydrogenation of ethylbenzene on activated carbon catalysts 1. Influence of surface chemical groups. *Applied Catalysis A: General* 1999, 184, 153-160.
3. Pereira MFR, Orfao JJM, Figueiredo JL. Oxidative dehydrogenation of ethylbenzene on activated carbon catalysts 3. Catalyst deactivation. *Applied Catalysis A: General* 2001, 218, 307-318.

Chapter 5 Characterization of carbon catalysts before and after reaction

In this chapter, a comparison of the properties of carbon samples before and after catalytic oxidation of butane was performed. The difference in chemical properties of carbon samples during the reaction process was identified, correlated with their catalytic performance. The influence of modification on chemical properties of catalysts and corresponding catalytic performance was also investigated. The systematic investigation could clarify the role of oxygenated surface groups in the catalytic oxidation of butane.

5.1 TEM

5.1.1 Nanocyl CNTs

The TEM images of pristine Nanocyl CNTs were display in Fig. 5.1. The CNTs have been acid-washed by manufacturer. It was shown that Nanocyl CNTs had a quite homogeneous morphology and distribution of diameters. The range of diameter is about 15-20nm and number of walls is about 5-10. CNTs were graphitized, but defects were also observed in high-resolution TEM (Fig. 5.1c and d).

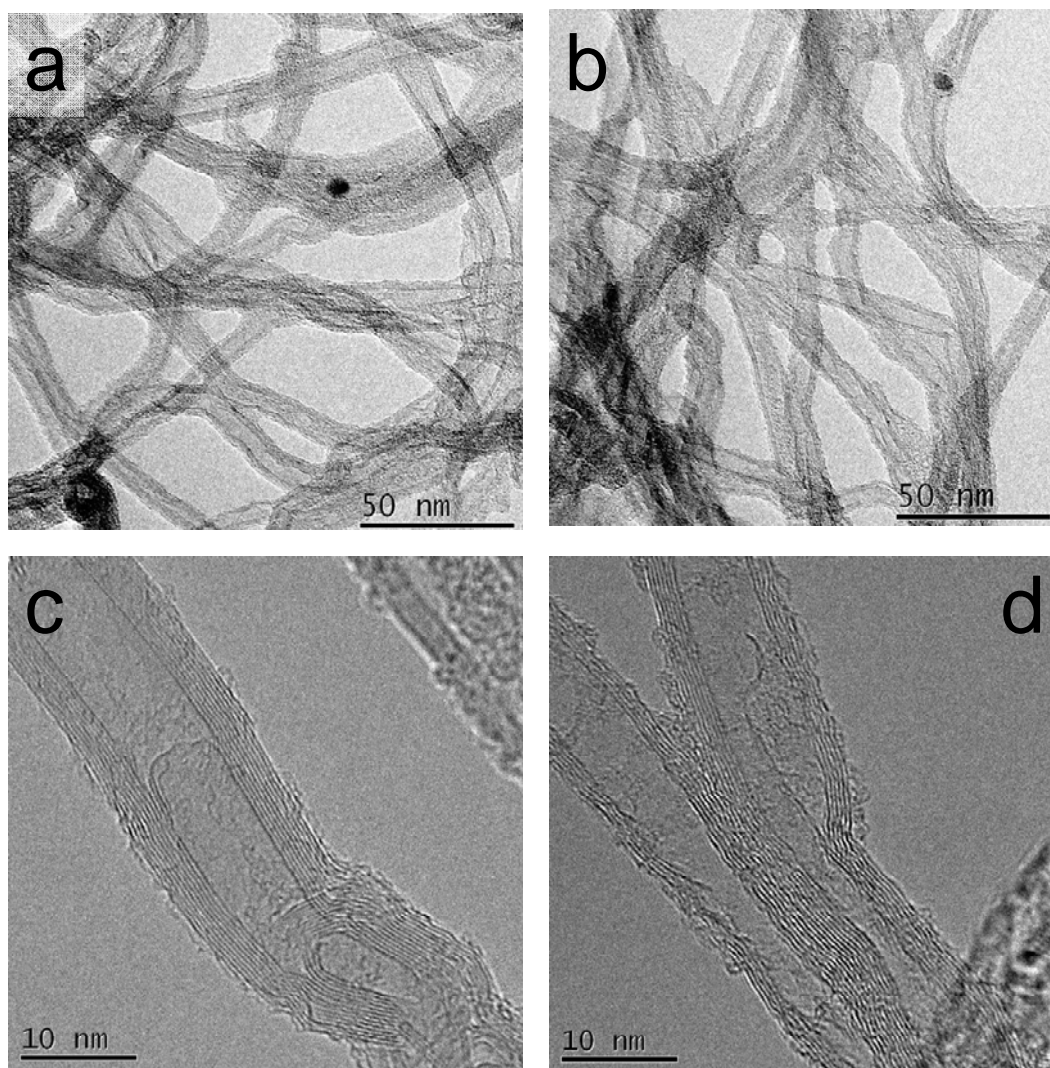


Fig. 5.1 TEM images of pristine Nanocyl CNTs: a and b) over view images; c and d) high resolution images

After two hours oxidation by concentrated nitric acid, no apparent difference was observed in the TEM images of Nanocyl-1 (Fig. 5.2b), but the amount of carbon nano particle was significantly decreased. The thermal treatment affected less on the morphology of oxidized Nanocyl CNTs at temperature of 973K (Fig. 5.2d and f). These suggest that the change in the bulk properties could be negligible during the calcination process.

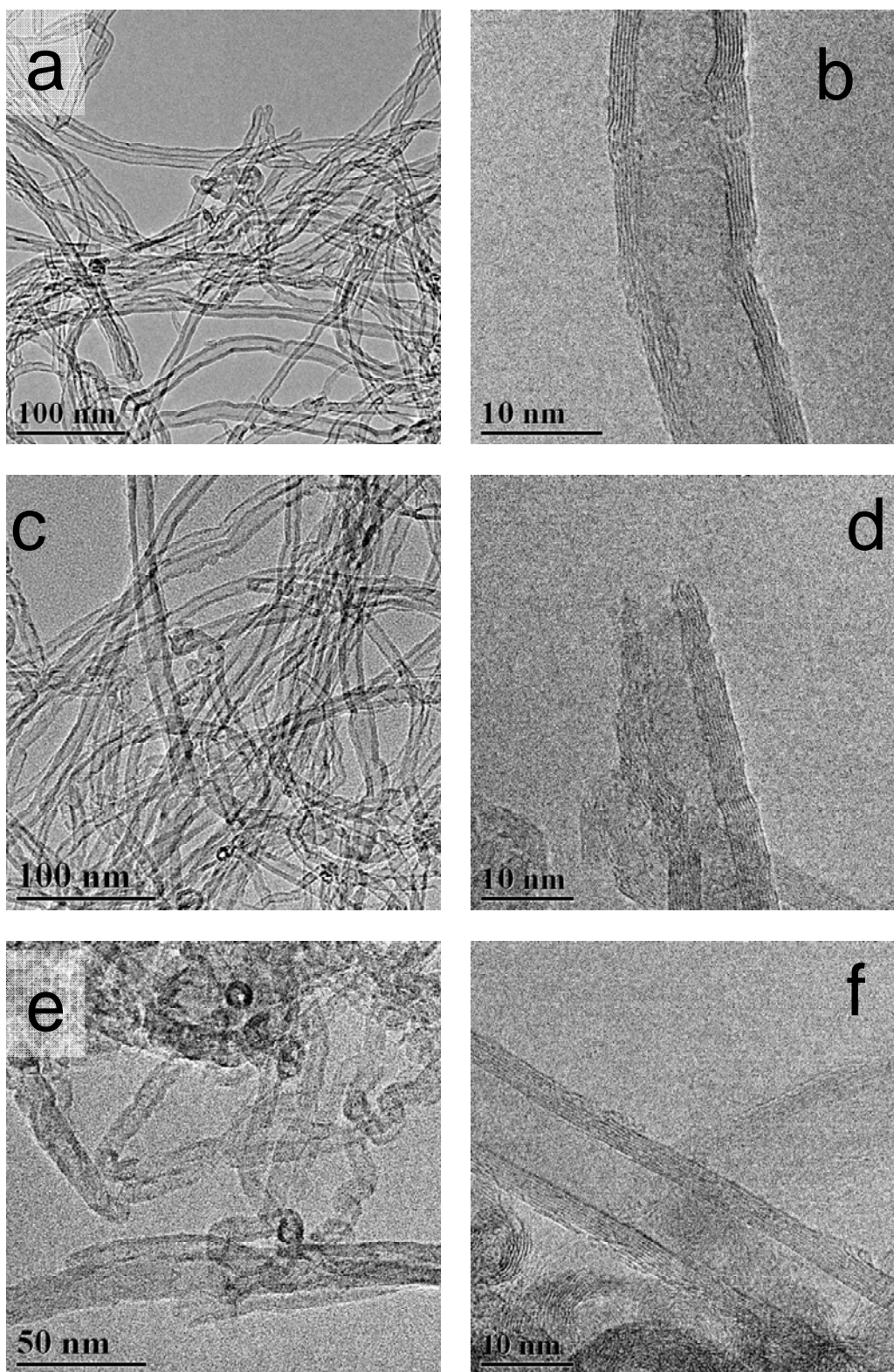
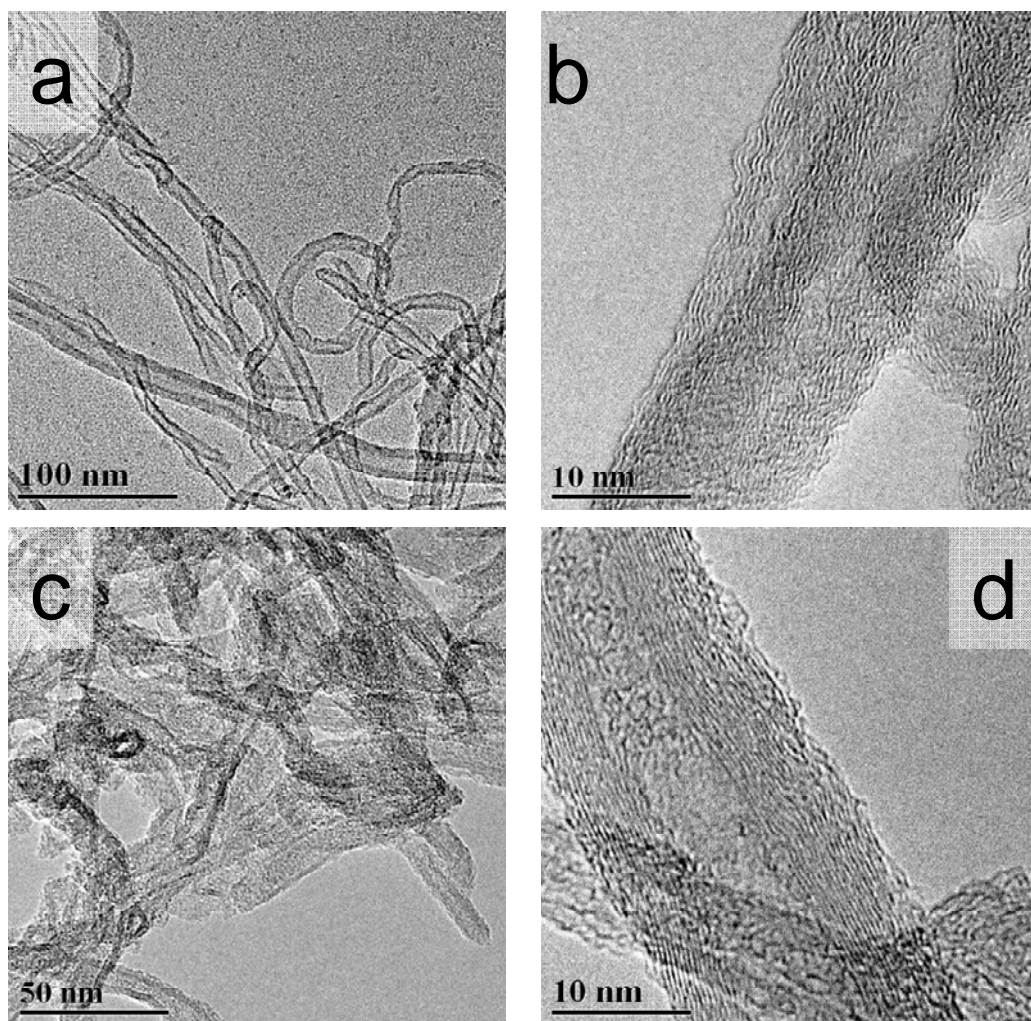


Fig. 5.2 TEM images of functionalized Nanocyl CNTs: a and b) Nanocyl-1; c and d) Nanocyl-2; e and f) Nanocyl-4;

The TEM images of phosphoric modified Nanocyl-2 were displayed in Fig. 5.3. Phosphate deposit on CNTs with low loading amount (2-5wt%) can not be observed in the HRTEM images, although it has been identified by EDX. However, the well distribution of phosphorus was observed in image of elemental maps (Fig. 5.3e). The phosphoric deposit turned out to be obvious when the loading amount was higher than 10 wt% (Fig. 5.3g and h, pointed by black arrow).



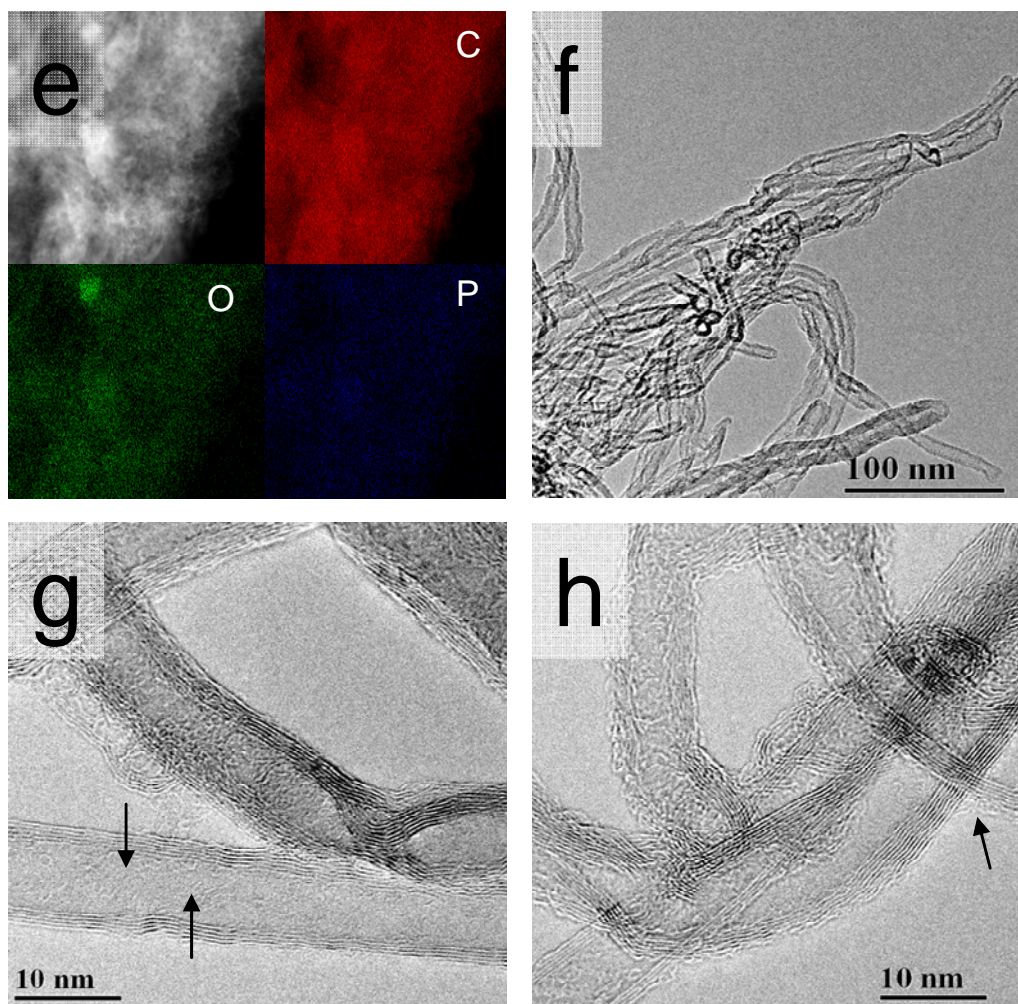


Fig. 5.3 TEM images of phosphoric modified Nanocyl-2 samples, a and b) 2%P₂O₅(N)-Nanocyl, c and d) 5%P₂O₅(N)-Nanocyl, e) element maps of 5%P₂O₅(N)-Nanocyl, f-h) 10%P₂O₅(N)-Nanocyl

The TEM images of carbon materials after reaction (Fig. 5.4) displayed less difference in morphology and microstructure of CNTs during reaction process, confirming the superior stability of CNTs catalysts during reaction process. It also suggests that the change in the catalytic performance of modified CNTs should not be related with their microstructure. It means that the investigation should be performed

using “organic surface groups” approach, corresponding to the chemical properties of modified or used catalysts. However, TEM is not a suitable method for this investigation.

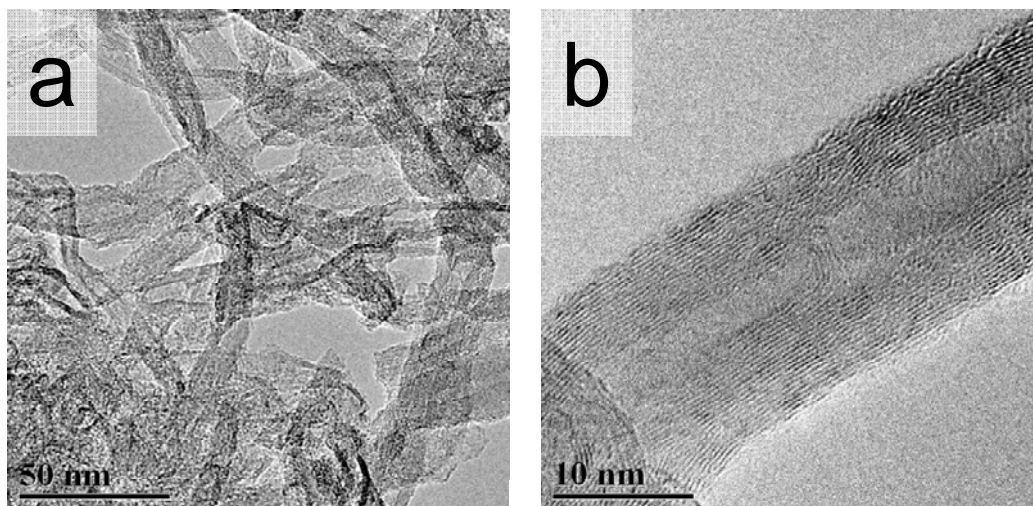


Fig. 5.4 TEM images of Nanocyl-2 sample after the catalysis reaction

5.1.2 PSLD CNTs

The TEM images of PSLD CNTs were displayed in Fig. 5.5. The diameter of CNTs ranges from 20nm to 200nm. The high resolution images displayed a composite microstructure: CNTs showed the herring-boned structure inside and poorly-graphitized layer outside. The thickness of those poorly-graphitized layers ranges from several nm to 50 nm. The angle between orientation of herring-boned graphene and axial of tube is about 30° (Fig. 5.5c and d). Impurities were also observed, like metal particles, carbon onion and amorphous carbon. The metal particles comprise of iron and nickel are deposited by graphitized carbon layers.

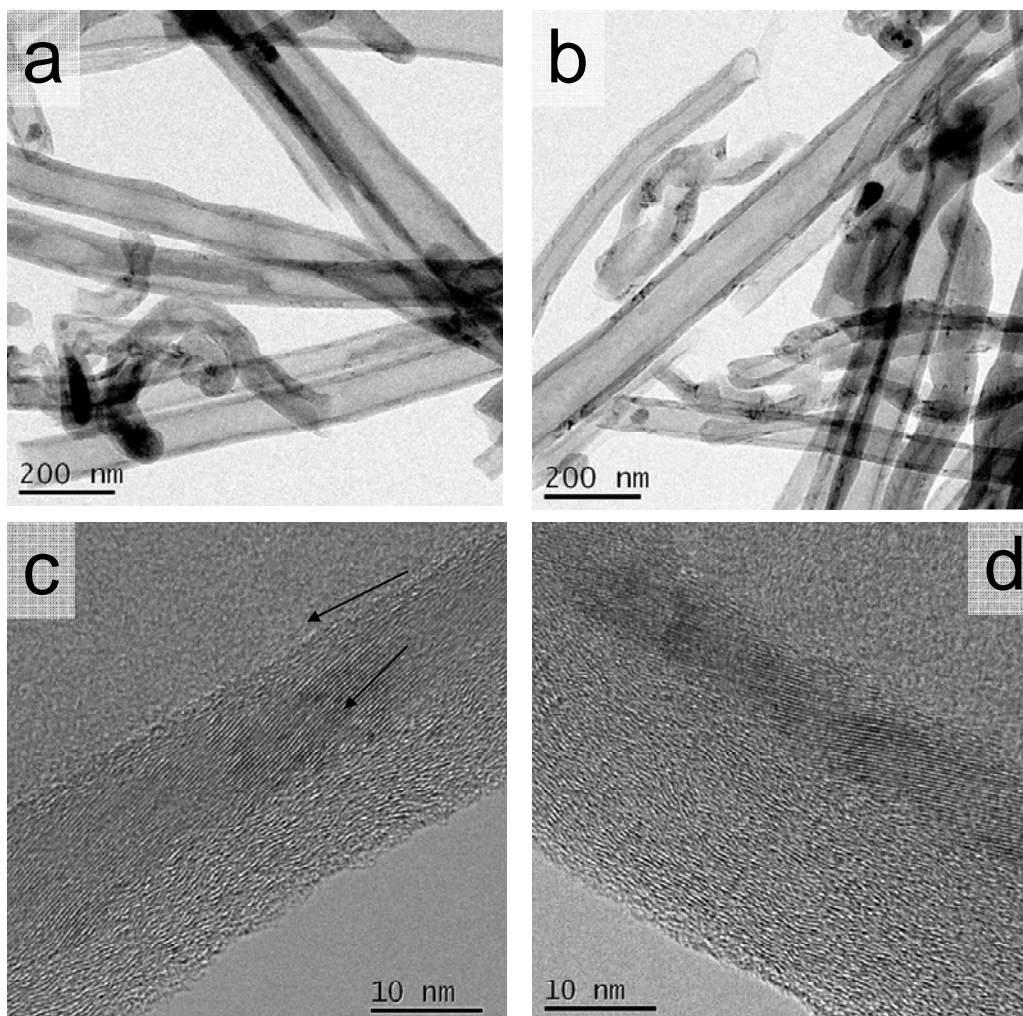


Fig. 5.5 a,b) TEM images of pristine PSLD CNTs c,d) HRTEM images of pristine PSLD CNTs

After 4 hours oxidation, less change in microstructure and morphology was observed in sample PSLD-4. The gradual removal of poorly graphitized carbon was displayed in the TEM images, attributed to further oxidation (Fig. 5.6 a-d). After 40 hours oxidation, only herring-boned nanofilaments were observed (Fig. 5.6 e and f).

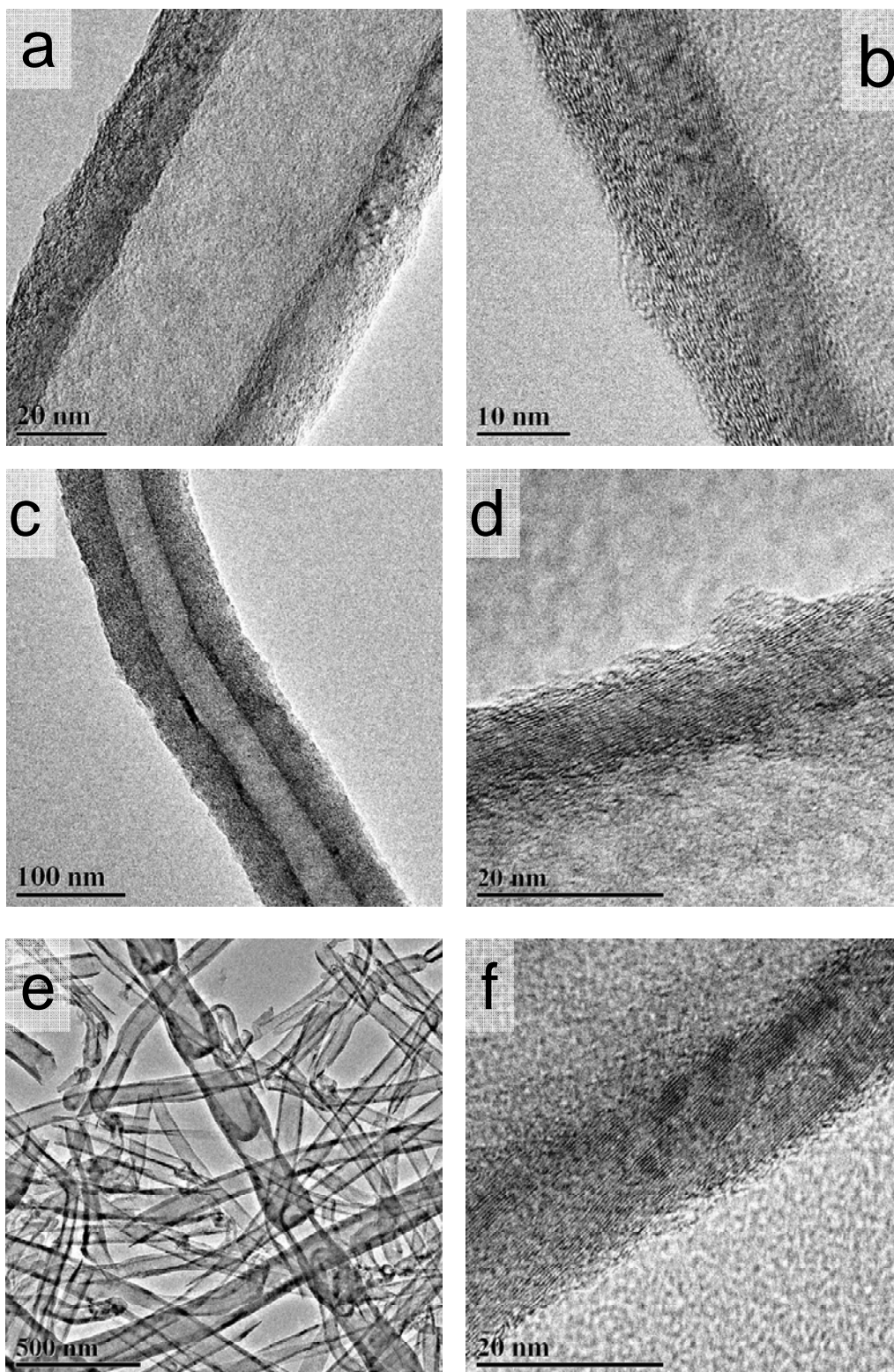


Fig. 5.6 TEM images of PSLD CNTs with different oxidation time, a and b)PSLD-4, c, d)PSLD-10, e, f)PSLD-40

No difference was also observed between the microstructure and morphology of samples before and after grafting (Fig 5.7), which can be attributed to the tiny size of moieties (several Å). But the immobilized molecules could also be destroyed by electron beams during TEM analysis. The more suitable characterization methods could be IR and XPS.

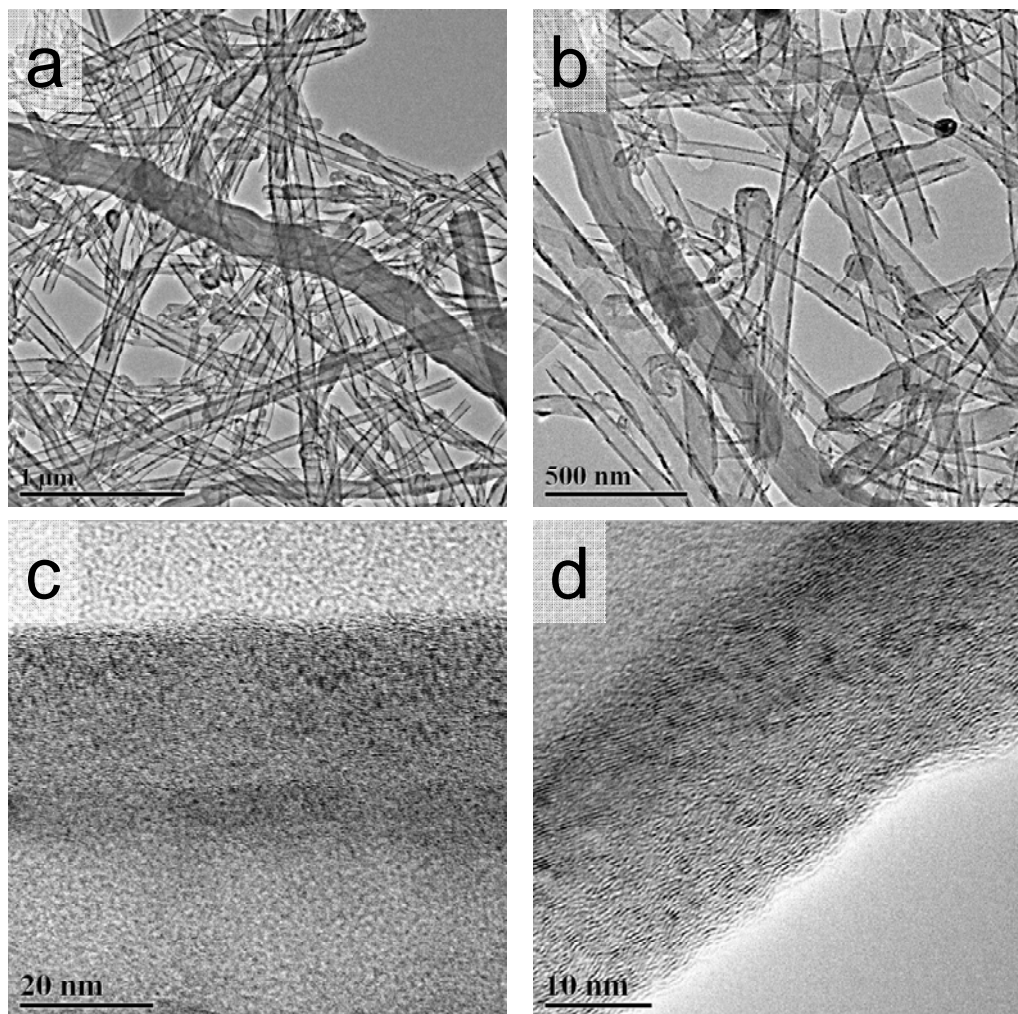


Fig. 5.7 TEM images of immobilized CNTs (M-PSLD-3)

No remarkable difference was observed in the HRTEM images of CNTs (PSLD and PSLD-40) before and after catalytic reaction (Fig. 5.8). The poorly graphitized layer of CNTs displayed a remarkable stability under the reaction condition. In addition,

carbon deposit can not be identified on the surface of either poorly graphitized layer or herring-boned carbon nanofilament.

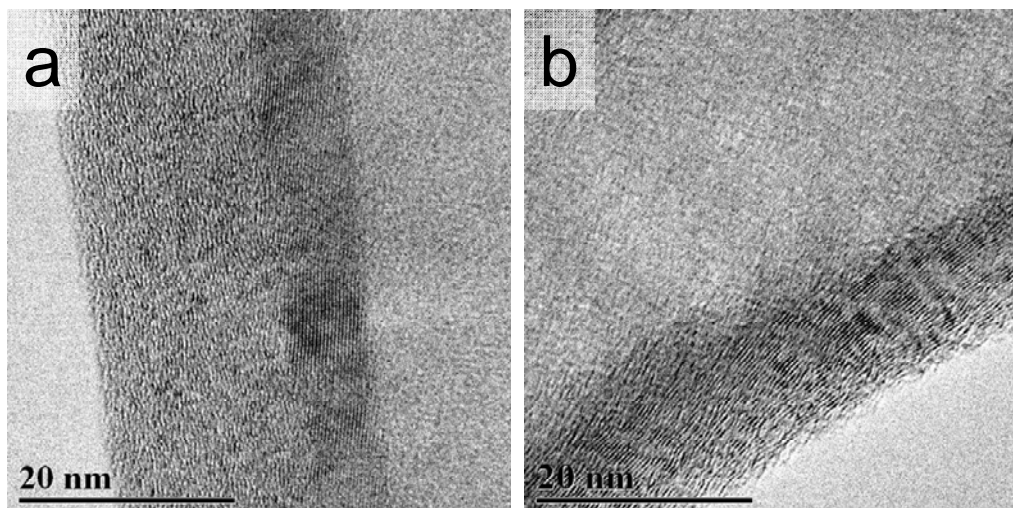


Fig. 5.8 HRTEM images of CNTs used in the catalysis reaction a) PSLD, b) PSLD-40

Less difference between morphology of pristine CNTs and modified CNTs was observed in the TEM images. The change in the microstructure and morphology of CNTs before and after reaction cannot be identified by TEM either. The observation gives the explanation of the catalytic stability of CNTs, confirming that there was not either combustion of CNTs or serious carbon deposition. It also suggests that the diversity in the catalytic performance of modified CNTs should not be related with their microstructure and morphology.

5.2 TPO, TPD, NH₃-TPD analysis of catalysts

5.2.1 Pristine Nanocyl CNTs

The pristine Nanocyl CNTs displayed a high activity but low selectivity to catalytic oxidation of butane. The TPD profiles displayed poorly functionalized nature of pristine Nanocyl CNTs, also confirmed by the NH₃-TPD profiles (Fig. 5.9). After

reaction, TPD profiles denoted even less functionalized properties of used CNTs with respect to a decreased amount of desorption CO and CO₂. It suggests that oxygenated surface groups were not involved in the reaction and other active sites on the surface of pristine CNTs should be mainly responsible for total oxidation. The variety of oxygen species at the edge sites and defects of graphene via dissociative or non-dissociative chemisorption process has been widely discussed.^[1-4] Obviously, the dissociative chemisorption didn't occur during the reaction process since the concentration of functionalities decreased after catalysis. The total oxidation could be attributed to the non-dissociated O₂⁻ and O₂²⁻ species on graphene sheet, which has been discussed in chapter 1.3.2.2.

Furthermore, the characterization proves that CNTs could not be functionalized and activated during the reaction process with the gaseous oxygen, hence challenging the assumption in literature.^[5-7] However, the prominent difference in chemical nature of carbon catalysts, reactants and reaction conditions was also observed. These also meant that the pre-treatment of catalysts, like chemical functionalization, should be necessary for improvement of catalytic activity. Then the further discussion about the chemical nature of carbon defects and oxygen functionalities would be denoted in Chapter 5.2.3.

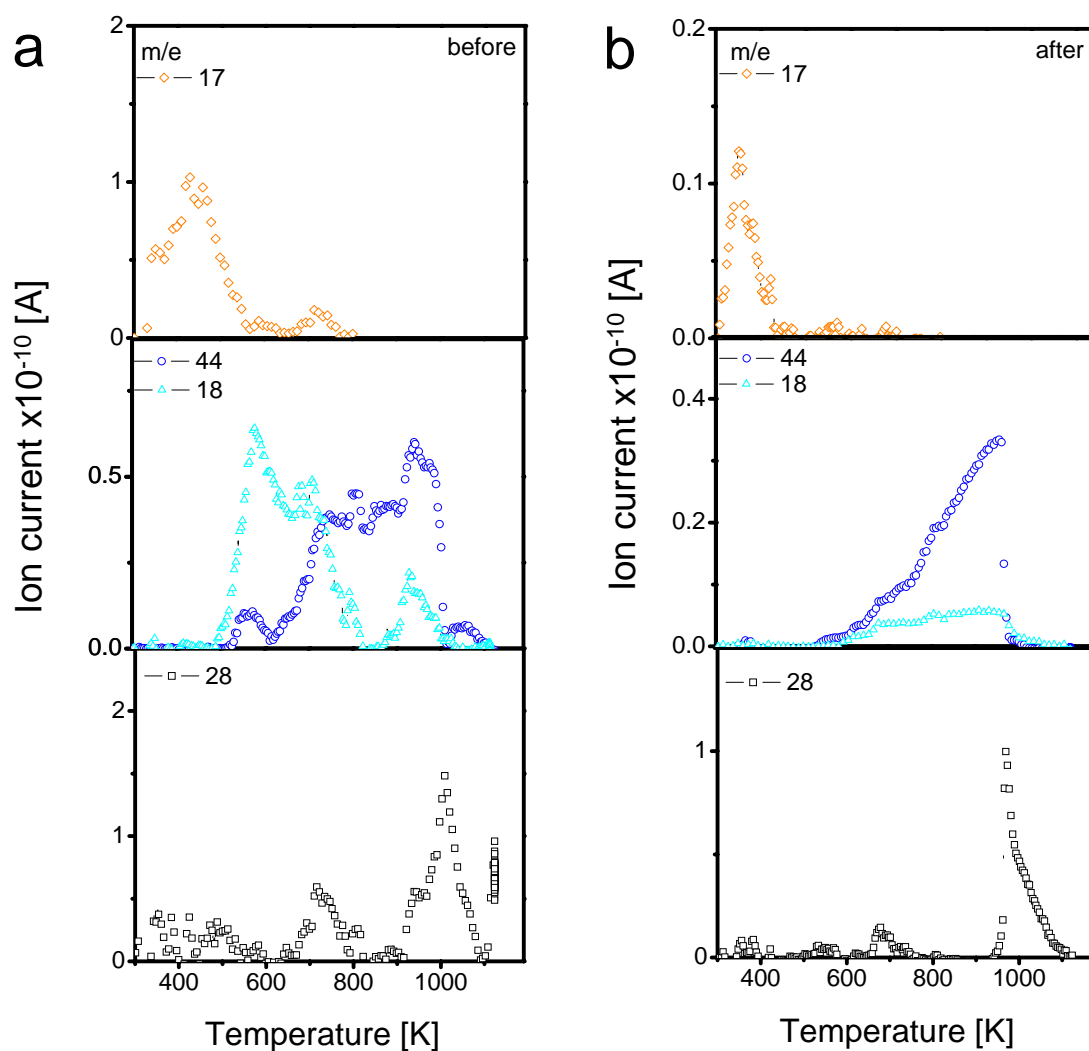


Fig. 5.9 TPD and NH₃-TPD profiles of pristine Nanocyl CNTs (Nanocyl) before (a) and after reaction (b)

A sharp peak with gasification temperature of 873 K was observed in the TPO profiles of the pristine Nanocyl CNTs, suggesting the homogenous feature of Nanocyl CNTs (Fig. 5.10). After reaction, the gasification temperature of CNTs increased 40 K higher. No peak was observed at low temperature in the used sample, suggesting that no coke formed during the reaction process.

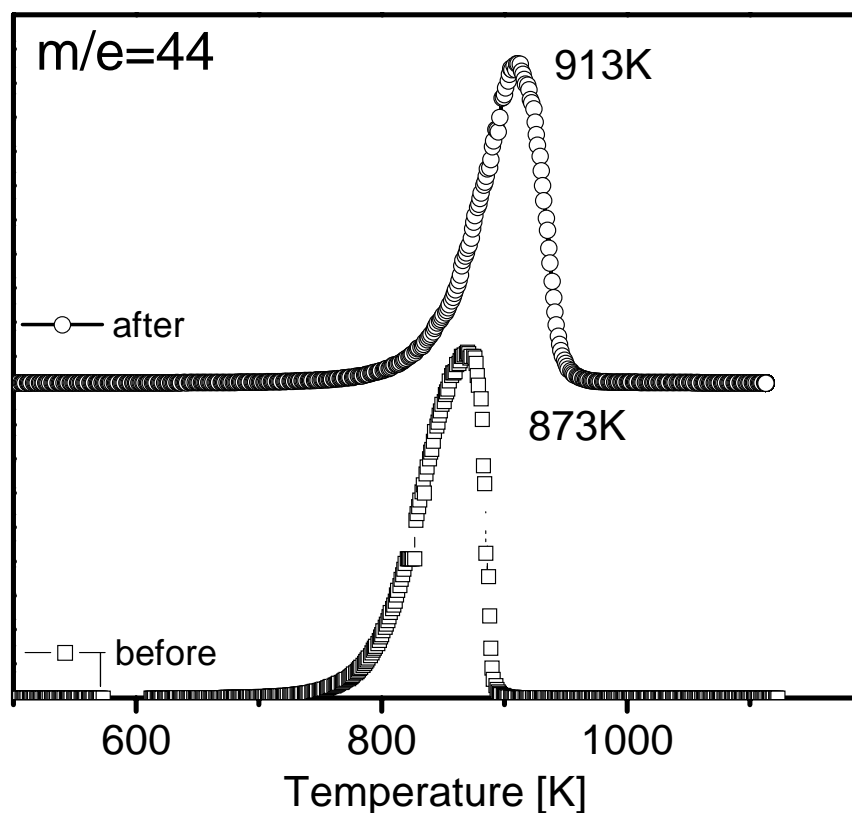


Fig. 5.10 TPO profiles of pristine Nanocyl CNTs (Nanocyl) before and after reaction

5.2.2 Oxidized Nanocyl CNTs

The easiest method to improve the oxygen amount on the surface of CNTs was oxidation, which was mentioned in Chapter 1.4.3.1. The TPD profiles of pristine Nanocyl CNTs and oxidized CNTs were displayed in Fig. 5.11. Apparently, the surface of oxidized CNTs (Nanocyl-1) was highly functionalized. In the TPD CO_2 profile, three peaks were identified at 560 K, 760 K and 970 K, assigned to the decomposition of carboxylic acid, anhydride and lactone, respectively.^[8] The deconvolution of CO profile of Nanocyl-1 displayed two CO desorption peaks at 770 K and 990 K, assigned to the

decomposition of anhydride and quinone groups, respectively. After calcination at 723K, a CO₂ desorption peak at about 630 K was observed, attributed to the remains of carboxylic acid groups. Furthermore, a broad CO₂ desorption peak observed at range of 800 to 1100 K should be assigned to co-desorption of anhydride and lactone. The calcination at 723 K significantly decreased the percentage of area of peaks at lower temperature in CO₂ desorption profile, contributed to the removal of thermally unstable functionalities. The same decrease was also observed in the CO desorption profile of Nanocyl-2 sample since the contribution of decomposition of anhydride to CO desorption species could be neglected. When further calcination was performed (≥ 973 K), few oxygenated surface groups were anchored in CNTs since relatively tiny peaks were observed in the profiles (Nanocyl-4). Notably, the desorption peak of CO assigned to the decomposition of quinone groups is quite broad (Fig.5.11b and c), suggesting the inhomogeneous nature of oxygenated surface groups on the CNTs. It means that there should be diversity in the chemical properties of quinone groups.

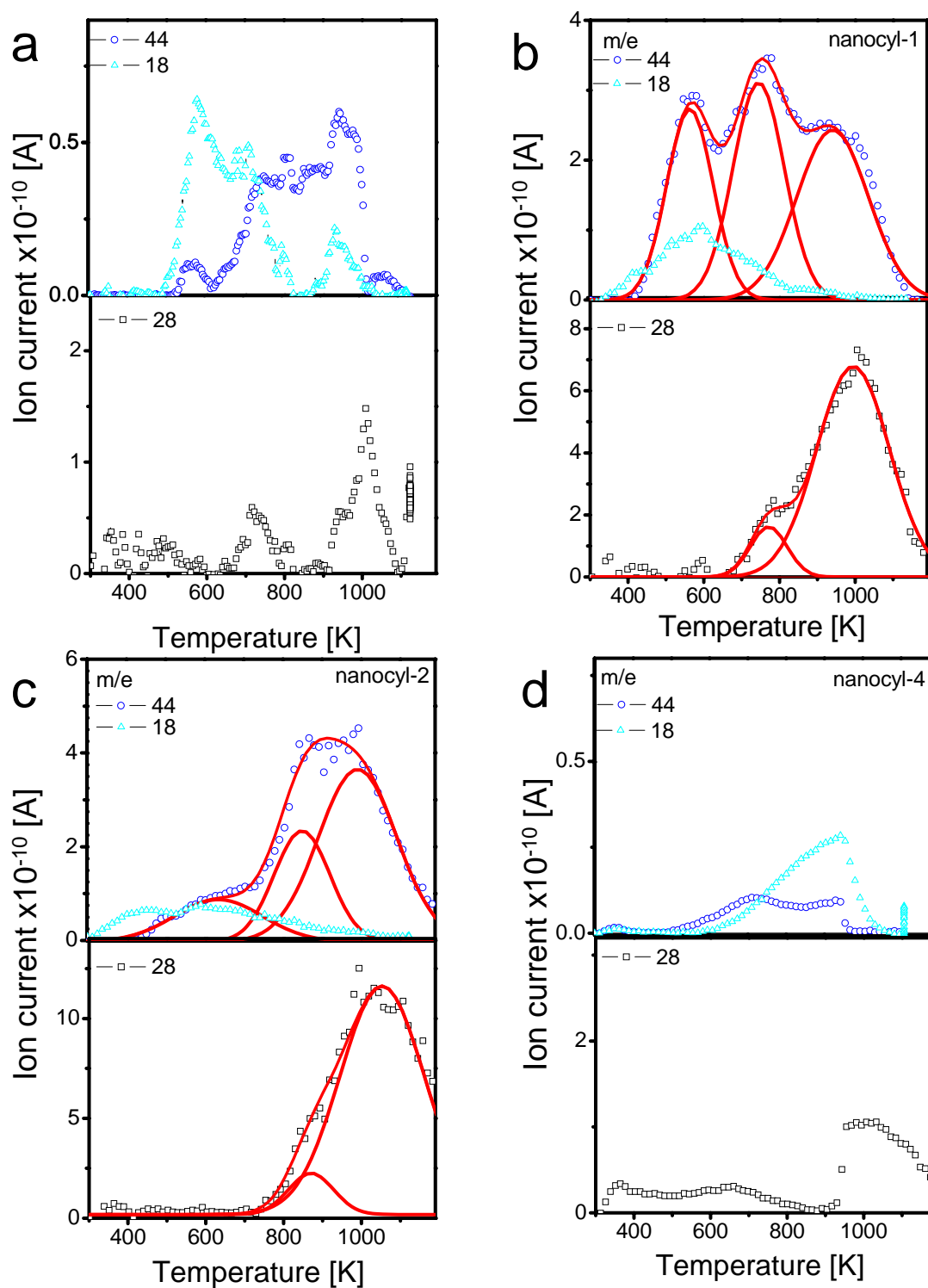


Fig. 5.11 TPD profiles of pristine and oxidized Nanocyl sample, a) Nanocyl, b) Nanocyl-1, c) Nanocyl-2, d) Nanocyl-4

The NH₃-TPD profiles of Nanocyl CNTs were displayed in Fig. 5.12. Apparently, the ammonia adsorption and desorption are related with surface oxygenated groups since no ammonia desorption peak was observed in the less functionalized CNTs (Nanocyl, and Nanocyl-4).

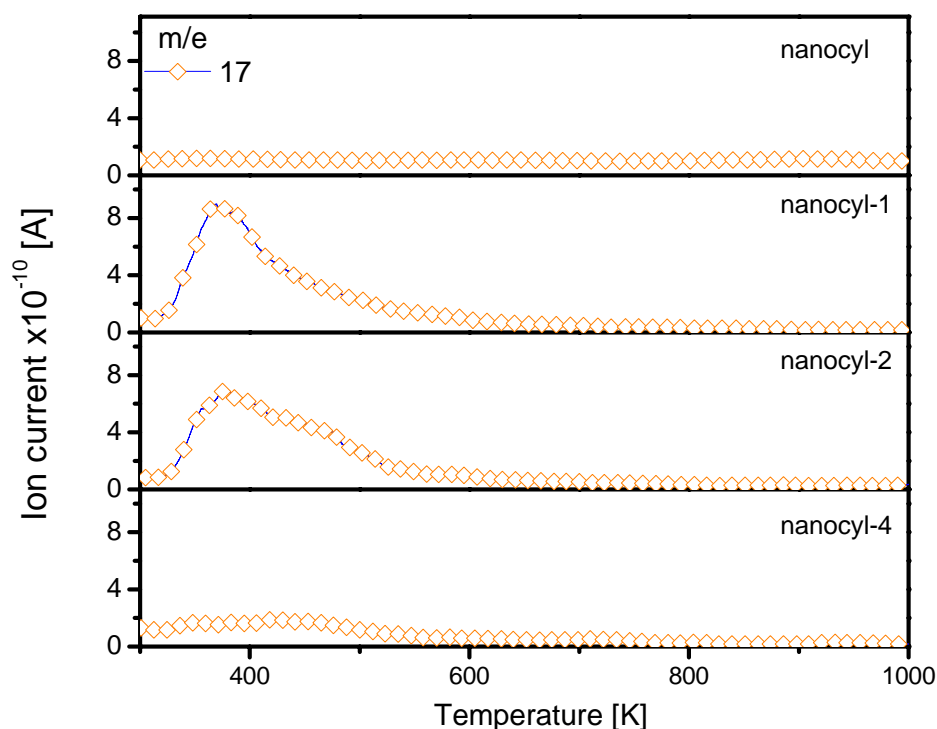


Fig. 5.12 NH₃-TPD profiles of pristine Nanocyl CNTs and oxidized Nanocyl CNTs

The oxidation treatment improved the catalytic performance of CNTs (Chapter 4.1). However, a significant loss in oxygen species was also observed in the catalyst (Nanocyl-2) during the reaction, even which has been calcined at 723 K for 2 hours (Fig. 5.13). Therefore, only a tiny desorption peaks of lactone at 973 K to 1073 K was observed in CO₂ profile of the used sample associated with the less desorption peak of NH₃. A similar decrease in amount of quinone groups was also observed. The significant

loss in oxygenated surface groups suggests that the majority of oxygen functionalities are not active sites for the catalytic oxidation of butane, which were removed during the reaction process.

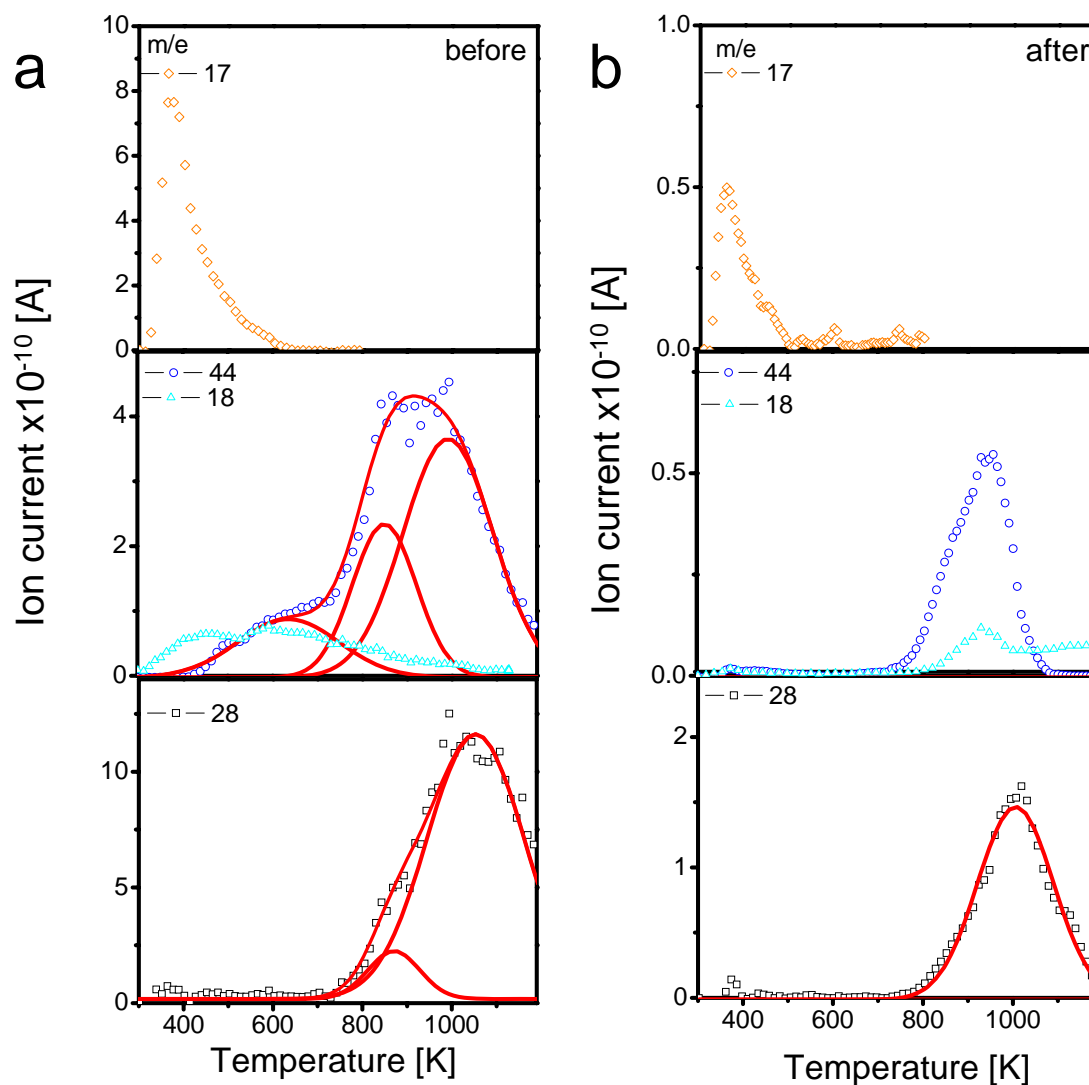


Fig. 5.13 TPD and NH_3 -TPD profiles of oxidized Nanocyl CNTs (Nanocyl-2) before (a) and after reaction (b)

The TPO CO_2 profiles of oxidized Nanocyl CNTs (Nanocyl-2) before and after the reaction were displayed in Fig. 5.14. Compared with the pristine CNTs, the gasification temperature of oxidized CNTs decreased 240 K lower. After reaction,

oxygenated surface groups were mostly removed and consequently the gasification temperature of used CNTs rose to 854 K. Correlated with TPO profiles of used pristine CNTs (Fig. 5.10), it means that the combustion of CNTs preferably occurred on the surface functionalization of CNTs.^[4]

Notably, carbon contamination was found in the used oxidized sample, as assigned to the small CO₂ peak at 603 K (circle dot, Fig. 5.14b). The carbon contamination could also be easily removed by water washing since the combustion peak at 603 K disappeared in the TPO profiles of the used CNTs after washing (Fig. 5.14c). It was also observed that the gasification temperature of washed sample increased, which might be attributed to the loss of smaller particle during the washing and filtering process.

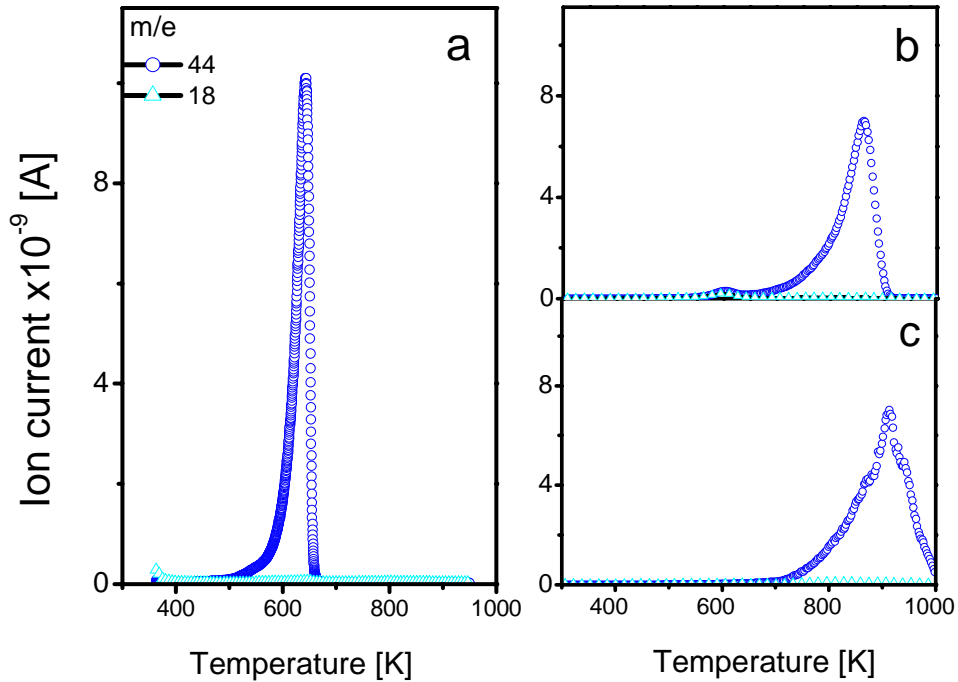


Fig. 5.14 TPO profiles of oxidized Nanocyl CNTs (Nanocyl-2) (a), used oxidized CNTs (b) and used sample washed by water (c)

5.2.3 Thermally treated Nanocyl CNTs

It was difficult to attribute the increase in selectivity to identical oxygenated surface groups, although oxidized CNTs displayed improved catalytic performance. The work done by Figureido revealed that the thermal treatment at low temperature affected less on catalytic performance, on the contrary, the thermal treatment at high temperature caused deactivation.^[12] However, the conclusion was quite questionable since the calcination at high temperature could change both of chemical nature and feature of activated carbons, resulting in the deactivation.

Therefore, the investigation method must be optimized, which has been demonstrated in Fig. 4.4 (P63). The TPD investigation was performed to identify oxygenated surface groups as well as to remove oxygenated surface groups out of surface of catalysts (Fig. 5.15).

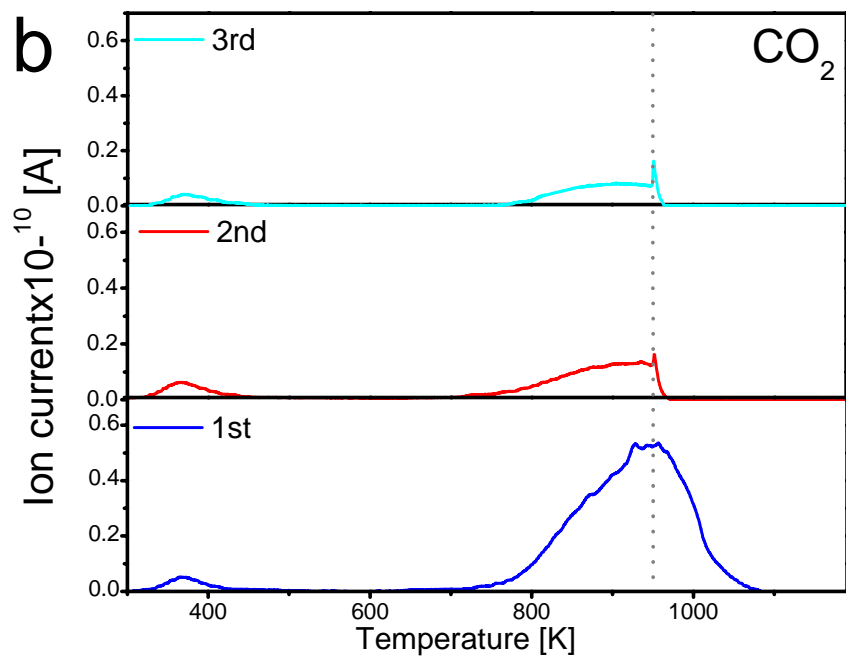
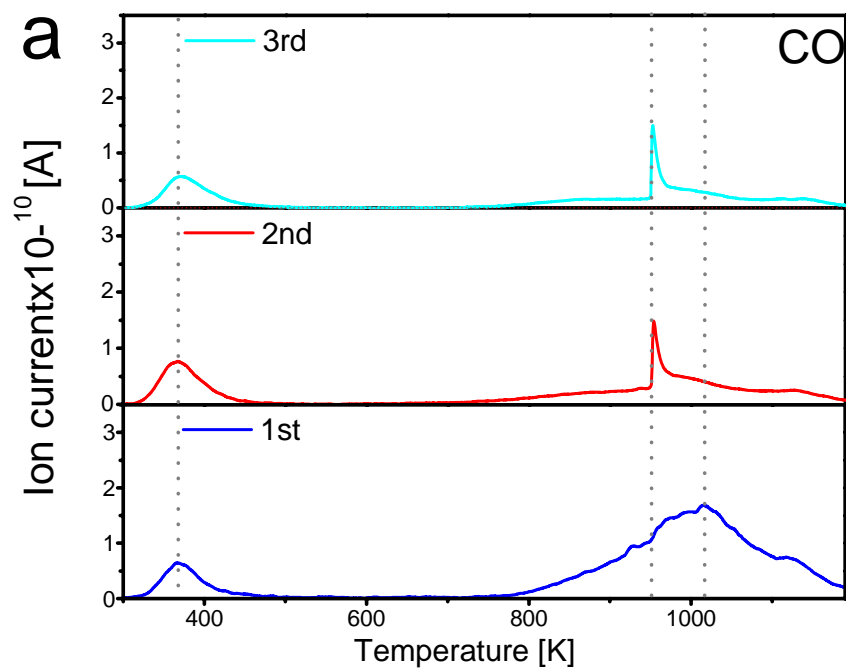
In the first TPD profiles, a broad CO desorption peak at 1000 K and CO₂ desorption peak at 950 K were observed, assigned to the decomposition of quinone groups and lactone groups, respectively. Although TPD performance could remove almost all oxygen species out of surface of CNTs, the regeneration of oxygen functionalities via chemisorption of gaseous oxygen was observed in the CNTs after catalytic test corresponding to the desorption of CO_x species in the second and third TPD performance. However, compared with the first TPD profiles, a significant difference was observed in the second TPD profiles: firstly, the area of desorption peak of CO_x species remarkably decreased; secondly, the shape of peaks also changed since a sharp peak at 950 K was observed in the CO desorption profiles. It means that after first TPD

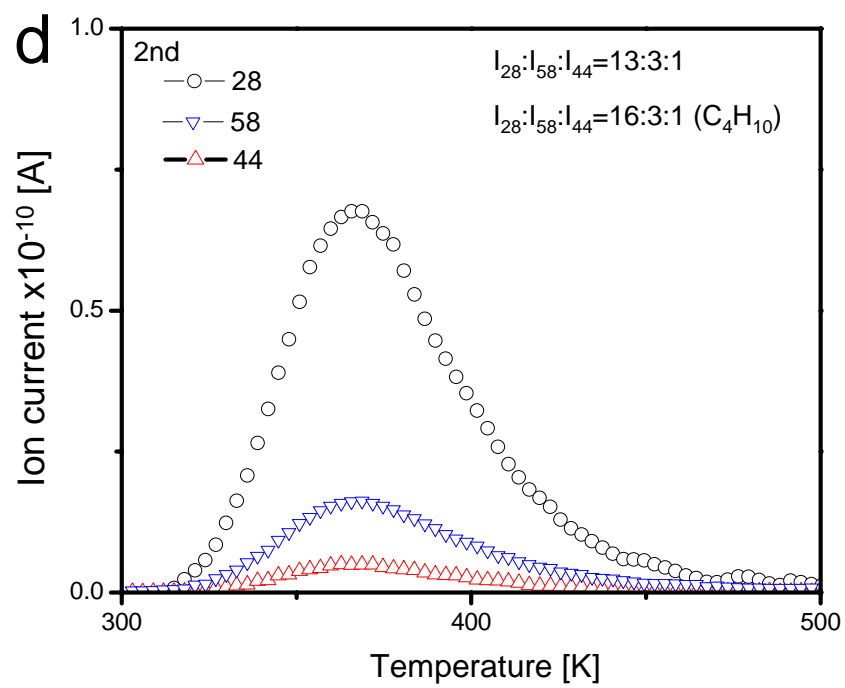
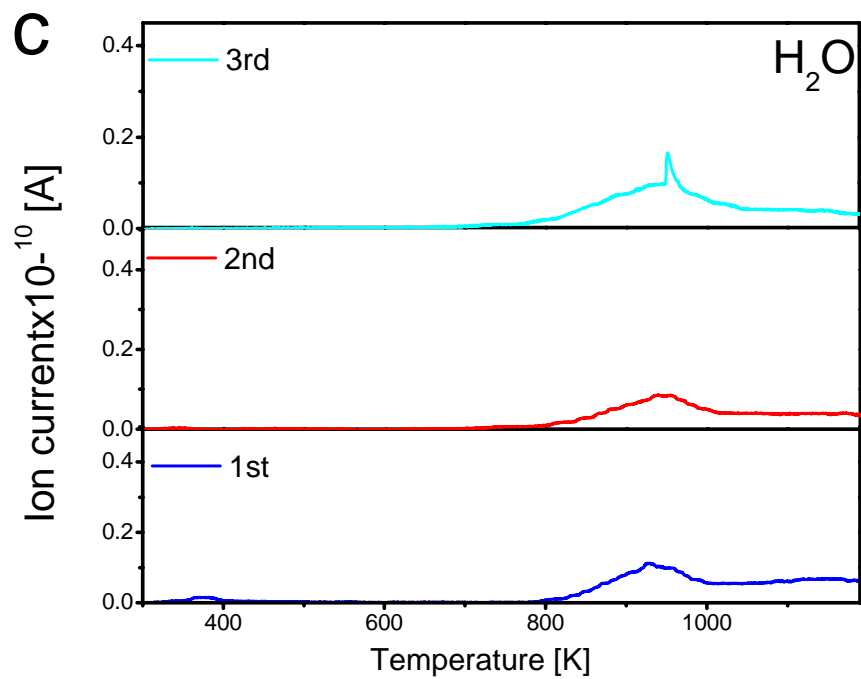
performance, a majority of carbon defects resulting from the removal of functionalities was less active for chemisorption of oxygen species. In addition, the oxygen functionalities regenerated from the chemisorption of oxygen were much different from the oxygen functionalities before first TPD performance.

The further TPD performance had less influence on the shape of CO_x desorption peaks (second and third TPD run), meaning there was less change in chemical nature of carbon defects during the further thermal treatment. The shape of CO desorption peaks in the second and third TPD performance was complicated, it is observed that the intensity increased slowly at the range of 650 K to 940 K and rapidly jump to a maximum at 950 K, afterward the intensity decreased slowly from 980 K to 1100 K. It could be attributed to the different oxygen functionalities. The sharp peak at 950 K should be associated with the homogeneity of chemical nature of some oxygen functionalities, resulting from the thermal treatment. However, the contribution of surface reaction between carbon oxides and surface defects, for instance, Boudouard reaction, should be considered associated with the sharp CO desorption peak at 950 K. A tiny water desorption peak at about 940 K was observed in all TPD performance due to the weak hydrogenation of oxygen functionalities during the catalytic oxidation. The similarity in peak shape and desorption temperature of water and CO₂ species suggests that the corresponding oxygen functionalities were hydrogenated. However, the less water desorption peaks implied that the re-oxidation of hydroxyl groups and following removal of water occurred quickly.

The desorption of some species with m/e equal to 44 and 28 was observed at low temperature (400 K) in all three TPD profiles, as well as species with m/e equal to 58.

The ratio of intensity of various peaks was shown in Fig. 5.15d, compared with the ratio of corresponding species in the reference gas (butane in He). It proved that the species with m/e equal to 28 and 44 could be attributed to the fragments of C_4 hydrocarbons, which were adsorbed on the surface of CNTs during the reaction process. It was also confirmed by isotopic experiment (Fig. 5.16) since no desorption peak of isotopic carbon oxides was observed at the same range of temperature. The mechanism investigation on the hydrocarbons adsorption on the CNTs has been reported, identifying the adsorption of butane on the different site of CNTs, for instance, interior, groove, and exterior sites.^[14] However, the identical desorption temperature ranged from 100 K to 200K, much lower than that in present work. The enhancement in interaction between hydrocarbon molecules with CNTs might be attributed to the functionalities. Notably, less change was observed among the three TPD profiles at low temperature (Fig. 5.15e), it means that the amount of active sites for adsorption of hydrocarbons should be similar even after TPD performance. For catalytic oxidation of hydrocarbons, the adsorption and activation of hydrocarbon molecules over active sites should be rate-determining steps. It implies that the catalytic performance of CNTs should be associated with the TPD profiles of hydrocarbons. This result supported the proposal that thermal treatment didn't change the amount of active sites for dehydrogenation.





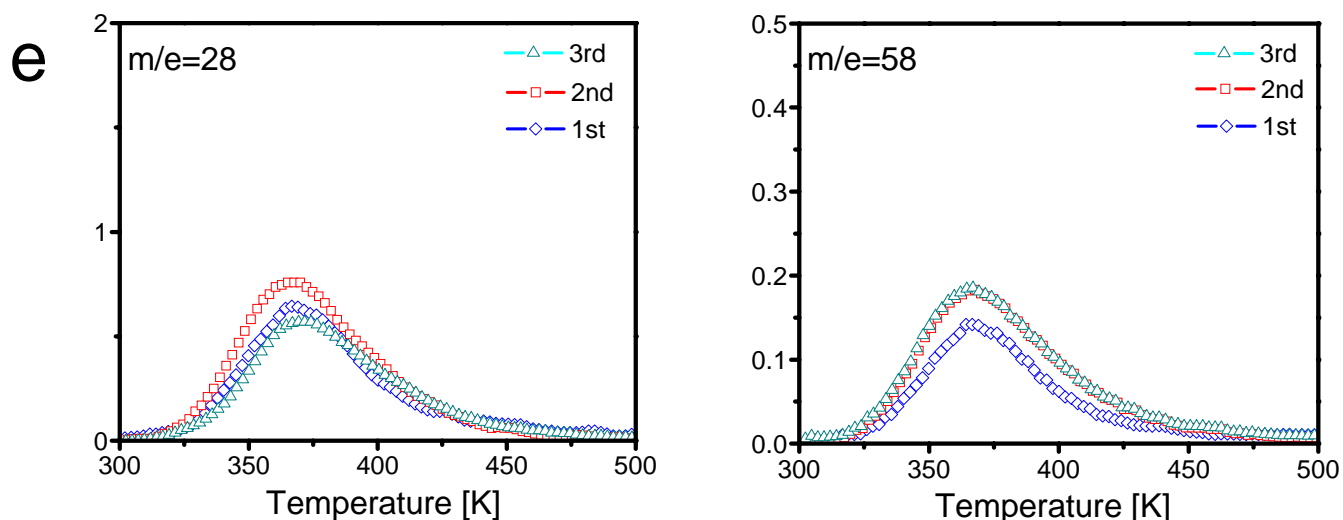


Fig. 5.15 TPD profiles of Nanocyl-2 CNTs during catalytic test-TPD cycling process, a) CO profiles; b) CO₂ profiles; c) H₂O profiles; d) desorbed species at low temperature in the second TPD performance and e) comparison between desorbed species (m/e= 28 or 58) during three TPD performance. In the third TPD profiles, the area of CO, CO₂ or H₂O includes the contribution of all isotopic species. For instance, the area (S) of CO is equal to the sum of area of peak with m/e=28 and area of peak with m/e=30. $S_{CO}=S_{28}+S_{30}$;

$$S_{CO_2}=S_{44}+S_{46}+S_{48}. S_{H_2O}=S_{18}+S_{20}.$$

Isotopic oxygen (¹⁸O₂) was used as oxidant instead of ¹⁶O₂ during the reaction process. The TPD performance demonstrated the exchanging of isotopic oxygen with oxygen functionalities during the reaction process, confirming that those functionalities should be active sites for the catalytic oxidation of butane. It means that the possible reaction pathway should include the recombination of hydroxyl groups (chapter 1, eq 1-13), not oxidation of hydroxyl groups (chapter 1, eq 1-15). Therefore, the regeneration of quinone groups occurred via the dissociative chemisorption of gaseous oxygen, wherein ¹⁶O was progressively being replaced by ¹⁸O.^[15, 16] The isotopic oxygen existed in both

CO and CO₂ desorption species, suggesting both quinone and lactone functionalities involved in the catalytic oxidation of butane. However, the readsorption and exchanging of carbon oxide species (isotopic scrambling) should also be considered.

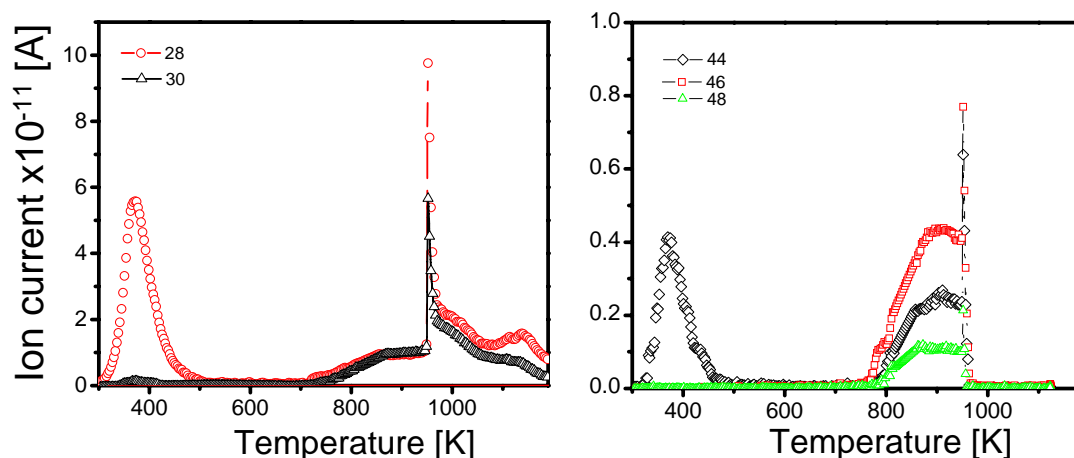


Fig. 5.16 Isotopic CO_x profiles in third TPD performance: left side CO and right side CO₂

The similar butane conversion and alkenes selectivity in the second and third catalytic test run were observed in Fig. 4.5 with respect to the significant release of CO_x species during TPD subsequent to catalytic test. It suggests that the catalytic oxidation of butane should be correlated with the oxygenated surface groups. However, a remarkable decrease in amount of oxygenated surface groups was observed during reaction process (Fig. 5.13), meaning that the majority of oxygenated surface groups generated via oxidation with acid was not involved in the catalytic reaction. It was confirmed by the observation that the CNTs with less oxygenated surface groups (after 1st, 2nd and 3rd TPD run) had similar catalytic activity to that with higher amount of functionalities (before TPD investigation). Although TPD treatment had less influence to butane conversion and C₄₌ products selectivity of oxidized CNTs, a significantly increase in butadiene yield was observed. The amount of active sites for the selective oxidation of butane was not

improved after TPD since the less change in butane conversion and alkenes selectivity was observed, which was supported by the same feature of desorption of hydrocarbon species at low temperature (Fig. 5.15e). The kinetic measurements confirmed that the butenes should be the primary products during the reaction process. It means that the increase in butadiene yield could be attributed to the stronger interaction between the hydrocarbon molecules and active sites, resulting in the further dehydrogenation. However, it is difficult to correlate the higher butadiene yield with increase in surface acidity since the significant decrease in amount of desorbed CO and CO₂ species was observed in first TPD performance. It implies that it should be attributed to the increase in the density of quinone groups in the relatively active site, facilitating the further dehydrogenation of butene products since neighbouring free quinone groups favoured the adsorption and further cleavage of C-H bond of hydrocarbon intermediate. For oxidized CNTs, the density of quinone groups in the active site was relatively lower due to the spontaneously generation of other oxygen functionalities via oxidation process. Therefore, the thermal removal of oxygenated surface groups facilitated the generation of zigzag or armchair carbon defects, wherein the consecutive formation of quinone groups resulting from the dissociative chemisorption of oxygen was thermodynamically favourable (Fig. 5.17).^[16] Consequently, the density of quinone in active sites was improved. In addition, homogeneity of quinone groups was also increased.

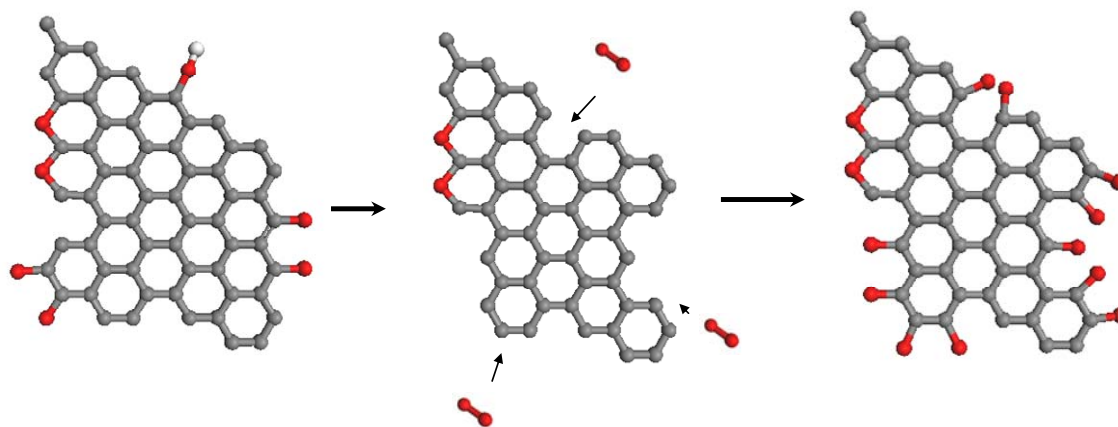


Fig. 5.17 Schematic illustration of removal and regeneration of oxygenated surface groups during the TPD and following catalytic test

The following conclusion can be drawn based on the thermal analysis on carbon samples. The pristine CNTs with poorly functionalized nature displayed a high activity and low selectivity to catalytic oxidation of butane, which should be attributed to the non-dissociative chemisorption of gaseous oxygen since less functionalization was observed during reaction process. After oxidation by nitric acid, the surface of CNTs was highly functionalized and its catalytic performance was improved either due to the generation of active sites, for instance, quinone groups, for the selective oxidation. However, the majority of oxygen species generated via oxidation didn't involve in the catalytic oxidation of butane, while progressively removed during the reaction process. The thermal treatment removed the most of oxygen functionalities, facilitating the generation of edge-side carbon defects and consecutive regeneration of quinone groups via the dissociative chemisorption of gaseous oxygen. The increase in density of quinone groups in active sites favored the further dehydrogenation of butane during the reaction process. However, the thermal treatment did not increase the amount of active sites. In addition,

the adsorption of educt at defects was observed, suggesting the strong interaction between hydrocarbon molecule and surface of CNTs.

The possible elementary steps proposed in chapter 1 (eq 1-8 to eq 1-12) were confirmed. The regeneration of quinone groups resulted from the recombination of hydroxyl groups and following dissociative chemisorption of gaseous oxygen. The strong adsorption of hydrocarbons at active sites and weakly hydrogenated nature of oxygenated surface groups suggests that the chemisorption and further cleavage of C-H bonds should be rate-determining step.

5.2.4 Phosphoric modified Nanocyl CNTs

After phosphoric addition, the shape and intensity of desorption peaks of oxygenated surface groups changed remarkably (Fig. 5.18). A comparison in TPD profiles of Nanocyl-2 and 5%P₂O₅(N)-Nanocyl displayed a significant decrease in both CO and CO₂ desorption peaks of phosphoric modified CNTs due to the calcinations of phosphoric modified samples. In CO₂ profiles, the peak at 1000 K should be assigned to the lactone groups. In CO profiles, the deconvolution displayed the contribution of two peaks at 980 K and 1100 K, assigned to the quinone groups and other high thermal stable functionalities. However, it is difficult to evaluate the contribution of phosphoric addition to desorption of CO_x species, even the shifting in the desorption temperature of CO species was observed. Compared to literature, it suggests that the decomposition of phosphoric carbon complexes should have contribution to the desorption peak of CO at 1100 K.

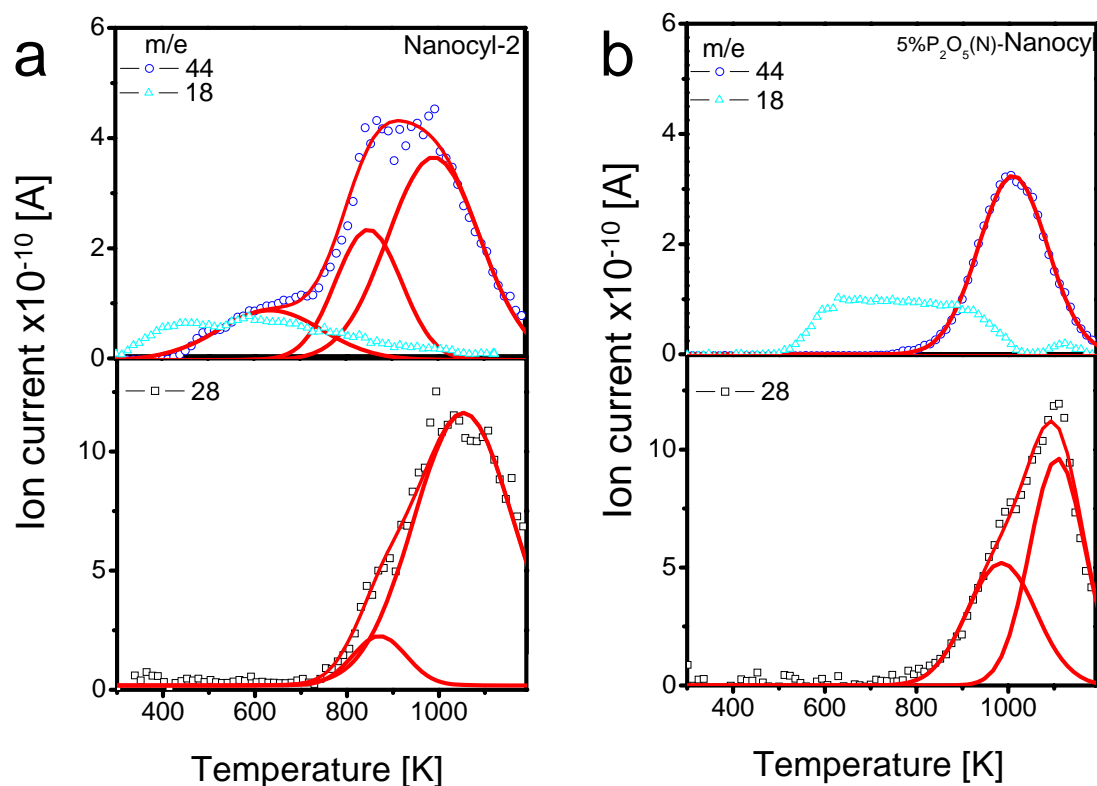


Fig. 5.18 TPD profiles of oxidized CNTs (left) and phosphoric modified CNTs (right)

When the loading amount was increased to 10wt%, less desorption amount of CO_2 and CO species was observed (Fig. 5.19). The decrease could be attributed to the calcination treatment after impregnation. We have discussed the contribution of phosphoric carbon complex to desorption of CO_x species at high temperature. It suggests that majority of oxygen functionalities of CNTs with high phosphoric loading amount (10wt%) was phosphoric carbon complexes. It means that the active sites for dehydrogenation were also covered by phosphoric addition in the case of CNTs with higher phosphoric loading amount, resulting in the decrease in both butane conversion and alkenes selectivity.

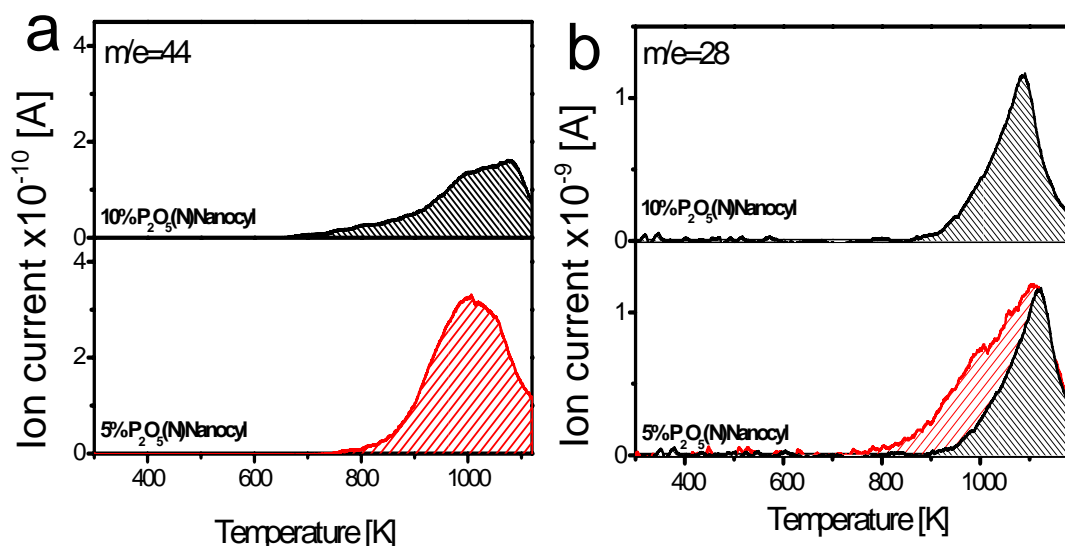


Fig. 5.19 TPD profiles of phosphoric modified Nanocyl samples, a) CO₂ , b) CO, for 10wt% and 5wt%P₂O₅ loading sample, the desorption species were labeled by dark shadow and red shadow, respectively

The TPD and NH₃-TPD profiles of phosphoric modified CNTs before and after reaction were displayed in Fig. 5.20. In CO₂ TPD profiles, a peak at 1000 K was observed in both TPD profiles, assigned to desorption of lactone. The deconvolution of CO TPD profiles displayed that there were two kinds of carbon oxygen complexes on the modified CNTs, whose desorption temperature was 1000 K and 1150 K, respectively. The former one should be attributed to desorption of quinone groups and the latter one should be attributed to the decomposition of phosphoric carbon complexes. No apparent water desorption peak was observed in the TPD profile of phosphoric modified sample after catalysis. It suggests that the quinone groups were not hydrogenated, in a good agreement with the TPD profiles of used oxidized CNTs. Obviously, after reaction, both decrease in CO_x desorption peak and ammonia desorption peak were observed, stating the less functionalized nature of catalyst after reaction. It confirmed that the majority of

oxygenated surface groups via oxidation did not have contribution to the catalytic performance at steady state. In the case of catalysts with higher phosphoric loading, a similar change in surface properties during the reaction process was observed in Fig. 5.21.

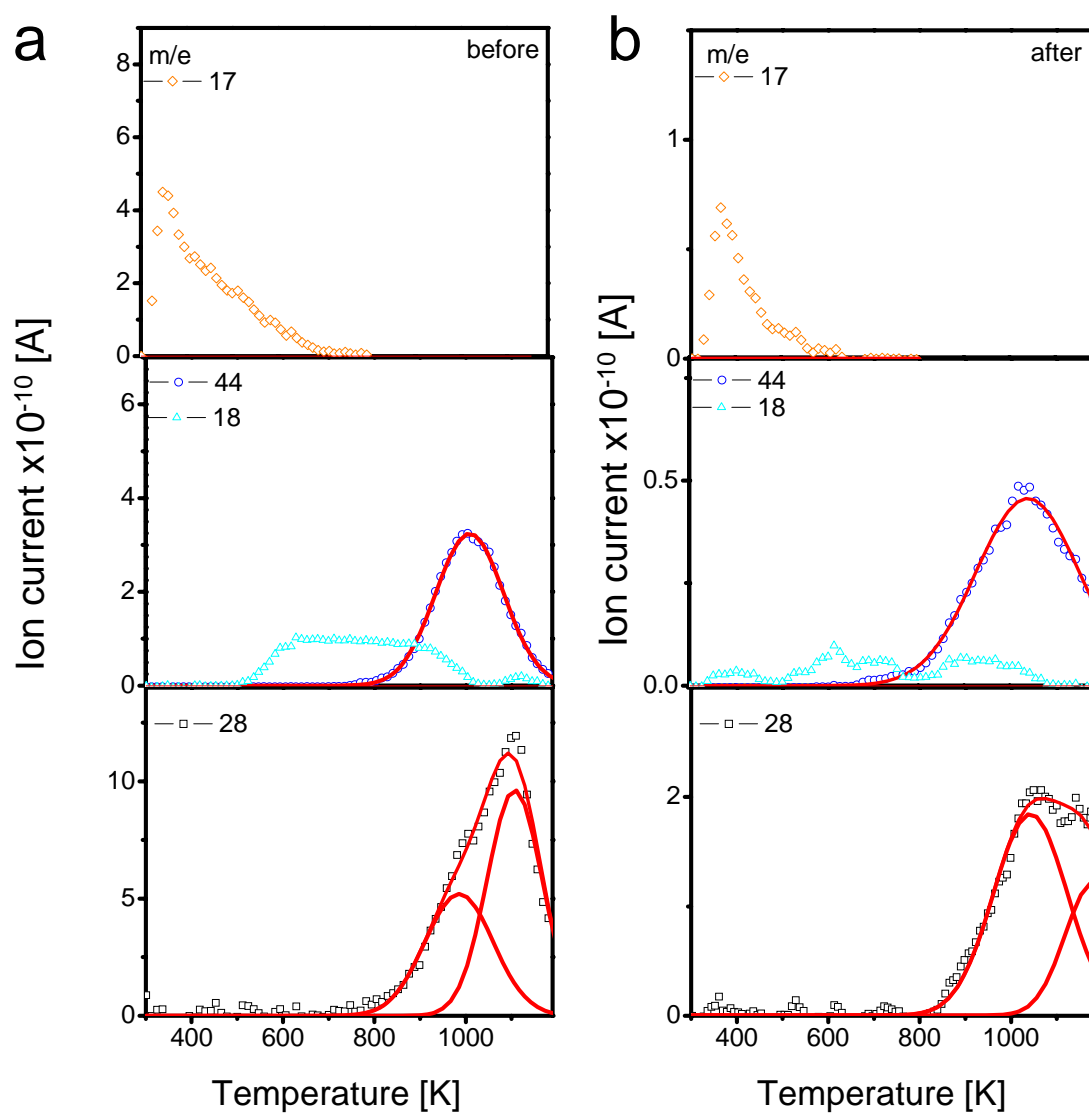


Fig. 5.20 NH_3 -TPD and TPD profiles of phosphoric modified Nanocyl CNTs (5% $\text{P}_2\text{O}_5(\text{N})$ -Nanocyl) before (a) and after reaction (b)

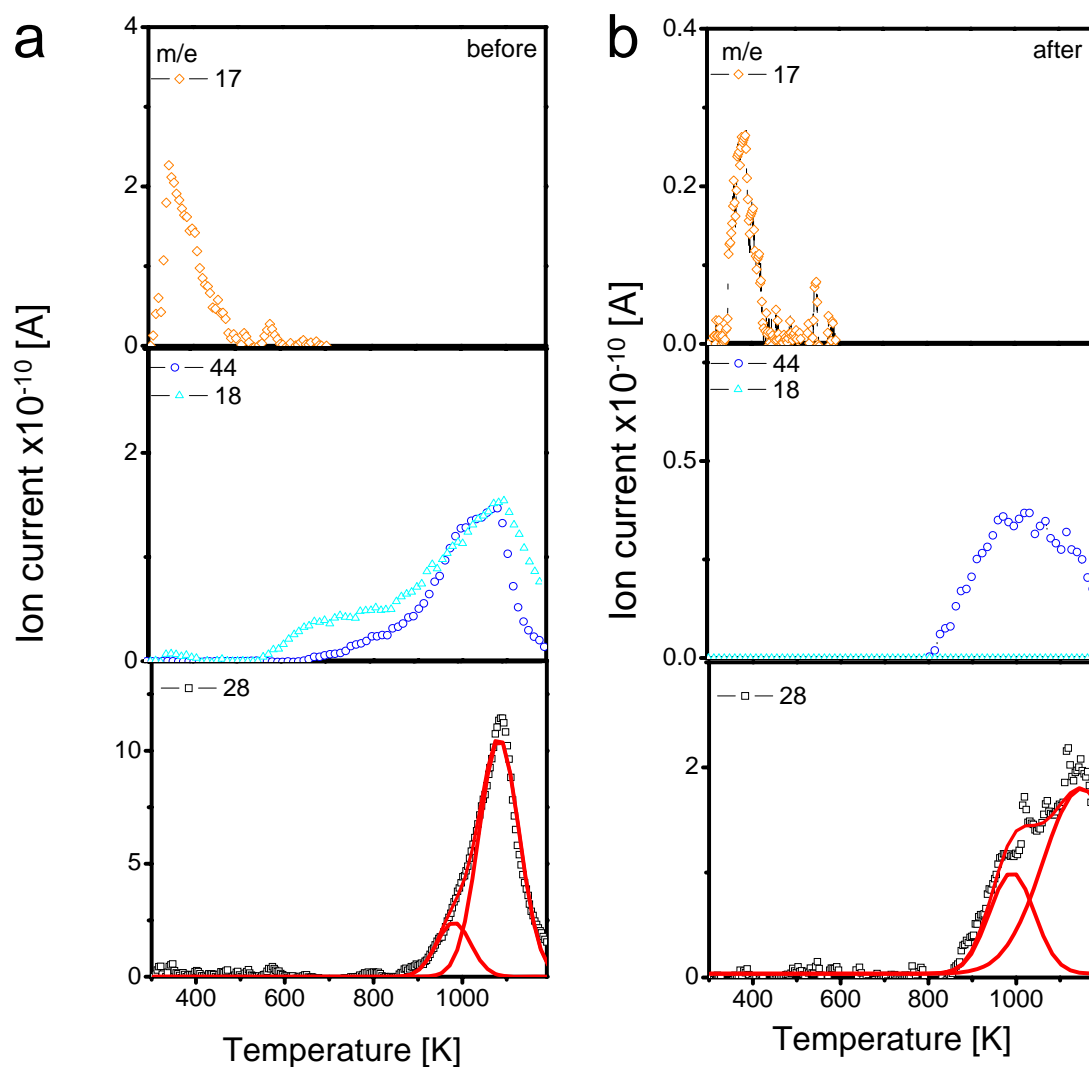


Fig. 5.21 NH₃-TPD and TPD profiles of phosphoric modified Nanocyl CNTs (10%P₂O₅(N)-Nanocyl) before (a) and after reaction (b)

The TPO profiles of phosphoric modified Nanocyl samples with different precursors and loading amount were displayed in Fig. 5.22. Obviously, phosphoric addition increased the gasification temperature of CNTs from 637 K (Nanocyl-2, Fig. 5.14) to about 936K (5%P₂O₅ (N)-Nanocyl). The loading amount had a positive influence on the temperature of gasification of CNTs. As can be seen, the gasification temperature

of CNTs with lower loading amount (5wt%) was 30 K lower than that with higher loading amount (10wt%) since there were still significant amount of oxygen functionalities free of phosphoric coverage on the surface of CNTs with lower phosphoric addition (5wt%). The change of precursors had less influence on the gasification temperature of carbon samples.

The increase in gasification temperature means the oxygen functionalities on the surface of CNTs were protected by phosphoric complexes from attacking of activated oxygen species.^[4, 17] Notably, It also confirmed that the addition of phosphoric acid could significantly inhibit the total oxidation of butane, though having no positive influence on C₄₌ products selectivity (in the case of activated carbon, chapter 4.5). In addition, the kinetic measurement proved that the increase in selectivity of phosphoric modified CNTs should also be attributed to the inhibition of total oxidation of butane.

Both inhibition of the oxidation of carbon catalysts (TPO) and total oxidation of butane (catalytic test) were observed in the case of phosphoric modified CNTs, displaying the correlation between the oxygenated surface groups and adsorbed hydrocarbons. It suggests that hydrocarbons should be adsorbed at the oxygenated surface groups, oxidized by activated oxygen species.^[18] Although it was ambitious that the inhibition should be associated with the physical barrier of phosphoric complex or the less reactivity of carbon defect strongly linked with phosphoric complexes.^[4] The improvement in catalytic performance of phosphoric modified CNTs (with low loading amount) and activated carbons suggests that the active sites for selective oxidation of butane were not poisoned by the phosphoric addition. The formation of phosphoric

carbon complexes should be attributed to the rearrangement of phosphoric oxide at high temperature. Although higher phosphoric addition amount favoured the inhibition of combustion of CNTs, the formation of phosphoric carbon complexes (Fig. 5.19) decreased the activity of active sites for selective oxidation of butane, resulting in the decrease in alkenes selectivity.

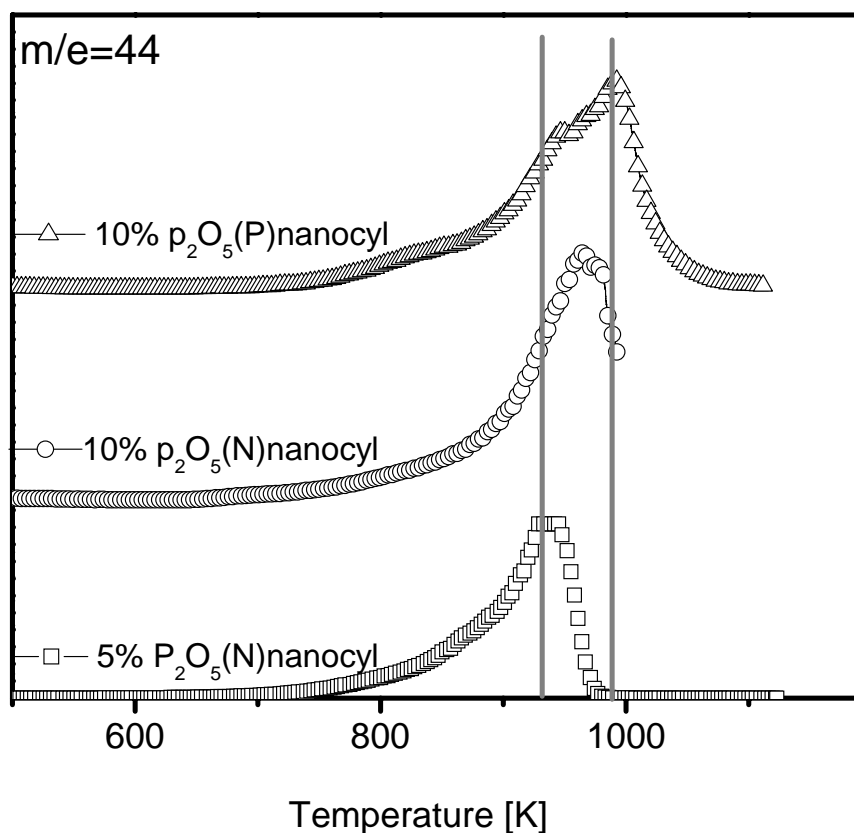


Fig. 5.22 TPO CO₂ profiles of 5%P₂O₅ (N)-Nanocyl, 10%P₂O₅ (N)-Nanocyl, and 10%P₂O₅ (P)-Nanocyl

A tiny peak with gasification temperature of 600 K in the TPO profile of used 5%P₂O₅ (N)-Nanocyl should be attributed to the contamination, similar to the TPO

profile of used Nanocyl-2 sample (Fig. 5.23). The loss in amount of oxygen functionalities was observed, but no significant difference was observed between the main gasification temperature of the samples before and after reaction.

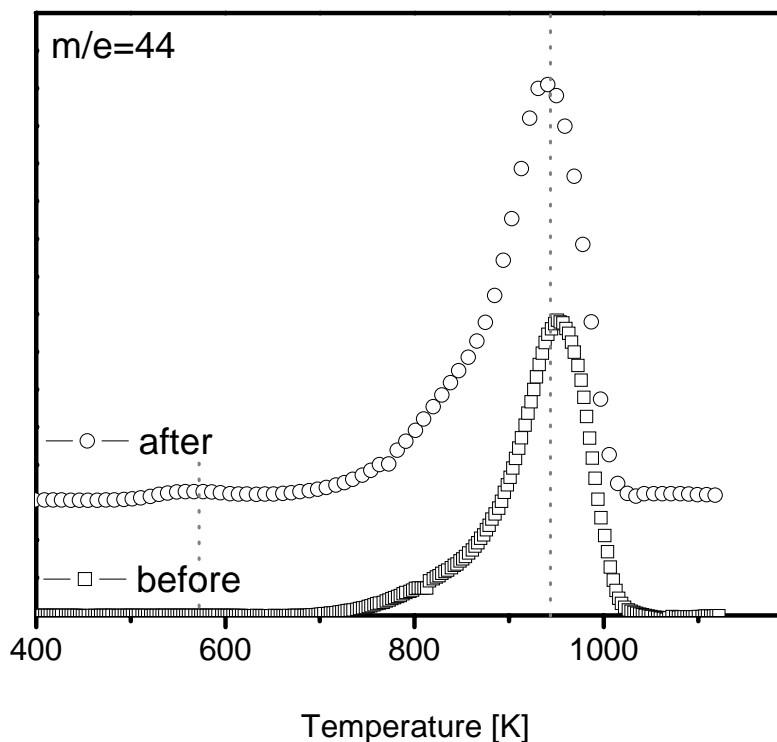


Fig. 5.23 TPO CO₂ profiles of 5%P₂O₅ (N)-Nanocyl before and after catalytic test

The gasification temperature of various Nanocyl CNTs catalysts before and after reaction was listed in Tab. 5.1. Obviously, for non-phosphoric-modified catalysts, the gasification temperature was associated with the functionalization degree since oxidized CNTs with the most functionality had lowest gasification temperature. The gasification temperature of used catalysts rose due to the removal of functionalities during the reaction process. Compared with the used pristine CNTs, the lower gasification temperature of used oxidized CNTs was observed due to the remains of quinone and

lactone groups. For phosphoric modified CNTs, the gasification temperature was less influenced by the amount of oxygenated surface groups. The gasification temperature of phosphoric modified CNTs was much higher than other non-modified samples, meaning that even quinone and lactone groups remained on the surface of used CNTs were also protected by phosphoric complexes.

Tab. 5.1 Gasification temperature of Nanocyl CNTs before and after reaction

Catalysts	Gasification temperature K	
	Before	After
Pristine Nanocyl CNTs	873	913
Nanocyl-2	634	854
5%P₂O₅ (N)-Nanocyl	936	930

Obviously, it confirmed that the increase in selectivity to alkenes could be attributed to the deposition of polyphosphoric acid over the CNTs since the attacking of activated oxygen species to carbon defects was hindered. The formation of phosphoric carbon complexes was also observed due to the rearrangement of phosphoric complexes at high temperature.

5.2.5 PSLD CNTs

The TPO CO₂ profiles of PSLD CNTs were shown in Fig. 5.24. In the CO₂ profile of the pristine PSLD CNTs, only one peak at 973 K was observed. The gasification temperature of oxidized samples decreased to 873 K due to creation of defects by oxidation. The TPO profiles of oxidized CNTs were complicated: the peaks were broad and asymmetric, attributed to the inhomogeneous feature of CNTs (Fig. 5.5). The existence of the poorly graphitized carbon layer could be one reason. In TPO CO₂ profile

of PSLD-4, two peaks were observed. One was 873 K and another was about 923 K. When the CNTs were further oxidized and the poorly graphitized outer layers were gradually exfoliated (Fig. 5.6), the relative intensity of first peak decreased. It means that the peaks at 873 K and 923 K could be assigned to the poorly graphitized layers and carbon nanofilaments, respectively. Particularly, TPO profile of over-oxidized sample (PSLD-40) still displayed asymmetric morphology, attributed to the wide distribution of diameter of CNTs.

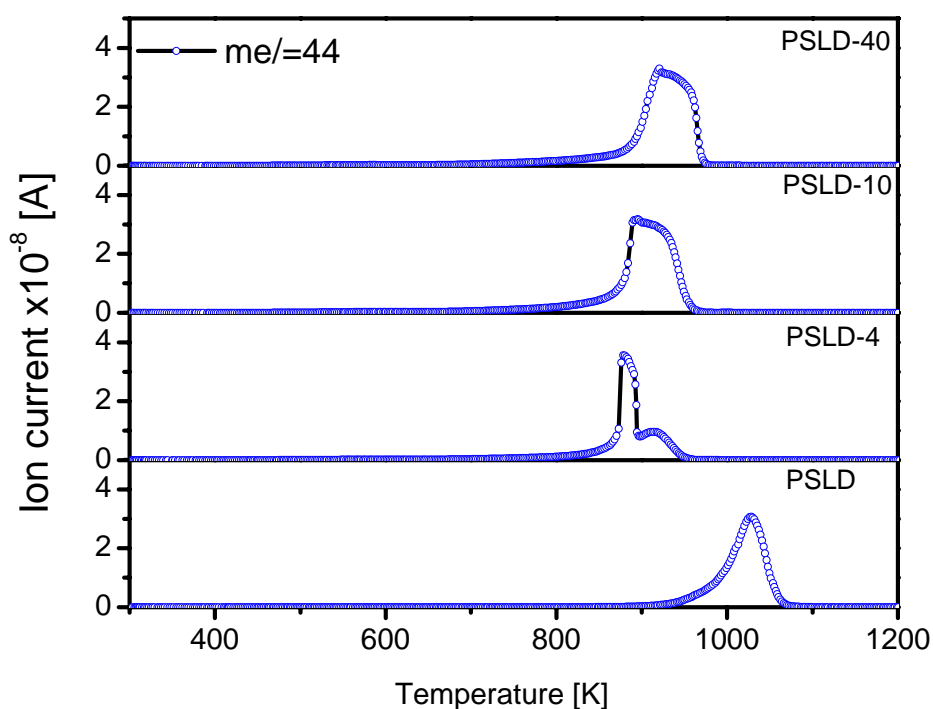


Fig. 5.24 TPO CO₂ profiles of pristine and oxidized PSLD CNTs

Obviously, phosphoric addition could increase the gasification temperature of carbon materials (Fig. 5.25). It was observed that there were two peaks, whose gasification temperature was about 823 K and 993 K, respectively. The loading amount

had slight influence on the gasification temperature, while increase of 20 K was observed in the gasification temperature of CNTs with higher loading phosphoric oxide. There was a significant difference between the peak shapes of oxidized CNTs and phosphoric modified CNTs, partially attributed to the characterization condition (heating ramp). The former one was operated with 10 K/min and latter one with 2 K/min. The higher heating ramp resulted in the problem of diffusion and shifting the gasification to higher temperature. The increase in gasification temperature of phosphoric modified CNTs could also be attributed to the surface modification.

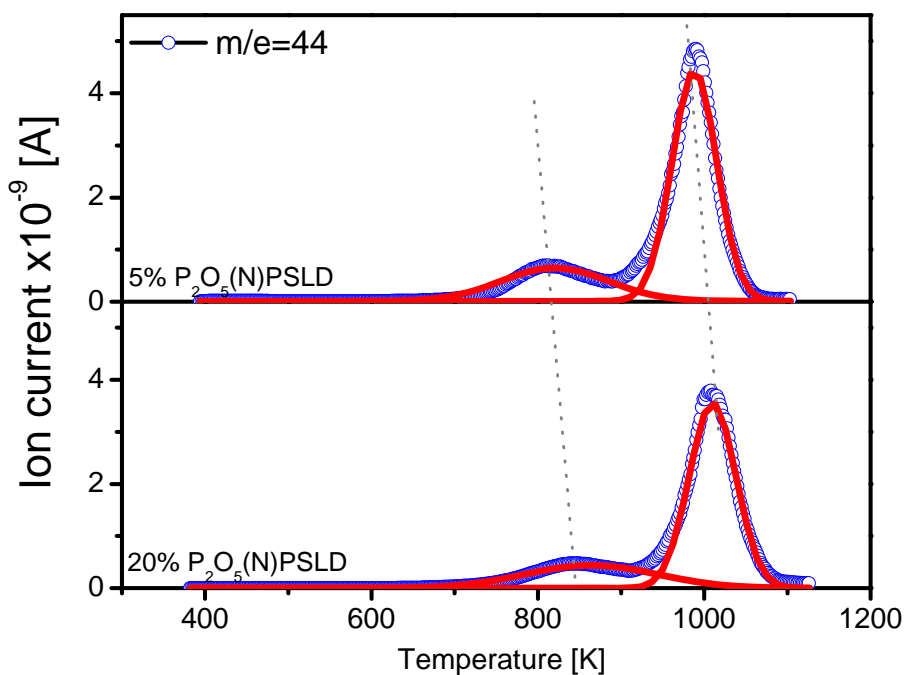
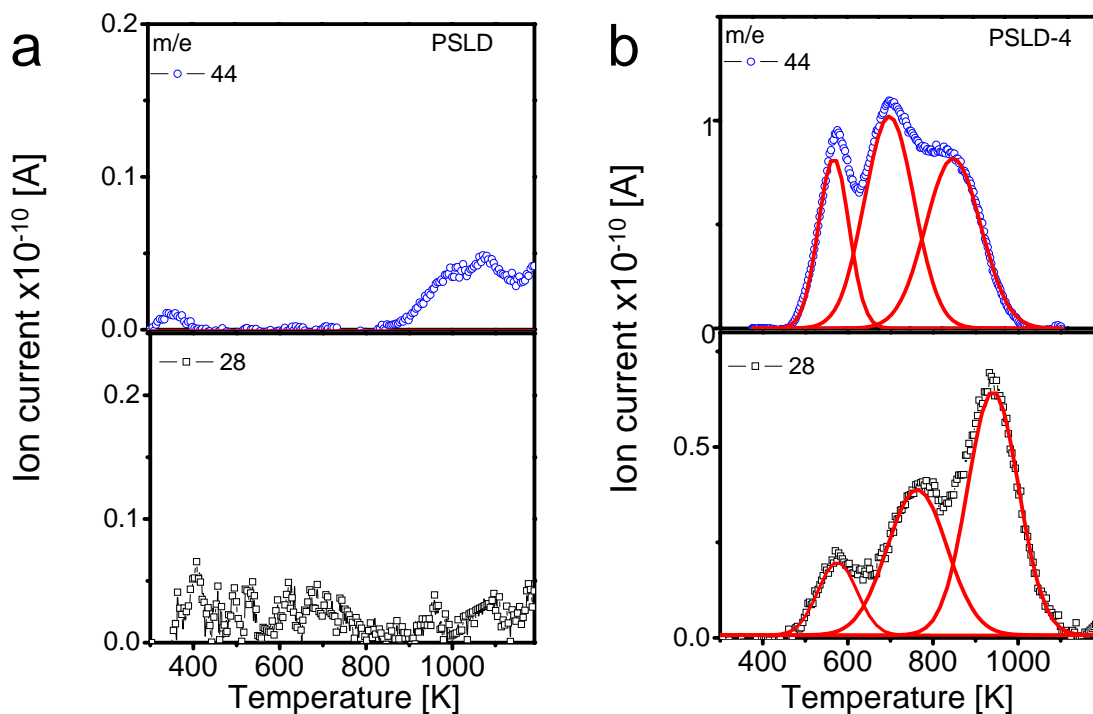


Fig. 5.25 TPO CO₂ profiles of phosphoric modified CNTs

TPD profiles of pristine and oxidized PSLD samples were illustrated in Fig. 5.26. Obviously, pristine PSLD sample was poor functionalized and then there was less carbon oxide and water peaks in the profiles. After oxidation, the surface was highly

functionalized since remarkable CO₂, CO and H₂O desorption peaks were observed. In CO₂ profiles of oxidized samples, three peaks appeared at 573 K, 733 K and 903 K, assigned to the decomposition of carboxylic acid, anhydride and lactone, respectively. There were three peaks at 530, 748 K and 944 K observed in the CO profiles of oxidized PSLD samples, attributed to the decomposition of some carboxylic acid, anhydride/phenol and quinone, respectively. Further oxidation (≥ 10 h) had less influence on the relative intensity of each desorption peak.



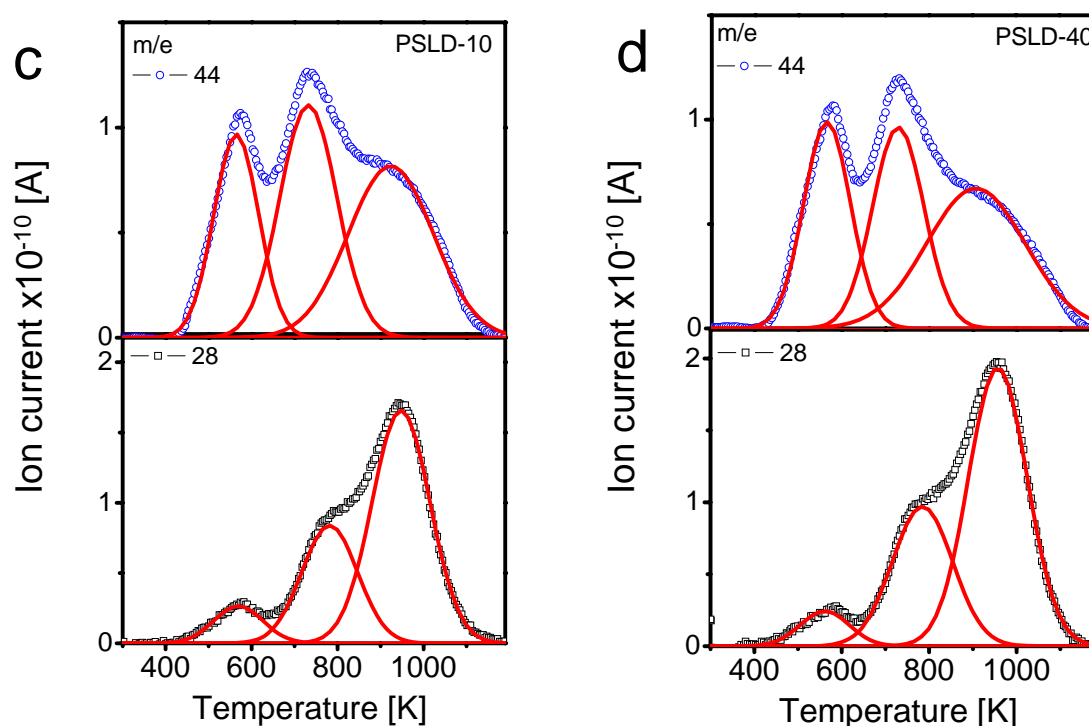


Fig. 5.26 TPD profiles of pristine and oxidized PSLD sample, a) PSLD, b) PSLD-4, c) PSLD-10, d) PSLD-40

The phosphoric addition significantly change the morphology of the CO₂ and CO desorption peaks, displaying no clear desorption peak below 773 K correlated with the desorption of carboxylic acid (Fig. 5.27). It means that the carboxylic groups and anhydride groups were removed from the surface of CNTs. In both of CO and CO₂ TPD profiles, two desorption peaks were observed at 973 K and 1123K. The CO₂ and CO desorption peaks at 973 K should be attributed to the decomposition of lactone and quinone, respectively. The desorption peak of CO_x at 1123 K should be attributed to the decomposition of phosphoric carbon complexes, which was also observed in the TPD profiles of phosphoric modified Nanocyl CNTs (Fig. 5. 18).

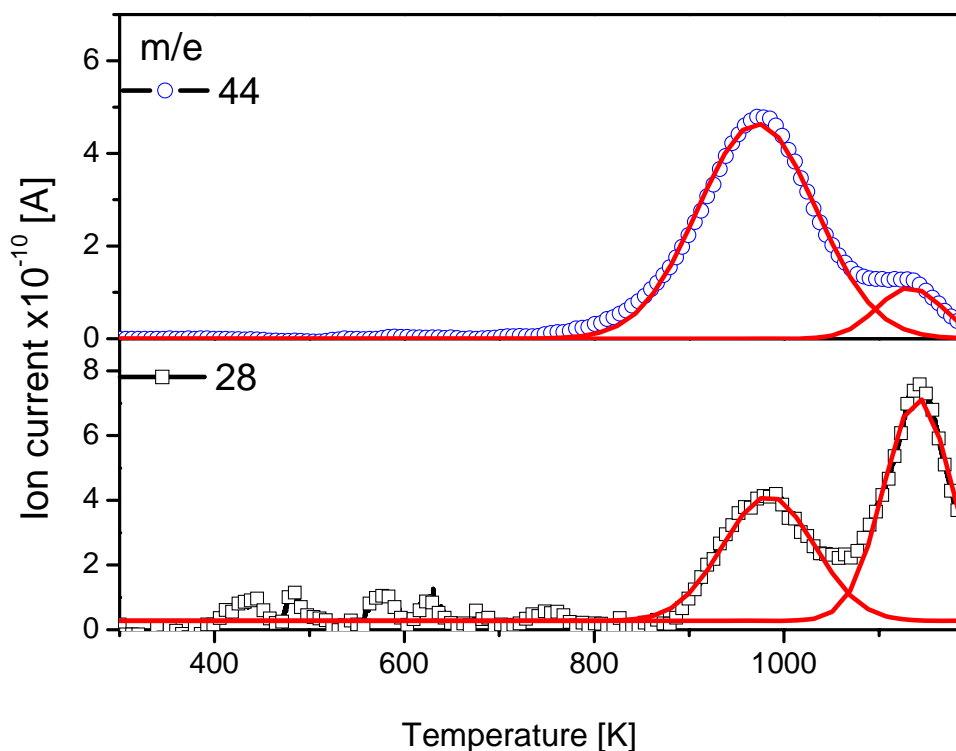


Fig. 5.27 TPD profiles of 5%P₂O₅(N)PSLD sample

5.3 XPS spectrum

The O1s XPS spectra of pristine Nanocyl CNTs before and after reaction were shown in Fig.5.28. For pristine CNTs, oxygen concentration was about 1.3%, and decreased to 1.2% after reaction. It confirms the poor functionalized nature of pristine CNTs, which was not improved during the reaction process. It was also observed that the intensity of C=O with binding energy of 531 eV increased after reaction.

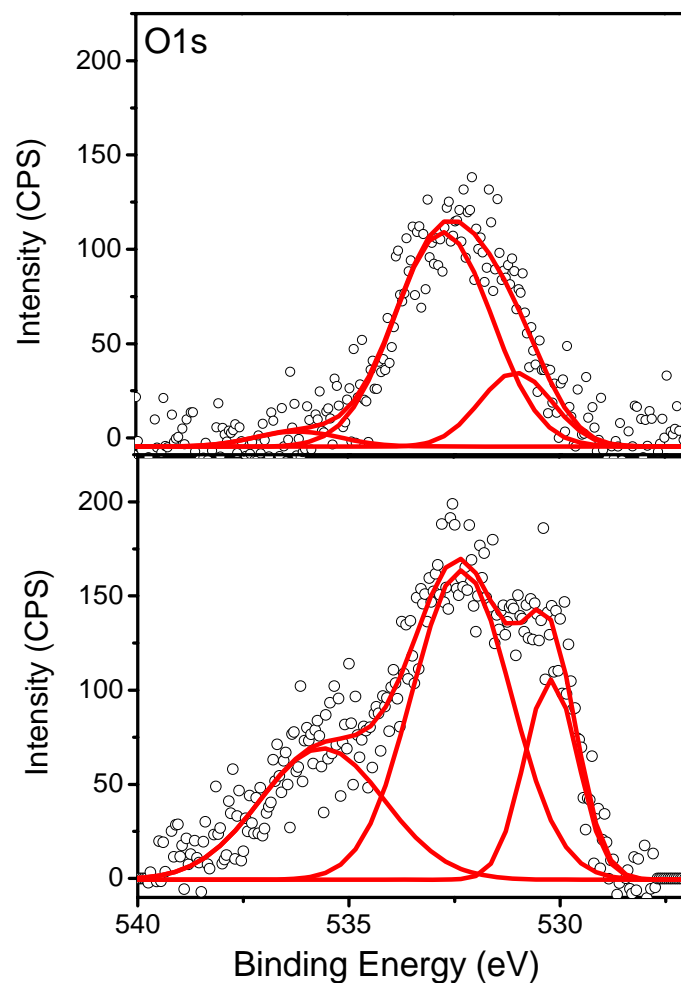


Fig. 5.28 O1s spectra of pristine Nanocyl CNTs before (upper) and after (lower) reaction

After oxidation treatment, the O mol% on the surface of CNTs increased from 1.3% to 5.5%, correlated with the highly functionalized nature of oxidized CNTs. The deconvolution of oxygen species was shown in Fig. 5.29. The phosphoric addition partially removed oxygenated surface groups out of surface of CNTs, resulting in a decrease in the surface oxygen concentration (2.6%). The relatively decrease in oxygen

species with lower binding energy of 531 eV was also significant, with respect to the TPD profiles of phosphoric modified CNTs (Fig. 5.18).

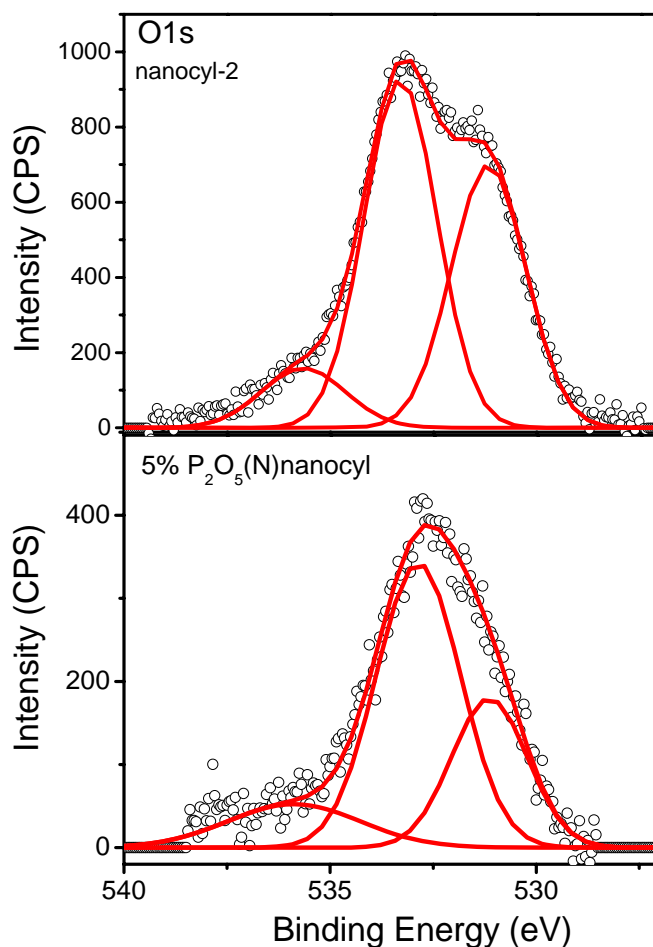


Fig. 5.29 O1s spectra of Nanocyl-2 (upper) and 5wt%P2O5(N)/Nanocyl (lower)

5.4 Infrared spectrum

The IR spectra of oxidized Nanocyl CNTs were shown in Fig. 5.30a. The band at 1630 cm^{-1} can be assigned to the absorbed water on the KBr. The peaks ranged from 1559 to 1509 cm^{-1} can be assigned to carbon skeleton vibration of aromatic ring.^[19] The tiny peak at 1460 cm^{-1} is assigned to CH_2 or CH_3 bending vibrations.^[20] The weak peak

at around 882 cm^{-1} can be assigned to isolated aromatic C-H out-of-plane bending vibrations.^[20] The 1714 cm^{-1} band may be associated with the C=O vibrations of carboxyl, lactone or ketone groups.^[21] The strong peak at 1381 cm^{-1} could be attributed to the combination of O-H deformation vibration and C-O stretching vibration in phenol groups. The peaks at 1260 , 1121 and 1046 cm^{-1} may be associated with C-O or C-O-C vibrations of ester, ether, phenol or carboxyl groups. After calcination at 723 K , no significant change was observed, except the decrease in intensity of peak at 1370 cm^{-1} . It should be attributed to desorption of oxygen functionalities with low thermal stability (see TPD profiles in Fig. 5.11). The change in the ratio of intensity of peak at 1121 cm^{-1} to that at 1046 cm^{-1} was also observed, which might be attributed to the dehydration process. A peak at 2328 cm^{-1} could be assigned to the asymmetric stretch of CO_2 from atmosphere. The O-H stretching vibration at 3441 cm^{-1} was observed in both samples. After reaction, the significant decrease at 1381 cm^{-1} was observed due to desorption of oxygen functionalities (Fig. 5.30b), confirmed by the decrease in the C-O vibration at 1046 cm^{-1} . Due to the less functionalities and strong light absorbance, signal with much noise ranged from 1400 to 1800 cm^{-1} was observed in the spectrum of used CNTs, even the background has been subtracted. The decrease in the C=O vibration in the used catalysts was observed in Fig. 5.30b, confirming the removal of functionalities during the reaction process.

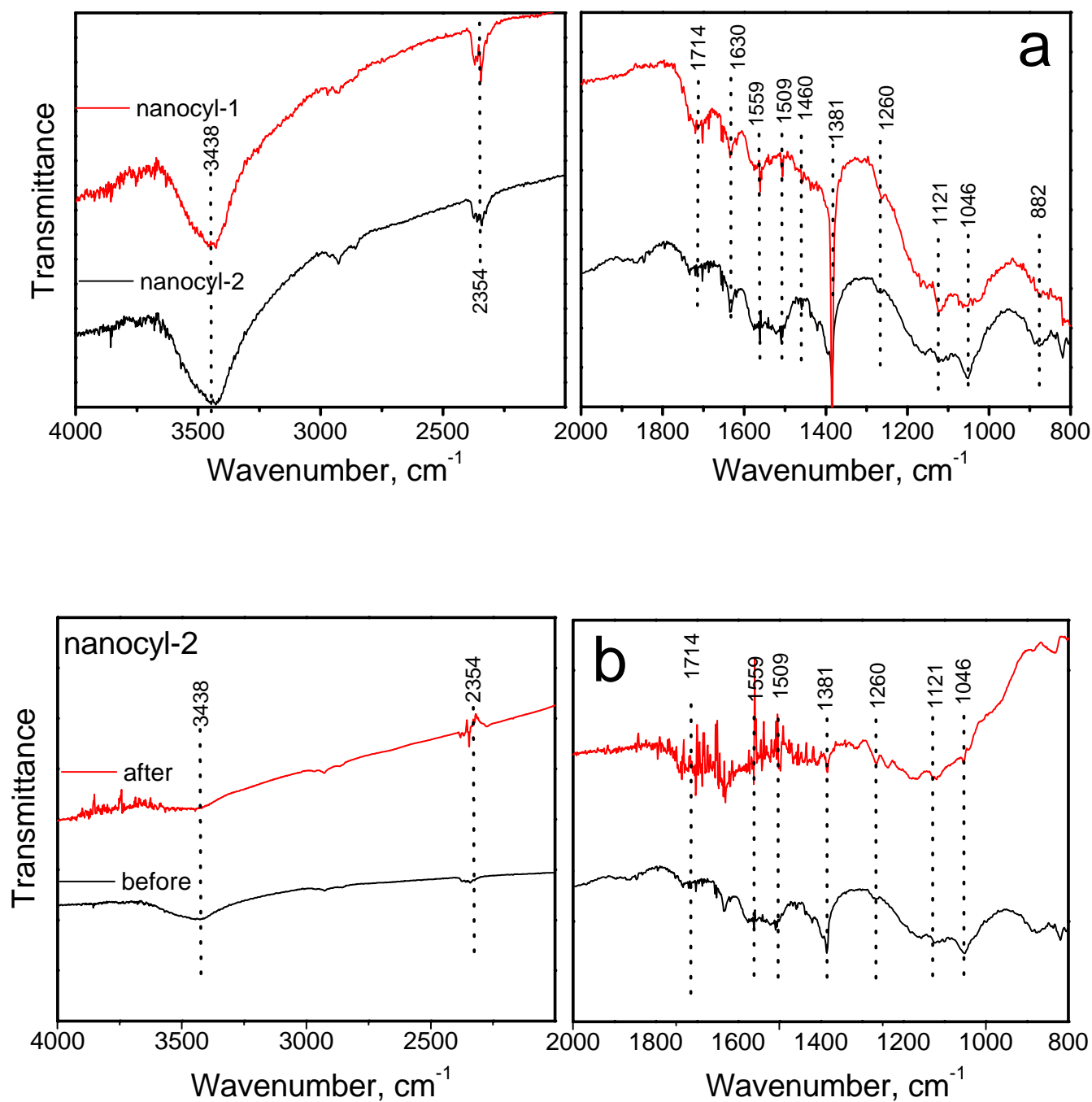


Fig. 5.30 IR spectra of oxidized CNTs: a) Nanocyl-1 and Nanocyl-2; b) Nanocyl-2

before and after reaction

The significant difference between IR spectra of modified CNTs and matrix was observed in Fig. 5.31, demonstrating the highly functionalized nature of modified CNTs. It confirms that the moieties have been grafted on the surface of CNTs. A strong peak at 1720 cm^{-1} was observed, assigned to the vibration of C=O. The peaks ranged between 1587 to 1500 cm^{-1} could be assigned to carbon skeleton vibration of aromatic ring. The peaks at 1381 , 1178 , 1121 and 1046 cm^{-1} were attributed to the vibration of C-O. The characteristic double peaks at 1229 and 1178 cm^{-1} were assigned to the vibration of C-O-C ring with respect to the immobilized furan ring on the surface of CNTs.^[23] The Peak at 1022 cm^{-1} should also be assigned to the ring breathing vibration, which was also observed in furoyl compounds. The peaks at 2970 and 2790 cm^{-1} should also be attributed to the vibration of O-H bond or heterocycles.

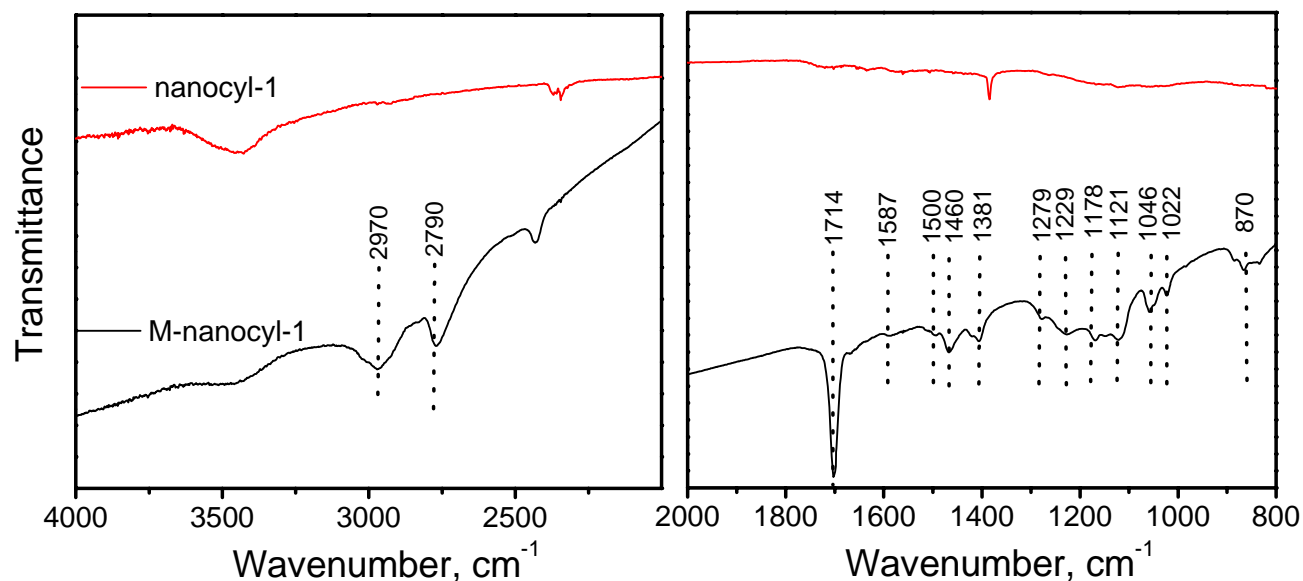


Fig. 5.31 IR spectra of oxidized Nanocyl samples before (Nanocyl-1) and after modification (M-Nanocyl-1)

For pristine CNTs, the active sites for dehydrogenation could not be generated during the reaction process, even with existence of gaseous oxygen (Fig. 4.1). The oxidation treatment was a useful but low efficient method to create active sites on the surface of CNTs. The idea of using grafting modification for catalysts preparation was new attempt to seek a new method to improve the catalytic performance efficiently, which also facilitates the mechanism investigation. The catalysts prepared by the grafting modification displayed a good catalytic activity and stability, although the immobilized moieties were significantly removed (Fig. 5.33). Therefore, this method can be used in the catalysts preparation with great potential. The peak at about 1200 cm^{-1} could be attributed to the vibration of C-O-C bonding in furan ring, meaning that there still is noticeable amount of grafted molecules on the surface of CNTs with respect to higher selectivity of modified materials for catalytic oxidation of butane to corresponding alkenes.^[23]

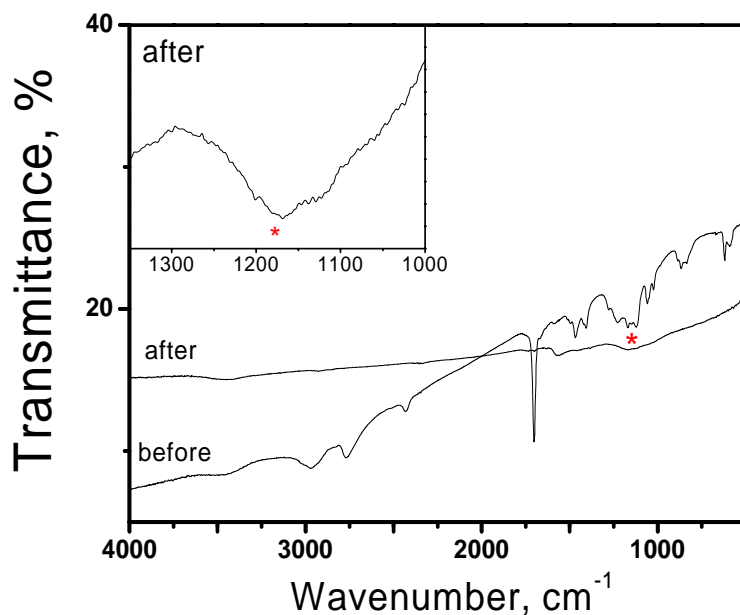


Fig. 5.33 IR spectra of grafted CNTs (M-Nanocyl-1) before and after reaction

5.5 XRF

The elemental analysis of different carbon samples was displayed in Tab. 5.2. Obviously, the influence of metal impurities could be neglected since the activated carbon with the highest purity (AA) displayed the superior catalytic performance to other activated carbon samples. The removal of metal impurities in CNTs by oxidation treatment associated with increase in selectivity confirmed that the active sites should not be impurities.

Tab. 5.2 Elemental concentration of carbon catalysts

	C wt%	Fe wt%	Ca wt%	Si wt%	Mg wt%	Cl wt%
AA	99.96	0.006	0.01	0	0	
PS	99.1	0.02	0.01	0.45	0.004	0.36
Norit	98.6	0.046	0.12	0.7	0.04	0.3
Nanocyl	99.85	0.11*		0.04		
Nanocyl-2	99.97	0		0	0.024**	

* including Ni ** including Co and Mn

5.5 Conclusions

In present work, the disadvantage of “solid state chemistry” approach was observed since the activated carbons with the highest BET surface area displayed the lowest alkenes formation rate (Tab .4.14). On the contrary, TPD method combined with mass-spectroscopy was widely used in present work to investigate surface complexes of CNTs before and after reaction, revealing the correlation between the catalytic activities and oxygenated surface groups. The elementary step of regeneration of quinone groups was also studied with isotopic method, stating the exchange of oxygenated surface groups with gaseous oxygen.

Therefore, conclusions can be drawn in the following: 1) there were two kinds of reaction processes on the surface of CNTs, i.e. the total oxidation and selective oxidation of butane, respectively; 2) oxygenated surface groups, like quinone, should be active sites for the adsorption and dehydrogenation of butane; 3) the total oxidation was attributed to the non dissociative oxygen species on the surface of CNTs, resulting from the weakly chemisorption; 4) the exchange between oxygenated surface groups and gaseous oxygen supported the assumption that the recombination of hydroxyl groups and regeneration of quinone groups via the dissociative chemisorption of oxygen were elementary steps, wherein quinone groups acted as active sites for dehydrogenation; 5) the phosphoric addition favoured the catalytic selectivity by protecting the carbon species (hydrocarbons and carbon defects) out of attacking of oxygen species via chemisorption and activation of oxygen; 6) initial chemical nature of carbon samples was a dominant factor for catalytic activity since no more active site generated during the reaction process; 7) grafting modification can efficiently improve the catalytic performance and significant amount of moieties could remain on the surface of CNTs after the catalysis reaction.

Reference:

1. Moos G, Hertel T, Ulbricht H, Interaction of Molecular Oxygen with Single-wall Carbon nanotube Bundles and Graphite, *Surface Science* 2003, 532–535, 852–856
2. Atamny F, Blocker J, Dubotzky A, Kurt H, Timpe O, Loose G, Mahdi W, Schlogl R, *Surface Chemistry of Carbon: Activation of Molecular Oxygen*, *Molecular Physics* 1992, 76(4), 851-886
3. Xu YJ, Li JQ, *The Interaction of Molecular Oxygen with Active Sites of Graphite: A Theoretical Study*, *Chemical Physics Letters* 2004, 400, 406–412
4. Backreedy R, Jones JM, Pourkashanian M, Williams A, *A Study of the Reaction of Oxygen with Graphite: Model Chemistry*, *Faraday Discuss* 2001, 119, 385-394

5. Mestl G, Maksimova NI, Keller N, Roddatis VV, Schlögl R, Carbon Nanofilaments in Heterogeneous Catalysis: An Industrial Application for New Carbon Materials? *Angew. Chem. Inter. Edit.* 10 2001, (11), 2066-2068
6. Su DS, Maksimova N, Delgado JJ, Keller N, Mestl G, Ledoux MJ, Schlögl R, Nanocarbons in Selective Oxidative Dehydrogenation Reaction, *Catalysis Today* 2005, 102, 110-114.
7. Delgado JJ, Vieira R, Rebmann G, Su DS, Keller N, Ledoux MJ, Schlögl R, Supported Carbon Nanofibers for the Fixed-bed Synthesis of Styrene, *Carbon* 2006, 44 (4), 809-812.
8. Toles CA, Marshall WE, Johns MM, Surface Functional Groups on Acid-activated Nutshell Carbons. *Carbon* 1999, 37, 1207-1214.
9. Sahoo SK, Raob PVC, Rajeshwer D, Krishnamurthy KR, Singh ID, Structural Characterization of Coke Deposits on Industrial Spent Paraffin Dehydrogenation Catalysts, *Applied Catalysis A: General* 2003, 244 , 311–321
10. Wolf EE, Alfani F, Catalysts Deactivation by Coking, *Catal. Rev. Sci. Eng.* 1982,24, 3, 329-371.
11. Macia-Agullo JA, Cazorla-Amoros D, Linares-Solano A, Wild U, Su DS, Schlögl R. Oxygen Functional Groups Involved in the Styrene Production Reaction Detected by Quasi In-situ XPS. *Catal. Today* 2005, 102, 248-253.
12. Pereira MFR, Orfao JJM, Figueiredo JL, Oxidative Dehydrogenation of Ethylbenzene on Activated Carbon Catalysts. I. Influence of Surface Chemical Groups. *Appl. Catal. A: General* 1999, 184, 153-160.
13. Trimm DL, The Formation and Removal of Coke from Nickel Catalyst, *Catal. Rev. Sci. Eng.* 1977,16, 155-189.
14. Funk S, Burghaus U, Adsorption Dynamics of Alkanes on Single-Wall Carbon Nanotubes: A Molecular Beam Scattering Study, *J. Phys. Chem. C* 2007, 111, 8043-8049
15. Zhuang Q, Kyotani T, Tomita A, Dynamics of Surface Oxygen Complexes during Carbon Gasification with Oxygen, *Energy & Fuels* 1995, 9, 630-634
16. Zhu X, Lee S, Lee Y, Frauenheim T, Adsorption and Desorption of an O₂ Molecule on Carbon Nanotubes, *Physical Review Letter* 2000, 85, 13, 2757-2760
17. Wu X, Radovic LR, Inhibition of Catalytic Oxidation of Carbon/carbon Composites by Phosphorus, *Carbon* 44 (2006) 141–151

18. Dejoz A, Nieto JML, Melo F, Vazquez I, Kinetic Study of the Oxidation of n-Butane on Vanadium Oxide Supported on Al/Mg Mixed Oxide. *Ind. Eng. Chem. Res.* 1997, 36, 2588-2596.
19. Mawhinney DB, Naumenko V, Kuznetsova A, Yates JTJr, Infrared Spectral Evidence for the Etching of Carbon Nanotubes: Ozone Oxidation at 298 K. *J. Am. Chem. Soc.* 2000., 122, 10, 2383-2384.
20. Moreno-Castilla C, Lopez-Ramon MV, Carrasco-Marin F, Changes in Surface Chemistry of Activated Carbons by Wet Oxidation, *Carbon* 2000, 38, 14, 1995-2001
21. Kuznetsova A, Mawhinney D, Naumenko BV, Yates JTJr, Liu J, Smalley RE, Enhancement of Adsorption inside of Single-walled Nanotubes Opening the Entry Ports, *Chem. Phys. Lett.* 2000, 321, 3-4, 292-296.
22. Griffiths PR, Haseth JA, *Fourier Transform Infrared Spectrometry*, Wiley 1986
23. Kul'nevich VG, Borisova NN, *Infrared Spectra of Furoyl Peroxides and Related Compounds Containing Carbonyl*, Translated from *Zhurnal Prikladnoi Spektroskopii* 1971, 14, 4, 648-653

Chapter 6 Catalytic oxidation of butene to butadiene

In this chapter, the catalytic performance of various carbon catalysts for catalytic oxidation of butene to butadiene was tested. The influence of modification (oxidation and phosphoric modification) to catalytic performance was also identified in present work.

6.1 Catalytic performance of carbon materials

6.1.1 Catalytic activity of pristine carbon materials

Several kinds of as-received carbon materials were applied as catalysts in the ODH of butene to butadiene, which displayed a remarkable catalytic performance as a function of reaction time (Fig. 6.1). The reaction products were butadiene, water, carbon monoxide and carbon dioxide. Trace amount of propene could be negligible. The ratio of oxygen to butene was changed to achieve the better performance. Under these reaction conditions, no combustion of carbon materials was observed and carbon balance was always kept at 100%. Before reaction, the pristine CNTs were washed by concentrated hydrochloric acid or nitric acid to remove metal particles. The influence of metal impurity on catalytic performance could be negligible.

An initial low activity was observed using the pristine PSLD catalyst for the catalytic oxidation of butene, which gradually increased during the activation process of 20 hours. When the feed was rich in oxygen, the higher conversion and yield were obtained, but selectivity decreased slightly. On the contrary, activated carbons exhibited the highest initial yield, which decreased as a function of reaction time. After ten hours deactivation, the catalysts reached the steady-state with about 30% yield under the richer

oxygen atmosphere. The catalytic properties of carbon catalysts in the steady state were displayed in Tab. 6.1. The worst catalytic performance with only 3-4% yield was obtained by using bay CNTs.

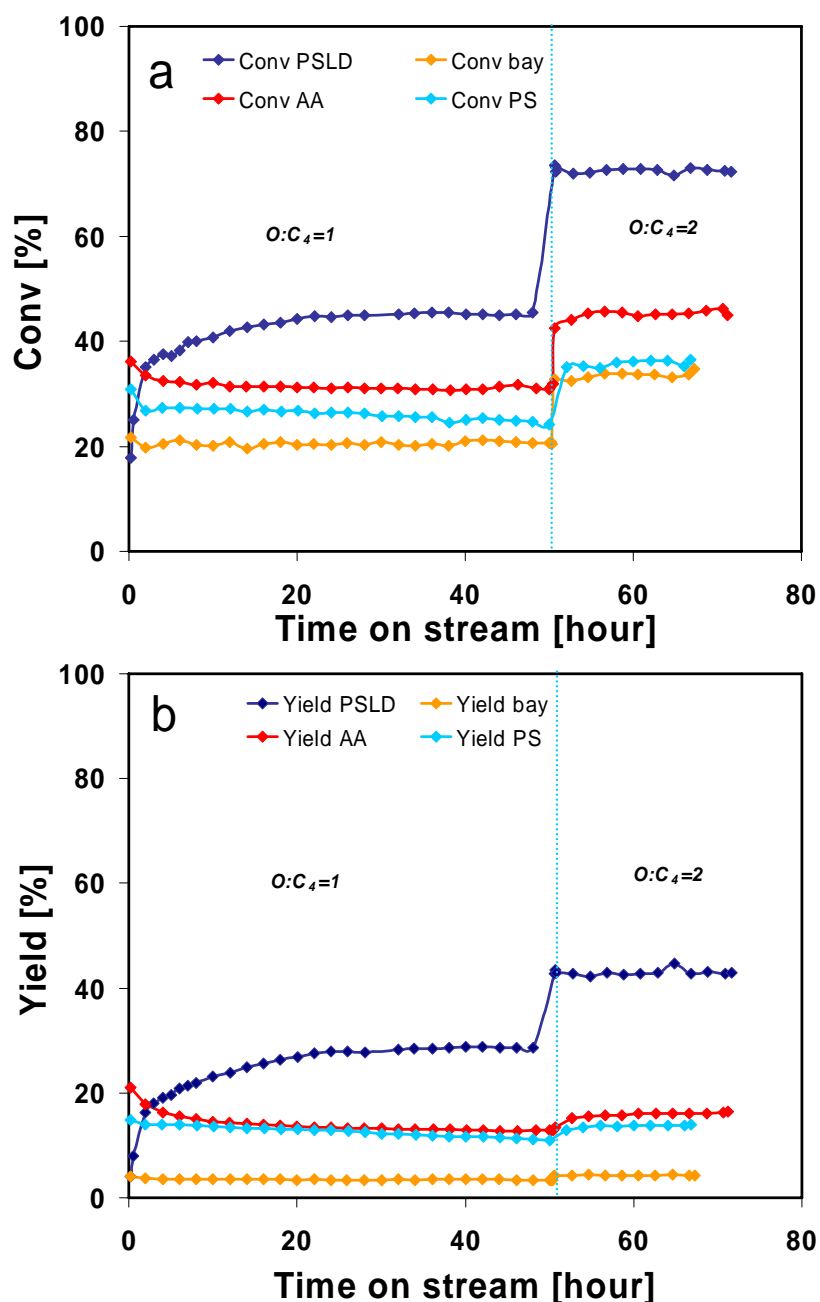


Fig. 6.1 Catalytic performance of pristine carbon materials with different ratio of oxygen/butene, a) conversion; b) butadiene yield reaction conditions: 673K, O_2 vol%=1.32%, 15ml/min, 180mg catalysts.

Tab. 6.1 Catalytic properties of pristine carbon catalysts with different ratio of oxygen/butene

catalysts	PSLD		Nanocyl		bay		AA		PS	
ratio of O ₂ / 1-bu	1	2	2		1	2	1	2	1	2
Con. %	45	72	55		21	34	31	45	24	36
S _{butadiene} %	63	60	54		16	12	42	36	46	38
Y _{butadiene} %	29	43	30		3.4	4.2	13	16	11	14

Fig. 6.2 illustrated the TPO and TPD profiles of pristine PSLD CNTs before and after catalysis reaction. A slight CO₂ desorption peak at 1073K was observed in the TPD profile of fresh CNTs. After reaction, the intensity of CO₂ formation rate increased significantly, which was attributed to highly functionalized nature of used CNTs. In TPO profiles, the gasification temperature of CNTs shifted from 1023K to 873K after catalytic reaction (Fig. 6.2b). The decrease of combustion temperature of carbon materials could also be attributed the functionalization of carbon materials.

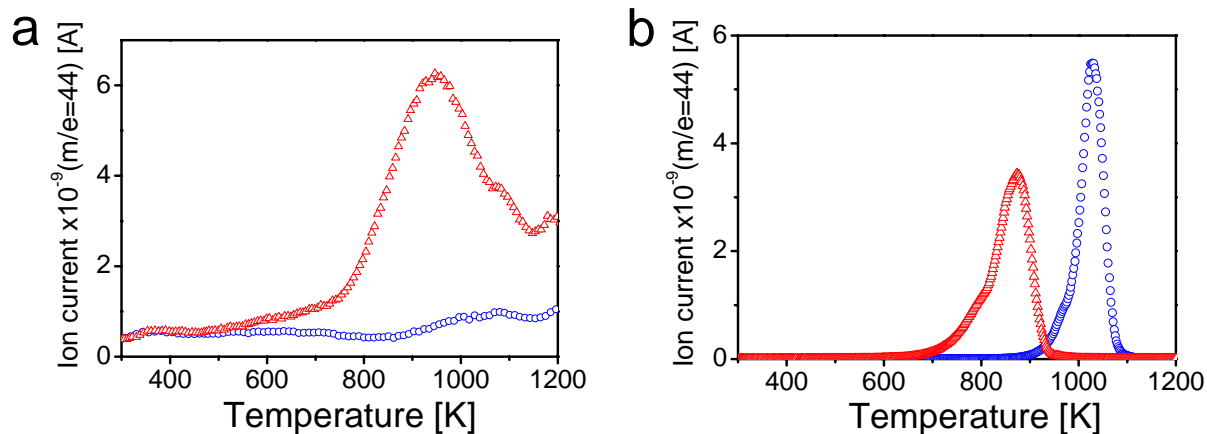


Fig. 6.2 CO₂-TPD (a) and TPO (b) profiles of pristine PSLD CNTs before (blue) and after (red) catalysis

Fig. 6.3 showed the C1s and O1s XPS spectra of pristine and used CNTs. It was observed that all the C1s spectra contained a typical graphitic peak at around 284.8 eV.^[2] There was no significant difference observed in spectra between CNTs before and after catalysis reaction, indicating that the intensity from functional groups on surface of used CNTs was much weaker than that of excitations of C1s electrons and was difficult to be detected in C1s spectra. However, the clear changes in the O1s spectra were observed indicating the difference between fresh and used CNTs. The deconvolution of O1s spectra was shown in Fig. 6.4b. The O1s peak mainly had three contributions that were able to be interpreted according to the literature on carbon materials, as ketone/C=O in carboxyl acids (around 531.1-531.8 eV), alcohol/C-OH in carboxyl acid (around 533.3 eV) and water (around 536.1 eV).^[3] Notably, the peak at 533.8 eV increased after catalysis reaction, which was attributed to the hydrogenated nature of oxygenated surface groups during the reaction process. It has been discussed in last chapter 5.2.2 (P132) and also been reported in literature.^[3]

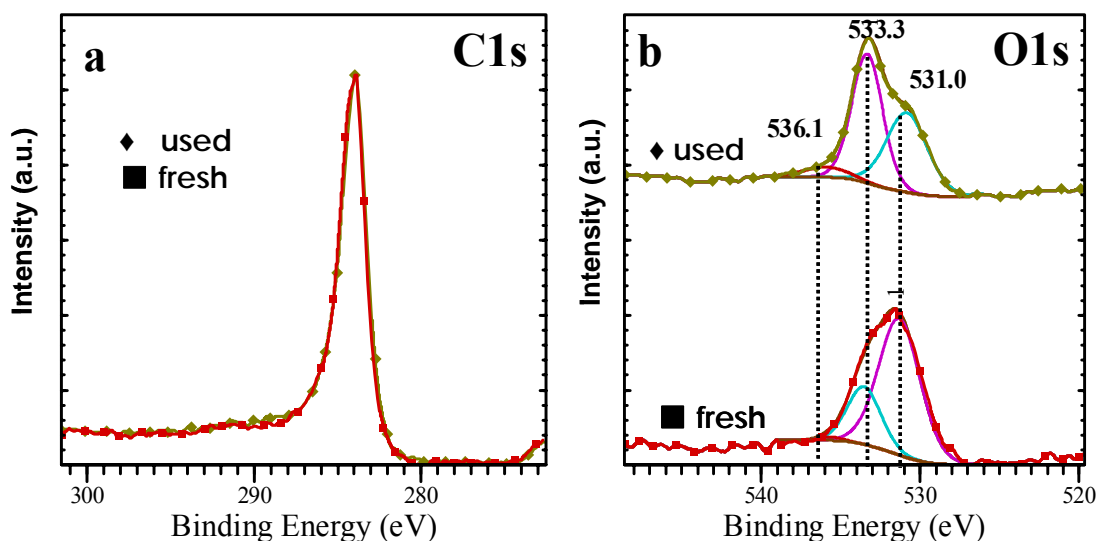


Fig. 6.3 XPS spectra of the fresh (■) and used CNT (♦): a) C1s spectra; b) O1s spectra

On the contrary, for Nanocyl CNTs, the loss in functionalities was observed during the reaction process. It must be pointed out that the difference in the feature and chemical nature of two kinds of CNTs was significant. The reaction condition was also different (poor oxygen in the catalytic oxidation of butane). Before further characterization was done, the diversity in catalytic performance of two kinds of CNTs might be attributed to their chemical nature.

6.1.2 Catalytic activity of oxidized carbon materials

The influence of oxidation treatment on catalytic behavior has been tested using oxidized PSLD CNTs as catalysts (Fig. 6.4). The deactivation was observed in each oxidized sample at initial period due to the removal of surface oxygenated groups. However, the activation process was observed by using PSLD-4 samples. When the oxidation time was longer than 10 hours, no activation process was observed. No significant difference in selectivity was observed by using CNTs with different oxidation time.

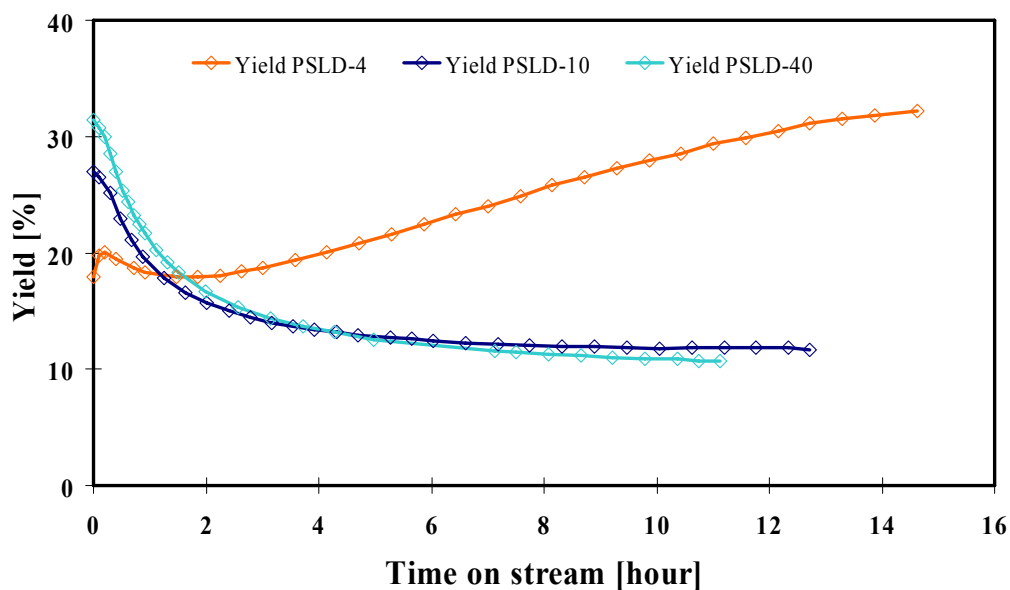


Fig. 6.4 Catalytic performance of oxidized PSLD CNTs: reaction conditions: 673K, O₂ vol%=1.32% and ratio of O₂:butene=2, 15ml/min, 180mg catalysts.

Tab. 6.2 Catalytic performance of oxidized PSLD CNTs

catalysts	PSLD-4	PSLD-10	PSLD-10
Con.	47	21	18
S _{butadiene}	68	55	61
Y _{butadiene}	32	12	11

The oxidation time had less influence on chemical nature of surface of CNTs, which was observed in the TPD profiles of oxidized CNTs (Fig. 5.26). It meant that the change in catalytic behavior could not be attributed to the surface oxygenated groups. However, the two-layer-microstructure of PSLD CNTs was observed in the TEM images. The HRTEM images displayed that the oxidation could progressively remove the outside carbon layer (poorly-graphitized carbon) (Fig. 5.6). The butene conversion of oxidized CNTs decreased from 47% to 20%, when the outside carbon layers were totally removed. It suggested that the high yield obtained over pristine PSLD and PSLD-4 samples could be attributed to the outside layer, poorly-graphitized carbon.

6.1.3 Catalytic performance of phosphoric modified CNTs

The catalytic activity of phosphoric modified PSLD CNTs was displayed in Fig. 6.5. Interesting experimental results were observed that phosphoric addition could improve the catalytic performance dramatically. The catalytic performance with 83% selectivity and 70% conversion was obtained by using 10wt% phosphoric loading PSLD. The high loading amount of phosphoric oxide resulted in the decrease in catalytic

performance of CNTs for the catalytic oxidation of butane. However, the increase in butene conversion and decrease in butadiene selectivity was observed in the catalytic oxidation of butene, associated with the increase in loading amount. For CNTs with lower P_2O_5 loading amount ($\leq 5\text{wt}\%$), the conversion reached the maximum at initial period and subsequently decreased as a function of reaction time, with respect to the same trend observed in the selectivity. The deactivation was significantly reduced by increasing the loading amount.

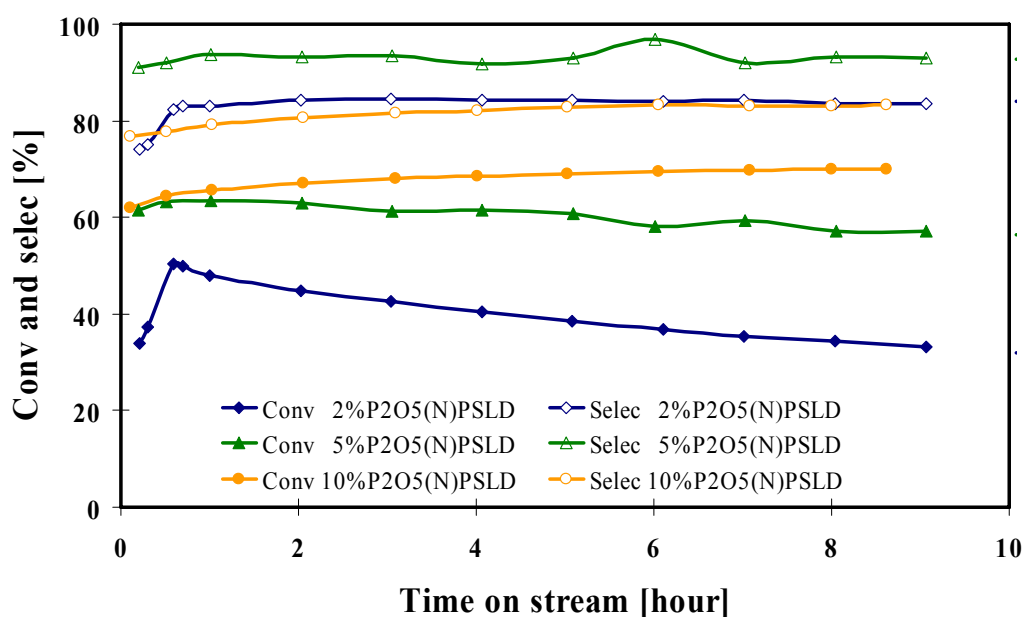


Fig. 6.7 Catalytic performance of phosphoric modified PS LD CNTs, 673K, O_2 vol%=1.32% and ratio of O_2 :butene=2, 15ml/min, 180mg catalysts.

Tab. 6.3 Catalytic performance of phosphoric modified PS LD CNTs

	Conv %	*ba Selec %	CO selec%	CO ₂ selec %	Yield %
2%P ₂ O ₅ (N)PSLD	28	82	7	12	23
5%P ₂ O ₅ (N)PSLD	53	91	4	5	48
10%P ₂ O ₅ (N)PSLD	70	83	7	10	58

*ba is the abbreviation of butadiene

The acid precursor, like phosphoric acid, was also used in the addition. It was observed that the precursors had less influence on catalytic performance of CNTs (Fig. 6.8). The similar catalytic performance was observed by using modified CNTs with same loading amount. The catalytic activity of modified CNTs was significantly inspiring, since it was higher than any other catalysts, even bismuth molybdate catalysts, which was well-known in the oxidative dehydrogenation.^[1-3]

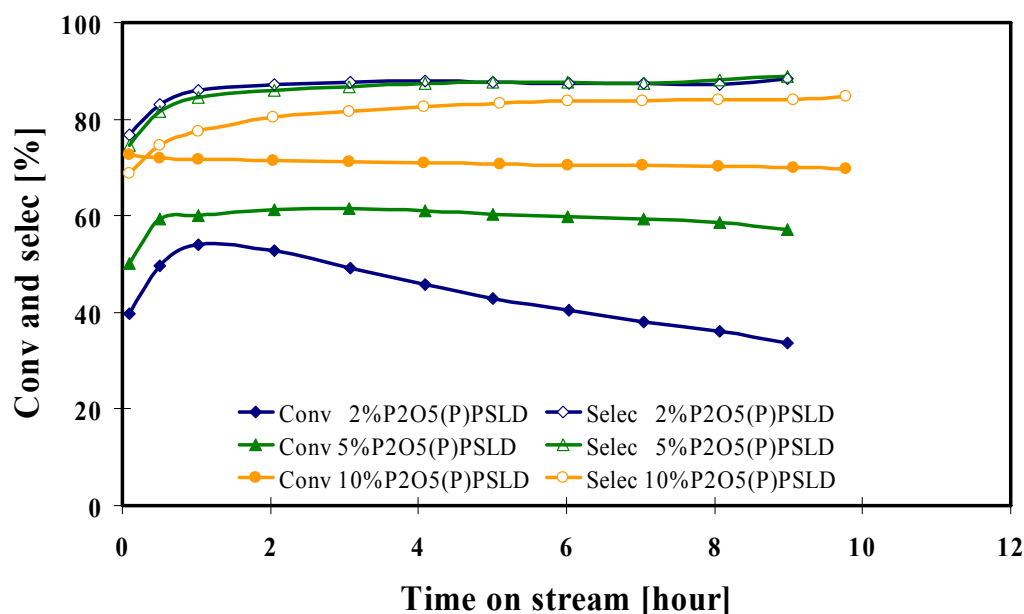


Fig. 6.8 Catalytic performance of phosphoric modified PSLD CNTs using phosphoric acid as precursor, 673K, O₂ vol%=1.32% and ratio of O₂:butene=2, 15ml/min, 180mg catalysts.

Tab. 6.4 Catalytic performance of phosphoric modified PSLD CNTs with phosphoric acid as precursor

	Conv %	*ba Selec %	CO selec%	CO ₂ selec %	Yield %
2%P ₂ O ₅ (P)PSLD	34	88	4	7	30
5%P ₂ O ₅ (P)PSLD	57	89	4	7	51
10%P ₂ O ₅ (P)PSLD	70	85	6	9	59

*ba is the abbreviation of butadiene

The TPO profiles of fresh and used 5wt% $P_2O_5(N)$ PSLD were display in Fig. 6.9. Obviously, no difference was observed between the TPD profiles of modified CNTs before and after reaction. It suggested that no coke formed on the used CNTs.

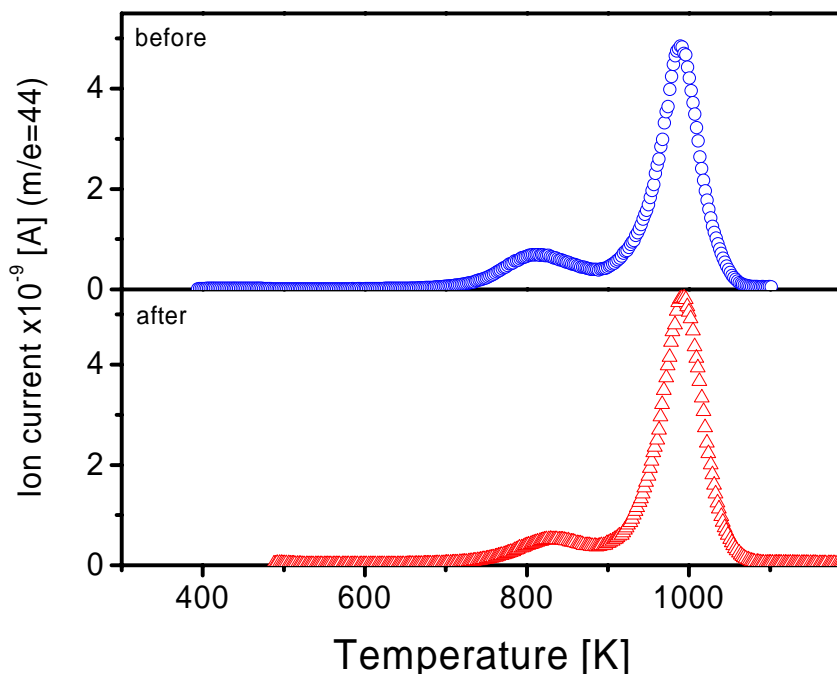


Fig. 6.9 TPO profiles of 5wt% $P_2O_5(N)$ PSLD before and after reaction

6.2 Oxygen order measurement

The outer diffusion and inner diffusion were diagnosed by experimental criteria.^[5] The outer diffusion diagnostic test with constant contact time (0.0067g·h/l) was shown in Fig. 6.10. The reaction rate kept constantly as the flow rate increased, demonstrating that the outer diffusion was negligible. Therefore, for oxygen order measurement, 6mg CNTs with 100mesh particle size was used as catalyst, which has been diluted with 500mg SiC.

The reaction temperature was 430°C and total flow rate was 15ml/min with 0.67 mol% butene.

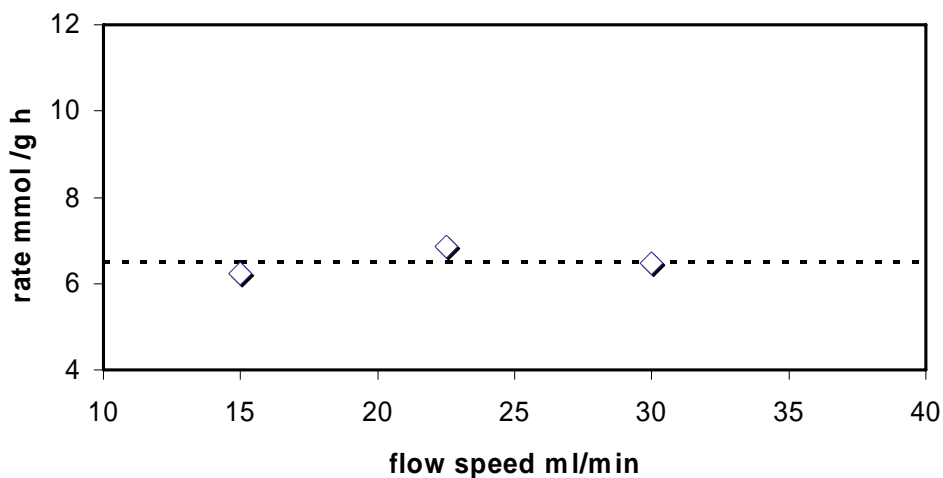


Fig. 6.10 Experimentally diagnostic test for outer diffusion, 430°C, O₂ vol%=1.32% and ratio of O₂:butene=2

The oxygen order was evaluated from the plots of $\log r$ again $\log (P_{O_2}/P_0)$. The result was shown in Fig. 6.11. The oxygen reaction order was 0.28, keeping a good agreement with literature.^[5-6] The oxygen order was higher than zero, meaning the oxygen adsorption and activation should also be the rate-determining steps for this reaction.

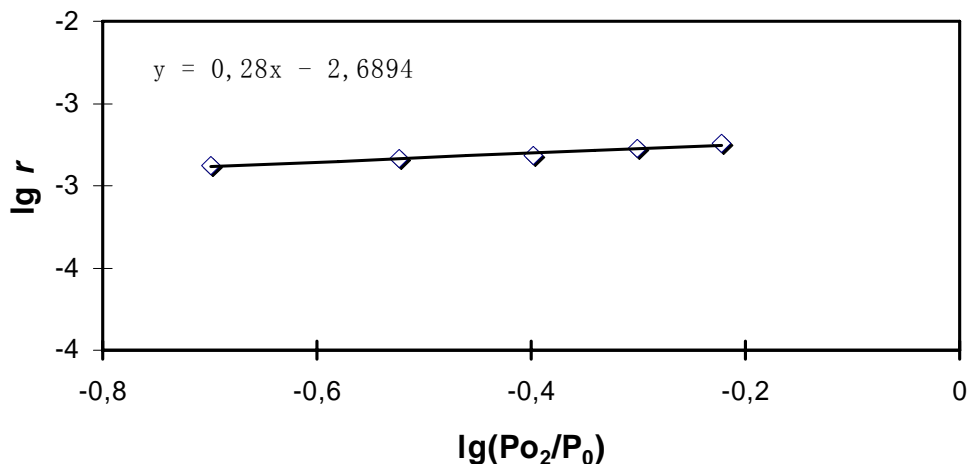


Fig. 6.11 Estimation of oxygen order

6.2 Conclusions

The catalytic activities of carbon materials were tested in this chapter. Pristine PSLD CNTs displayed low selectivity to dehydrogenation of butane, but high selectivity to dehydrogenation of butene. The different catalytic performance should be attributed to the chemical nature of educts. The intermediates like alkenyl radicals could be stabilized by conjugating π bond.

The phosphoric modified CNTs displayed a superior catalytic activity and stability, even better than that of the best metal catalysts in the literature. No coke formation was observed after reaction. The inspiring catalytic performance of modified CNTs really develops the industrial application of CNTs.

Reference:

1. Jung JC, Kim H, Chung YM, Kim TJ, Lee JS, Oh SH, Kim YS, Song IK, Unusual Catalytic Behavior of β - $\text{Bi}_2\text{Mo}_2\text{O}_9$ in the Oxidative Dehydrogenation of n-Butene to 1,3-Butadiene, *Journal of Molecular Catalysis A: Chemical* 2007, 264, , 237–210
2. Jung JC, Kim H, Choi AS, Chung YM, Kim TJ, Lee SJ, Oh SH, Song IK, Effect of PH in the Preparation of γ - Bi_2MoO_6 for Oxidative Dehydrogenation of n-Butene to 1,3-Butadiene: Correlation Between Catalytic Performance and Oxygen Mobility of γ - Bi_2MoO_6 *Catalysis Communications*, 2007, 8, 625–628
3. Portela MF, Oliveira MM, Pires M J, Mechanism of Oxidative Dehydrogenation of 1-Butene Over Bismuth Molybdate Polyhedron 1986, 5, 119-121
4. Ertl G, Knozinger H, Weitkamp J, *Handbook of Heterogeneous Catalysis*, Vol 3, 1232-1233
5. Chaar MA, Patel D, Kung HH, Selective Oxidative Dehydrogenation of Propane over VMgO Catalysts. *J. Catal.* 1988, 109, 2, 463–467.
6. Madeira LM, Portela MF, Catalytic Oxidative Dehydrogenation of n-Butane, *Catalysis reviews* 2002, 44(2), 247-286

Chapter 7 Reaction mechanism and outlook

When we talk about “carbon”, somehow, the meaning is complicated and ambivalent. Carbon materials display metallic, semi-conductive or dielectric electronic properties; they are composed of sp^2 hybrid carbons, sp^3 hybrid carbons or the combination with different ratio of sp^2 to sp^3 hybridization; they are crystal or amorphous; they displayed long-range order or short-range order of crystalline microstructure. Furthermore, the surface of carbon materials is always terminated by abundant guest elements, especially oxygen and hydrogen. Therefore, when the “chemical properties” are taken in to account in the discussion of catalytic performance of carbon materials, it is always associated with their microstructure, crystallization degree, raw material and previous preparation and functionalization history. Generally, two approaches have been widely performed in the surface chemistry of carbon, one is “solid state chemistry” approach and the other is “organic surface groups” approach.^[1] The former one focuses on the crystalline microstructure of carbon materials and the latter one focuses on the organic character of the surface groups.

In the “solid state chemistry” approach, the catalytic activity of carbon materials should be associated with their microstructure and crystal defects. For activated carbons and amorphous carbons, the low crystalline degree and small particle size significantly favor the increase in the ratio of number of carbon atoms at edge-side to that in the bulk. Consequently, the activity of those carbon materials is remarkably higher than that of highly-ordered graphitic materials since those edge-side carbon defects display higher reactivity. On the other hand, the difference of chemical properties between anisotropic

“basal plane” and “prismatic plane” of graphitic materials has also been observed due to the same reason.^[1] Furthermore, the increase in the chemical activity could also be attributed to the curvature and distortion of graphene with respect to the single-walled carbon nanotubes and low-graphitized carbon materials.

The so-called “organic surface groups” approach deals with the nature and the functionality of surface complexes of oxygen and other compounds chemisorbed at the surface defects. It means that the chemical nature of carbon materials is mainly attributed to the surface functionalities and complexes. Obviously, both “solid state chemistry” approach and “organic surface groups” approach should be considered in present work, corresponding to the great diversity in the catalytic performance of carbon materials. It must be emphasized that both factors are not isolated. For instance, the chemical properties of oxygen functionalities are notably influenced by the chemical environment, as confirmed by the observation of the shifting in the desorption temperature of functionalities.^[2] Furthermore, the carbon defects are always terminated by other atoms, resulting in the formation of surface functionalization of carbon materials. Those functionalities have significant influence on the chemical properties of carbon materials even with similar microstructure.^[3] However, less information has been obtained about the chemical state of functionalities on the carbon surface during the reaction process due to the absence of a characterization method, and the correlation between the chemical state of carbon materials and their reactivity is still under debate.

Fig. 7.1 displays the catalytic performance of carbon materials measured in the present work, combined with the catalytic performance of metal catalysts from literature

(Fig. 1.1). It is observed that butane conversion of carbon catalysts ranged from about 8% to 22%, with respect to the great diversity in alkenes selectivity ranged from 10% to 74%. The difference in the catalytic performance of various carbon materials has been discussed in chapter 4.

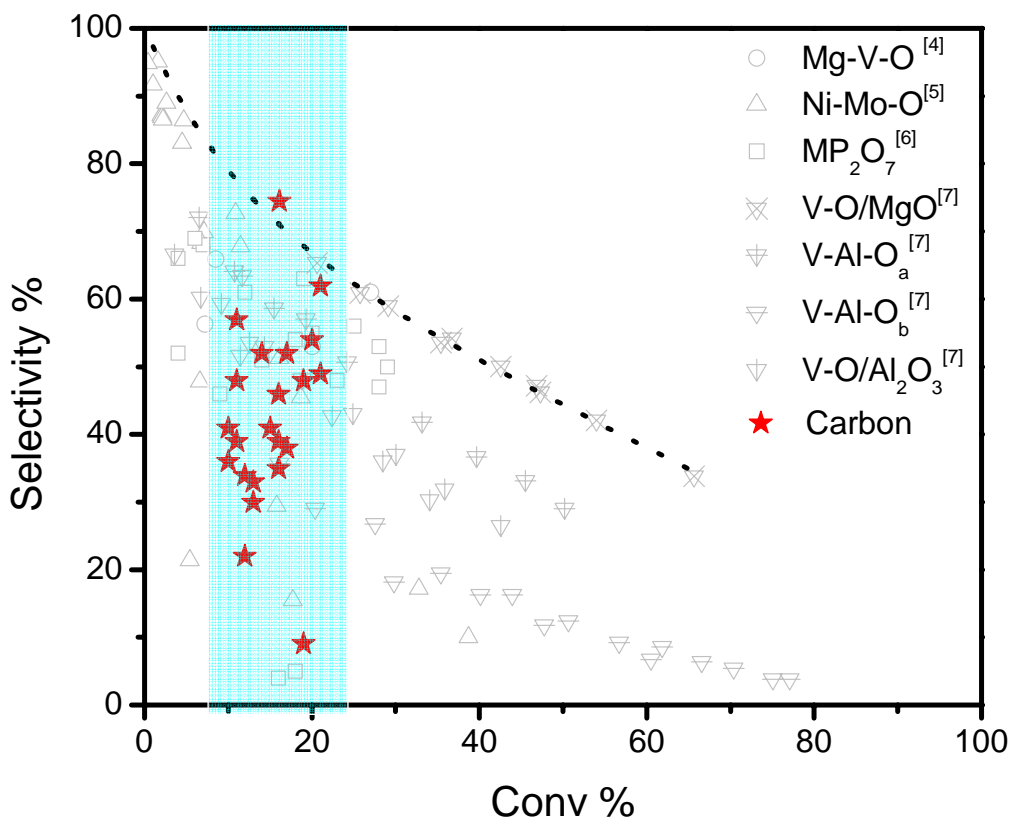


Fig. 7.1 catalytic performance of carbon and metal catalysts* and metal catalysts (*from reference, Fig. 1.1)

Obviously, the microstructure has significant influence on the catalytic performance. For activated carbon, the decrease in the catalytic performance was observed after oxidation treatment with respect to the increase in the functionalization degree. On the contrary, the functionalization significantly favored the catalytic

performance of CNTs. In addition, the removal of oxygenated surface groups of oxidized activated carbon had less influence to the catalytic performance in steady state. It means that the catalytic activity of activated carbons could not be directly related with the functionalization degree. The microstructure and nature of carbon defects should be the most important factor for catalytic performance of activated carbons, which could be easily changed due to the low crystalline feature. However, the investigation on the microstructure of activated carbons is hindered due to the absence of technique. For instance, the remarkable difference in the catalytic performance of three kinds of activated carbons has been observed, but it is difficult to be related with the difference in the microstructure such as BET surface area.

The microstructure should be also an important factor for the catalytic activity of carbon materials. However, the crystalline degree of graphene in the CNTs is much higher than that in activated carbons, meaning that the oxidation treatment used in present work could not change the microstructure of CNTs. Therefore, the contribution of change in the microstructure of CNTs to catalytic activity could be neglected. The thermal and chemical stability of CNTs have been confirmed in the chapter 5 since no significant difference is observed in TEM images of pristine CNTs, oxidized CNTs and CNTs before and after reaction. However, the remarkable availability of CNTs for functionalization has been widely reported due to the chemical nature of CNTs with abundant surface defects.^[8] It proves that the chemical reactivity of CNTs could be associated with the surface functionalities. Therefore, the effort should be focused on the edge-side carbon defects, for instance, defects and ends of CNTs.

The pristine CNTs with poorly functionalized feature display high activity but low selectivity for the catalytic oxidation of butane. The surface of pristine CNTs after reaction was still absent of oxygen. The various oxygen activation models have been proposed, including the non-dissociative chemisorption and dissociative chemisorption of oxygen.^[9] It implies the absence of dissociative chemisorption of oxygen during the reaction process, corresponding to the poorly functionalized nature of used catalysts. Therefore, non-dissociative chemisorption of oxygen species on the surface of CNTs should have more contribution to the total oxidation of butane.

The oxidation treatment favors the catalytic performance of CNTs, corresponding to the highly functionalized surface of catalysts. The increase in catalytic activity should be attributed to the surface functionalities. However, the complexity of surface functionalities has been described in the literature.^[1,2] It is always difficult to value the contribution of different oxygenated surface groups to the catalytic activity of CNTs. The thermal treatment and in-situ XPS characterization in literature proved the role of quinone groups in the catalytic oxidation of ethylbenzene to styrene, as also confirmed by theoretical calculation. However, a great diversity in the desorption temperature of carbon oxides species in TPD profiles was observed, suggesting the variety of chemical nature of functionalities including quinone groups. Therefore, the detailed reaction mechanism catalyzed by CNTs is worthy of in-depth clarification.

The catalytic performance of CNTs after TPD investigation has proved that the majority of oxygen functionalities, which were generated from the oxidation, does not have contribution to the catalytic performance. However, the observation that there was

exchange between surface oxygen functionalities and gaseous oxygen confirms that the quinone groups should be active sites for the catalytic oxidation of butane. Those quinone groups generated via the dissociative chemisorption of gaseous oxygen species at the defects of CNTs. Accordingly, the elementary steps of dehydrogenation of butane over CNTs are proposed in Fig. 7.2. The strong adsorption of C_4 hydrocarbon molecules on the surface of CNTs was firstly identified in present work, which should be associated with the adsorption and activation of hydrocarbons on active sites.

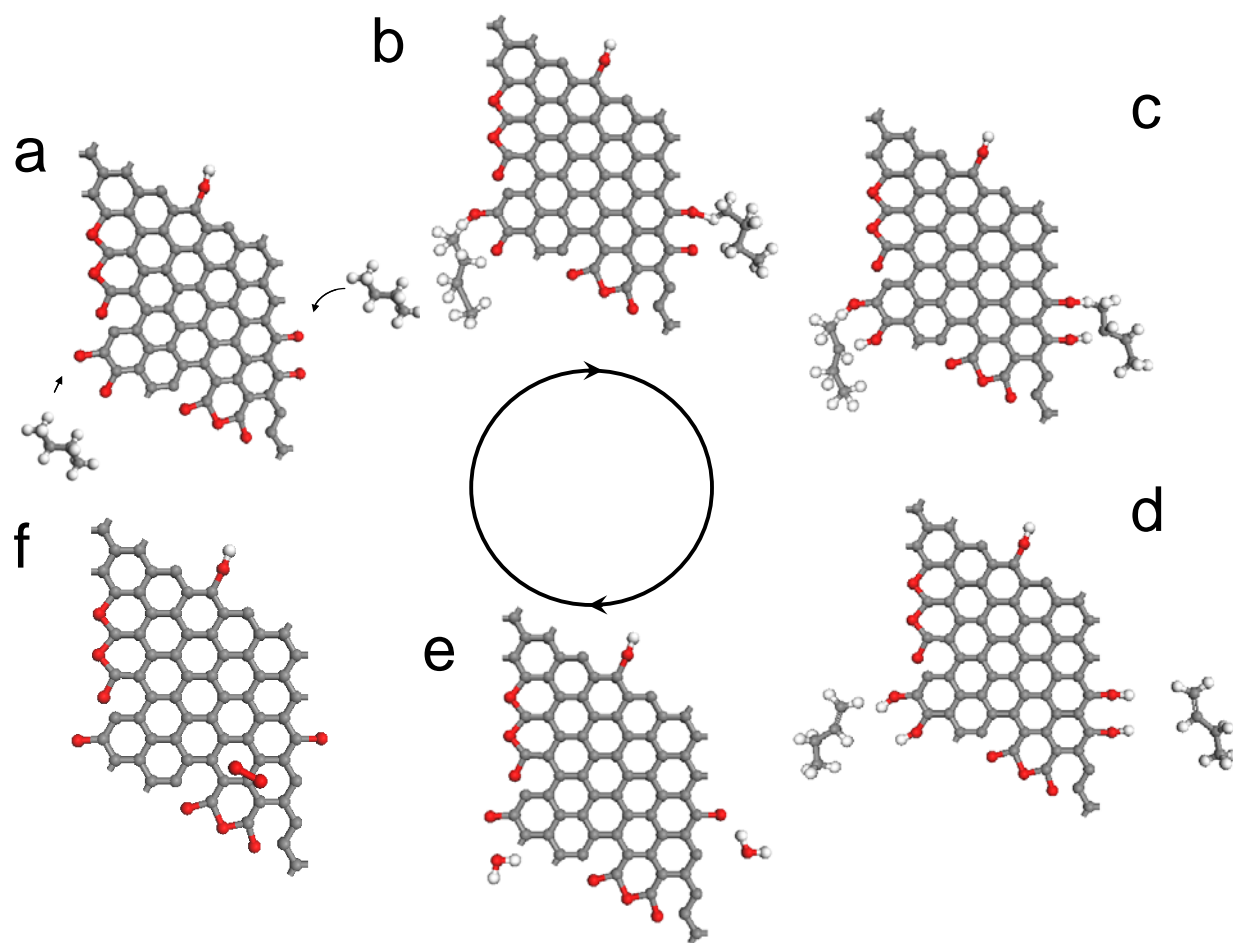
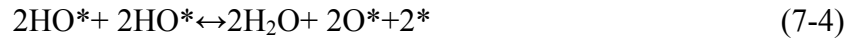
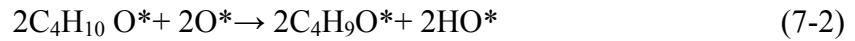


Fig. 7.2 Schematic illustration of oxidative dehydrogenation of butane to butene: a, b) chemisorption of butane at quinone groups, c,d) dehydrogenation and following desorption of butene, e) recombination of hydroxyl groups, following desorption of water and f)

regeneration of quinone groups via chemisorption of oxygen

Therefore, the possible reaction pathway for the dehydrogenation of butane occurred via a set of elemental steps (eq7.1 to eq7.5). Firstly, butane molecule is adsorbed on the surface of CNTs by interaction with quinone groups. Then C-H bond was activated and followed by abstraction of H atom from adsorbed butane occurred by using neighboring quinone groups. The further dehydrogenation happened, resulting in the formation and consequent desorption of butene molecule. In sequence, water generated via the recombination of OH groups and the dissociative chemisorption of O₂ occurred afterwards, resulting in the regeneration of quinone groups. The adsorption of butane and following cleavage of C-H bonding is rate-determining step for the dehydrogenation of butane.



The whole reaction network included parallel and sequential oxidation steps has been illustrated in chapter 4, reinforced by the kinetic measurement. Butenes are primary products and carbon oxides (CO_x) form as byproducts via butane oxidation and corresponding alkenes oxidation. It has been found that the high butadiene selectivity was achieved by using carbon nanotube after TPD performance. Notably, the removal of oxygenated surface groups could generate carbon defects, like zigzag and armchair defects, wherein the dissociative chemisorption of oxygen was thermodynamically

favorable (Fig. 7.3). This means that the density of quinone groups in active sites should be improved after thermal treatment. Therefore, the transportation and re-adsorption of butene molecule at the neighboring quinone groups are much easier.

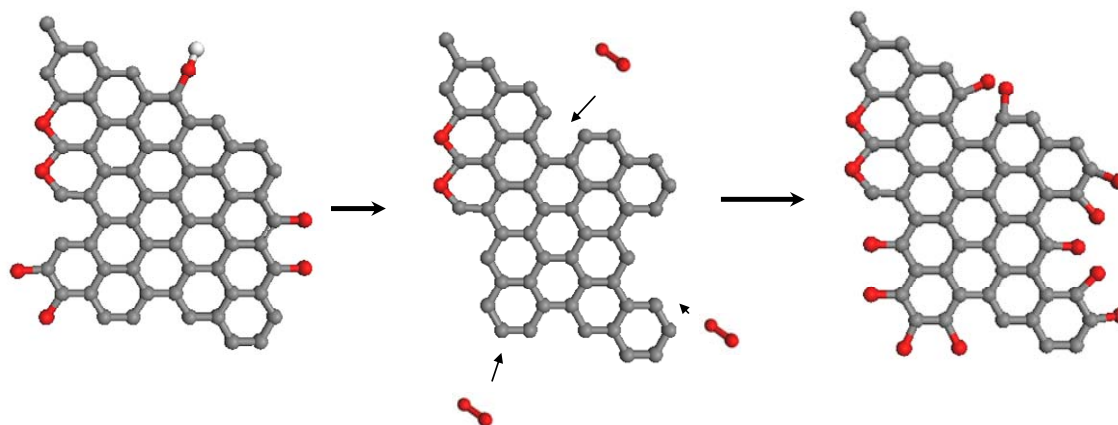


Fig. 7.3 Schematic illustration of removal and regeneration of oxygenated surface groups during the TPD and following catalytic test

The different contribution of oxygen species resulting from the dissociative and non-dissociative chemisorption of gaseous oxygen was observed. The total oxidation could be related with the electrophilic oxygen species (O_2^- , O_2^{2-}), which are weakly chemisorbed on the surface of CNTs. The electron-rich region of hydrocarbons, like C-C bonds, would be attacked by the electrophilic oxygen species, leading to the rupture of carbon sketch. The total oxidation could be effectively inhibited by using phosphoric addition, with respect to coverage of carbon surface by phosphoric oxide and, consequently, protecting the functionalities out of attacking of activated oxygen species.

The present work studied the contribution of surface functionalities of CNTs to the catalytic oxidation of butane to alkenes. It was found that majority of oxygenated surface groups did not have contribution to the catalytic activity of CNTs. The exchange

of gaseous oxygen and oxygenated surface groups was firstly identified, confirming that the elementary steps should include the dissociative chemisorption of oxygen and recombination of hydroxyl groups. It also confirmed that the catalytic behavior should be attributed to the quinone groups at active sites.

Two modification methods were conducted in the present work to improve the catalytic performance of CNTs. The phosphoric addition could efficiently inhibit the total oxidation, consequently improving the catalytic selectivity. The molecules grafting could improve the catalytic selectivity by immobilizing the molecules moieties on the surface of CNTs. A remarkable and stable catalytic performance was achieved by using the modified CNTs as catalysts, even better than the best metal catalysts. It displays the great potential of carbon materials in catalysis. The modification methods applied in the present work smartly develop the knowledge on the fabrication and modification of catalysts in a designed manner.

References

1. Rand B, Appleyard SP, Yardim MF, Design and Control of Structure of Advanced Carbon Materials for Enhanced Performance, NATO Science Series E, Vol. 374, 2001, Softcover
2. Figueiredo, JL; Pereira, MFR; Freitas, MMA, Modification of the Surface Chemistry of Activated Carbons, Carbon 1999, 37, 1379-1389
3. Pereira MFR, Orfao JJM, Figueiredo JL, Oxidative Dehydrogenation of Ethylbenzene on Activated Carbon Catalysts 1. Influence of Surface Chemical Groups, Applied Catalysis A: General 1999, 184, 153-160.
4. Kung HH, Oxidative Dehydrogenation of Light (C2 to C4) Alkanes, Advances in Catalysis 1994. 40, 1-38.

5. Martin-Aranda RM, Portela MF, Madeira LM, Freire F, Oliveira M, Effect of Alkali Metal Promoters on Nickel Molybdate Catalysts and Its Relevance to the Selective Oxidation of Butane. *Appl. Catal. A: Gen.* 1995, 127 (1–2), 201–217.
6. Marcua IC, Sandulescu I, Millet MJM, Oxidehydrogenation of n-Butane over Tetravalent Metal Phosphates Based Catalysts, *Applied Catalysis A: General* 2002, 227, 309–320
7. Nieto JML, Concepcion P, Dejoz A, Knozinger H, Melo F, Vasquez MI, Selective Oxidation of n-Butane and Butenes over Vanadium- Containing Catalysts, *Journal of Catalysis* 2000, 189, 147–157
- 8 . Balasubramanian K, Burghard M, Chemically Functionalized Carbon Nanotubes, *small* 2005, 1, 2, 180–192
9. Atamny F, Blocker J, Dubotzky A, Kurt H, Timpe O, Loose G, Mahdi W, Schlögl R, Surface chemistry of carbon: activation of molecular oxygen R, *Molecular Physics* 1992, 76(4), 851-886

APPENDIX

Curriculum Vitae

Liu Xi (P.R. China)

Working Experience:

2002.7-2004.6

Chinese South Glass Holding Co. LTD, Construction Glass Co. LTD, Department of Research and Development, Shenzhen, China

1997.7-1999.7

Chengdu Institute of Organic Chemistry, Chinese Academy of Science, Chengdu, China

Education:

PhD Physical chemistry 2004.7-2008.6

Fritz-Haber-Institut der Max-Planck Gesellschaft, Berlin, Germany

Master Physical chemistry 1999.9-2002.7

Chengdu Institute of Organic Chemistry, Chinese Academy of Science, Chengdu, China

Bachelor Material Science 1992.9-1997.7

University of Science and Technology of China, Department of Inorganic material , Anhui, China

Acknowledgements

I extend my sincere gratitude and appreciation to many people who made this doctoral thesis possible. Special thanks are due to my supervisor Prof. Dr. R. Schlögl to believe in me and for his attentive criticism which helped me to correct many ideas about catalysis and about myself. Thanks are also due to my supervisor Dr. Dangsheng Su, who help and teach me in my scientific work.

I would like to thank my colleagues, Dr. Xiaowei Chen, Dr. Jean-Philippe Tessonnier, Dr. Di Wang, Dr. Bo Zhu, Dr. Aihua Zhang, Dr. Jian Zhang, Rosa Arrigo, Manfred Schuster and Ali Rinaldi for the valuable scientific discussion. They also give me great support, helping me to overcome the difficulty in life.

I am highly in indebted to Dr. Bernd Kubias, Dr. Juan Jose, Delgado Siegfried Engelschalt and Manfred Swoboda for the help in construction of my apparatus.

I would also to thank Achim Klein-Hoffmann, Rolf Jentoft, Christian Hess, Raoul Blume, Edith Kitzelmann, Kristina Chakarova, Jutta Kröhnert, Gisela Lorenz for the excellent characterization of catalysts.

I would also thank Norbert Pfänder and Gisela Weinberg for TEM and SEM training.

I wish to express my profound gratitude to Dr. Yijun Xu, who help me to check the all content of my thesis and I also would gratefully appreciate kind help from Gisela Weinberg, who help me to translate the abstract from English to German.

I am grateful to Ning An, Almudena Celaya Sanfiz, Rhys Lloyd, Till Wolfram, Carine Chan Thaw, Rita Herbert, Jörg Thielemann, [Patrick Kurr](#), Peter Schnörch and others my friends.

I would also like to thank the Fritz-Haber-Institut der Max-Planck-Gesellschaft for the scholarship and the financial support of the projects CANAPE.

I wish to express my special thanks to my mother, brother and my family numbers for their cooperation, support and encouragement during the time of my research. They always be the part of my happiest memory. I am also very grateful to the people I love.